Electronic Appendices for JNCC Report 447

Stevens, C.J.[a], Smart, S.M.[b], Henrys, P.[b], Maskell, L.C.[b], Walker, K.J.[c], Preston, C.D.[d], Crowe, A.[b], Rowe, E.[e], Gowing, D.J.[a] & Emmett, B.A.[e]

[a] Department of Life Sciences, The Open University, Walton Hall, Milton Keynes MK7 6AA
[b] Centre for Ecology and Hydrology, Bailrigg, Lancaster LA1 4YQ
[c] Botanical Society of the British Isles (BSBI), c/o 97 Dragon Parade, Harrogate, North Yorkshire, HG1 5DG
[d] Centre for Ecology and Hydrology, Maclean Building, Benson Lane, Crowmarsh Gifford, Wallingford, Oxfordshire, OX10 8BB
[e] Centre for Ecology & Hydrology, Environment Centre Wales, Deiniol Road, Bangor,
Gwynedd, LL57 2UW

Download JNCC Report 447: http://jncc.defra.gov.uk/page-5894

October 2011

ISSN 0963–8091

For further information please contact:

Joint Nature Conservation Committee
Monkstone House
City Road
Peterborough
Cambridgeshire
PE1 1JY

Tel: +44 (0)1733 562626
Fax: +44 (0)1733 555948
Website: www.jncc.defra.gov.uk

This report should be cited as:

Stevens, C.J., Smart, S.M., Henrys, P., Maskell, L.C., Walker, K.J., Preston, C.D., Crowe, A., Rowe, E., Gowing, D.J. & Emmett, B.A. 2011. Collation of evidence of nitrogen impacts on vegetation in relation to UK biodiversity objectives. *JNCC Report*, No. 447

This project was jointly funded by Defra, the Joint Nature Conservation Committee, Natural England, the Countryside Council for Wales and Scottish Natural Heritage.

Electronic Appendix 1 for JNCC Report 447

Vascular Plant Database

Spatial analysis

Acid grassland – lowland

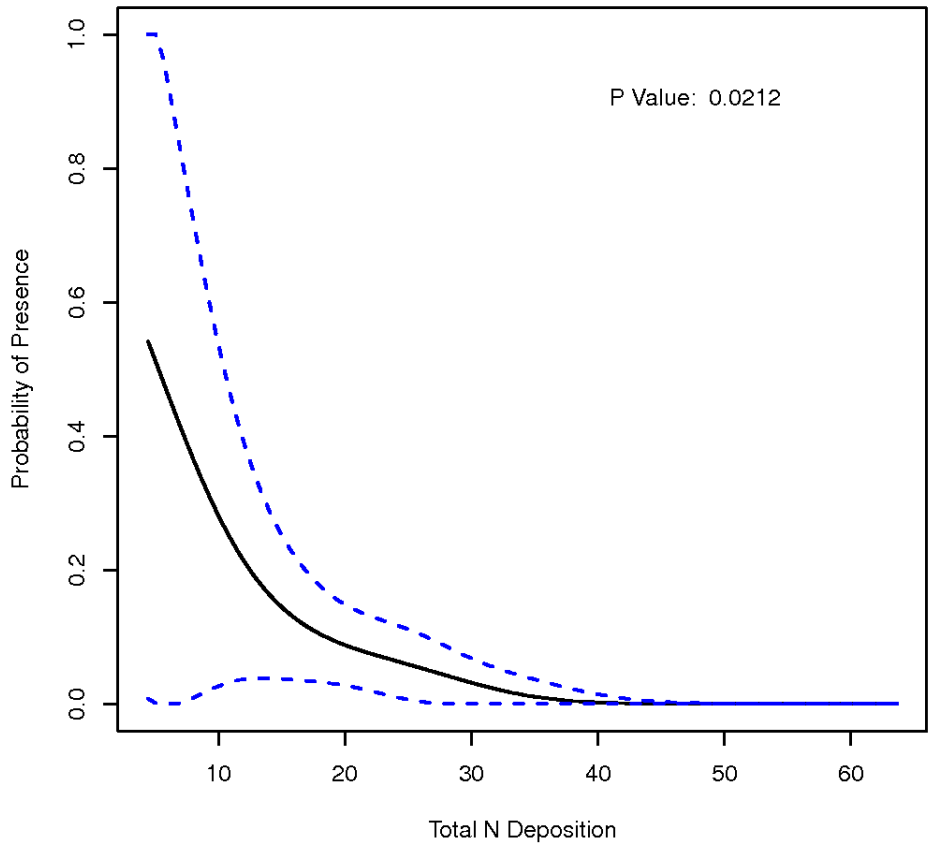

Figure A1.1. Spatial change in the probability of presence of *Cerastium arvense* in lowland acid grassland with increasing total current inorganic N deposition (kg N ha^{-1} yr^{-1}). Data from Vascular Plant Database.

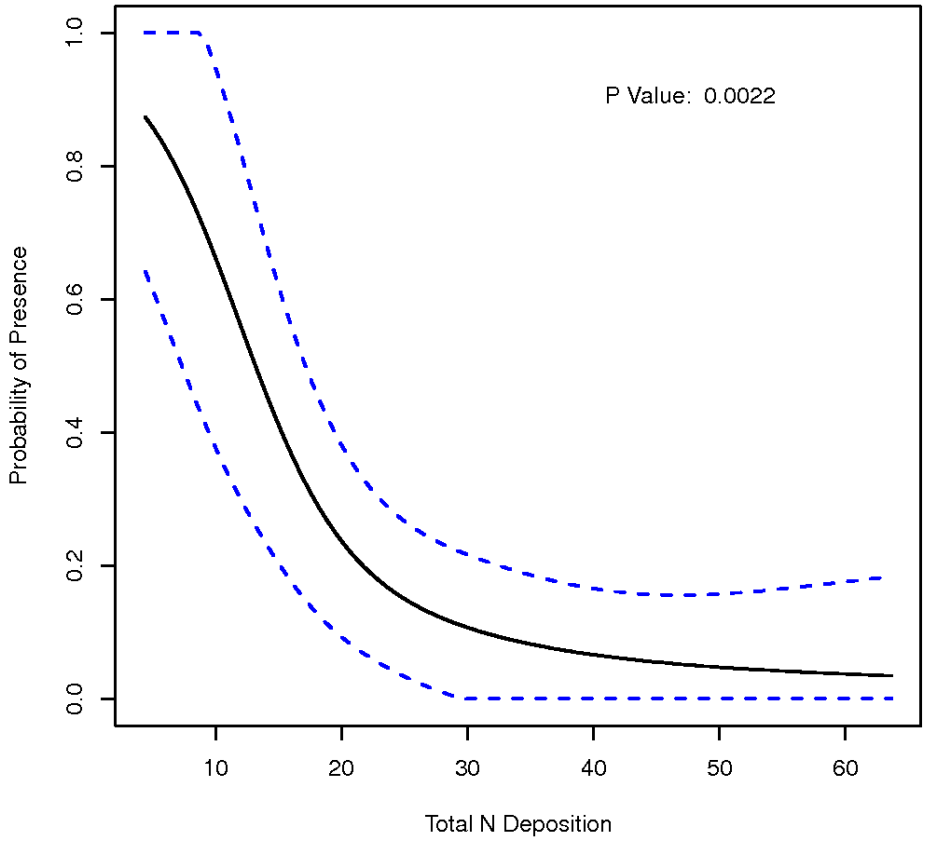

Figure A1.2. Spatial change in the probability of presence of *Cerastium semidecandrum* in lowland acid grassland with increasing total current inorganic N deposition (kg N ha^{-1} yr^{-1}). Data from Vascular Plant Database.

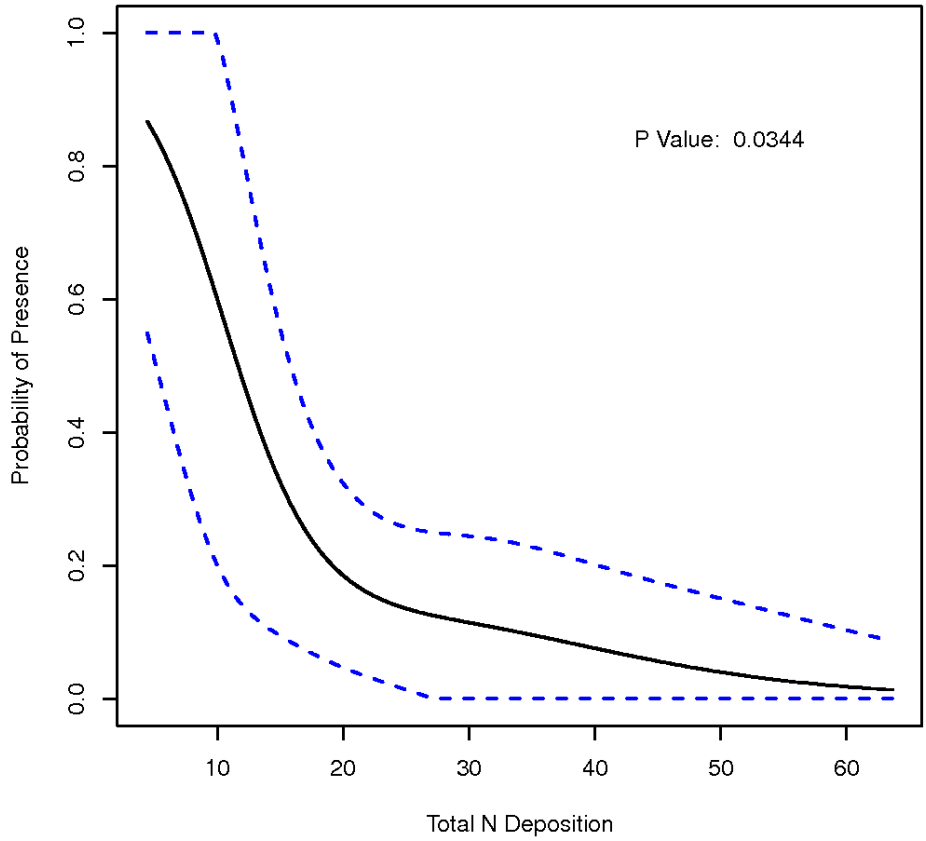

Figure A1.3. Spatial change in the probability of presence of *Trifolium arvense* in lowland acid grassland with increasing total current inorganic N deposition (kg N ha^{-1} yr^{-1}). Data from Vascular Plant Database.

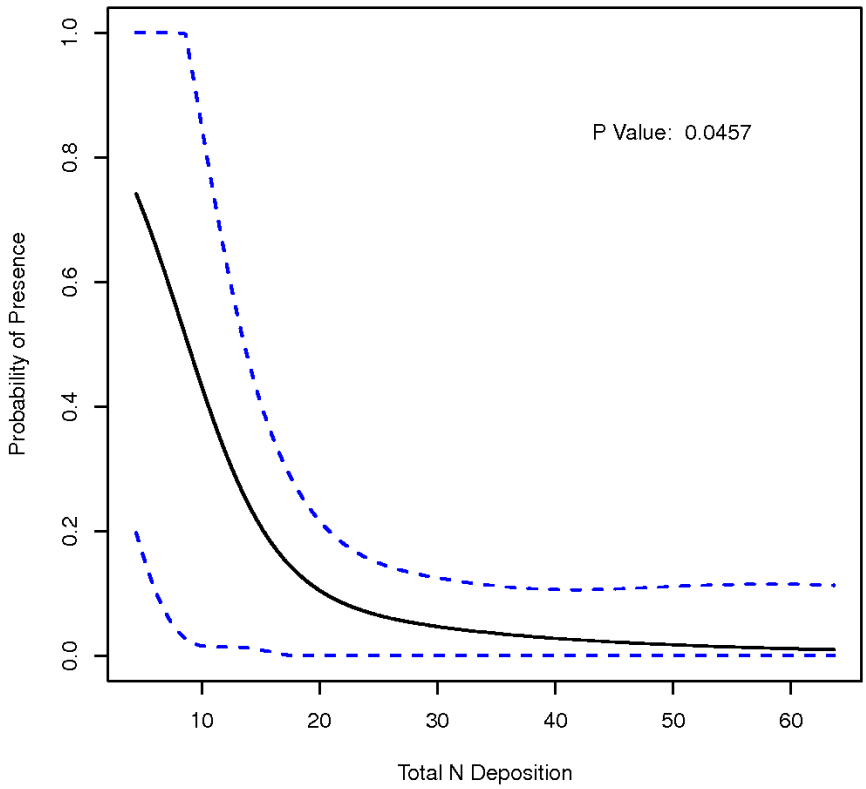

Figure A1.4. Spatial change in the probability of presence of *Vicia lathyroides* in lowland acid grassland with increasing total current inorganic N deposition (kg N ha^{-1} yr^{-1}). Data from Vascular Plant Database.

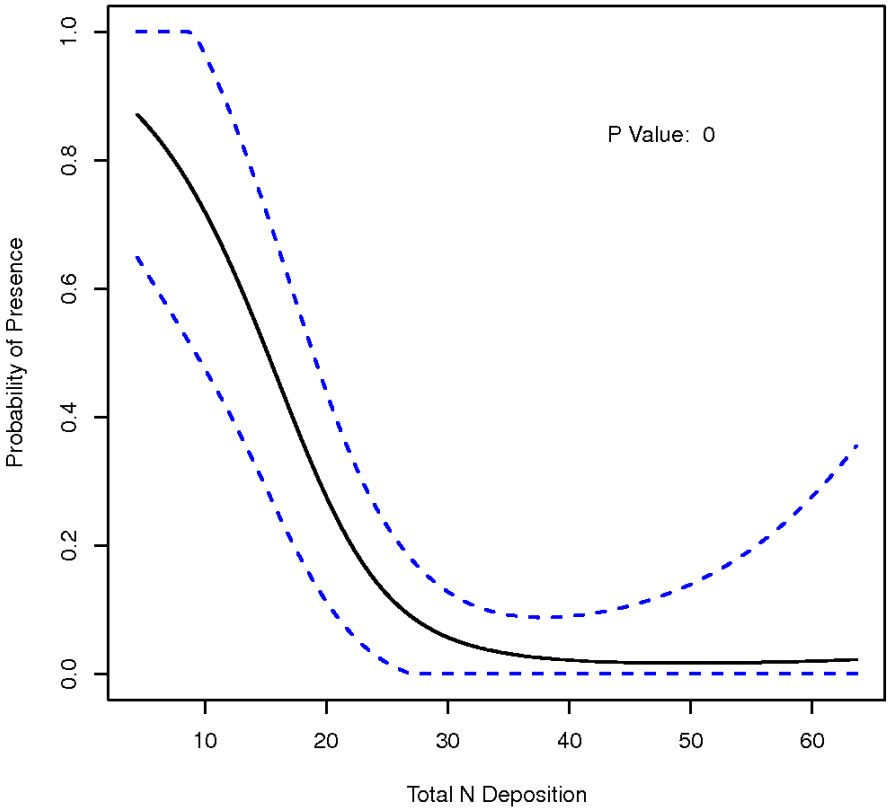

Figure A1.5. Spatial change in the probability of presence of *Viola canina* in lowland acid grassland with increasing total current inorganic N deposition (kg N ha^{-1} yr^{-1}). Data from Vascular Plant Database.

Calcareous grassland – lowland

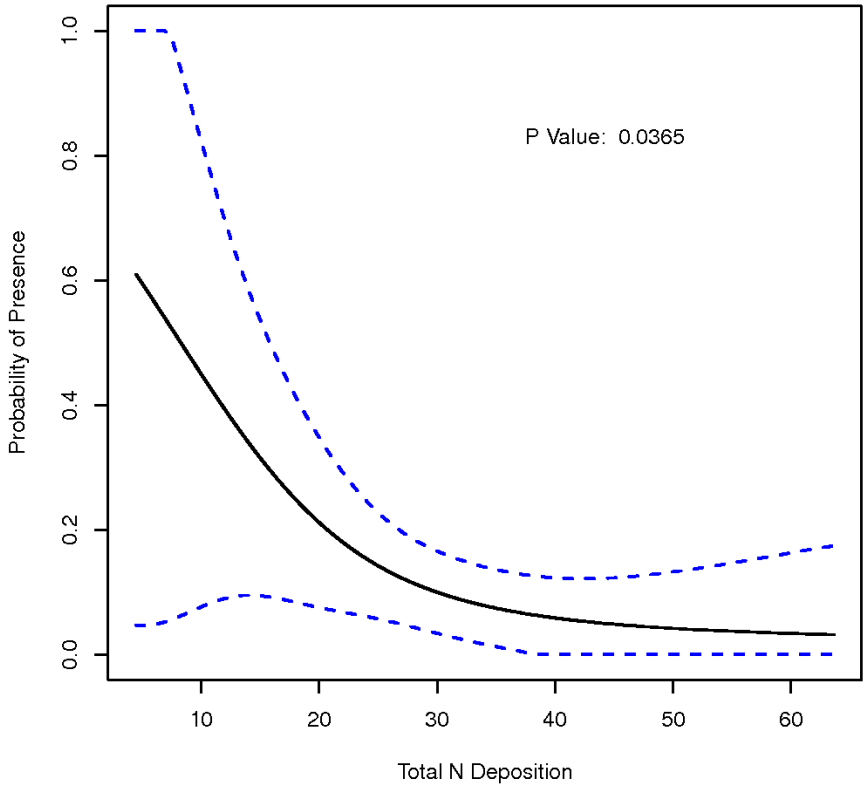

Figure A1.6. Spatial change in the probability of presence of *Allium vineale* in lowland calcareous grassland with increasing total current inorganic N deposition (kg N ha^{-1} yr^{-1}). Data from Vascular Plant Database.

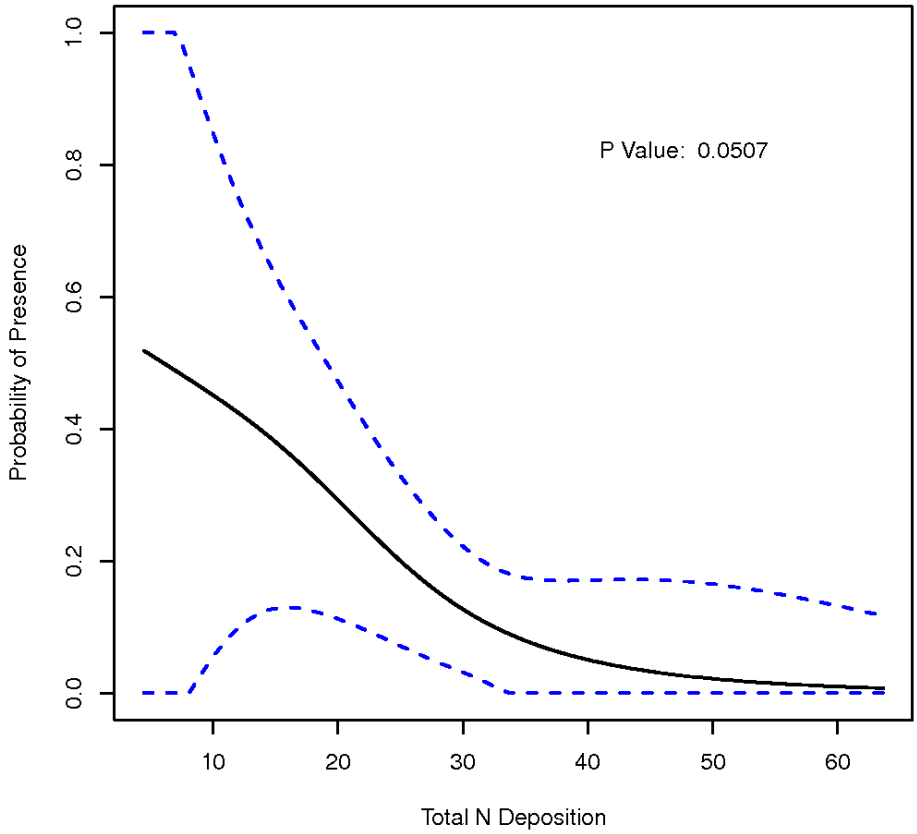

Figure A1.7. Spatial change in the probability of presence of *Anacamptis pyramidalis* in lowland calcareous grassland with increasing total current inorganic N deposition (kg N ha^{-1} yr^{-1}). Data from Vascular Plant Database.

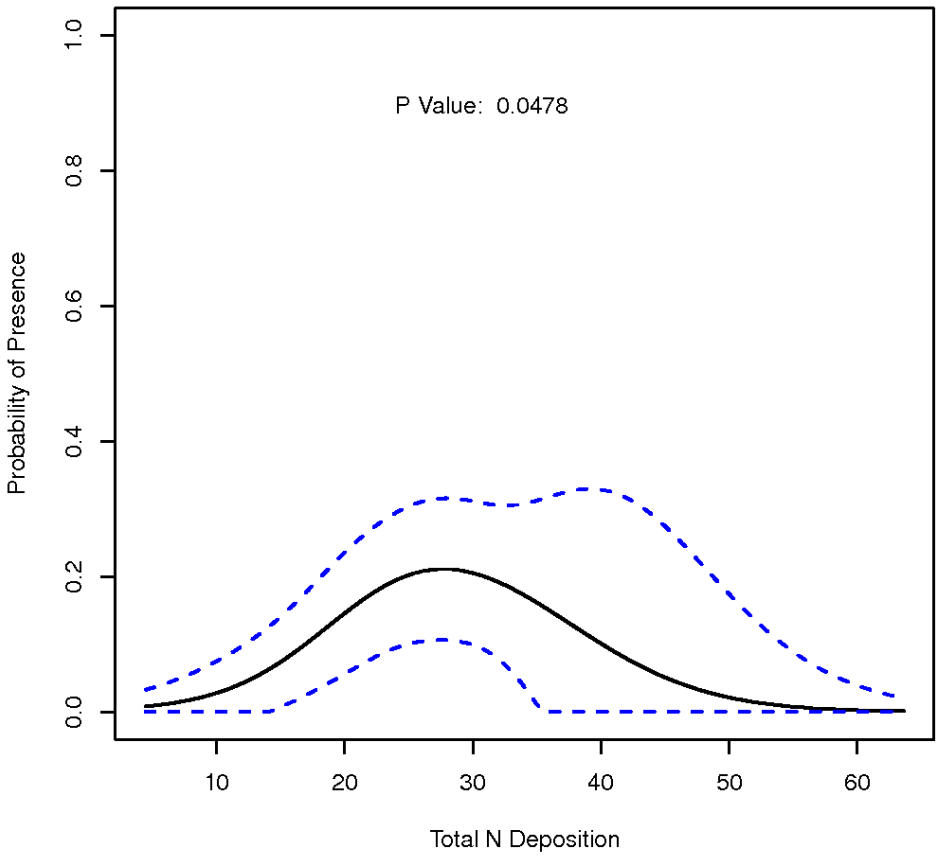

Figure A1.8. Spatial change in the probability of presence of *Carex spicata* in lowland calcareous grassland with increasing total current inorganic N deposition (kg N ha^{-1} yr^{-1}). Data from Vascular Plant Database.

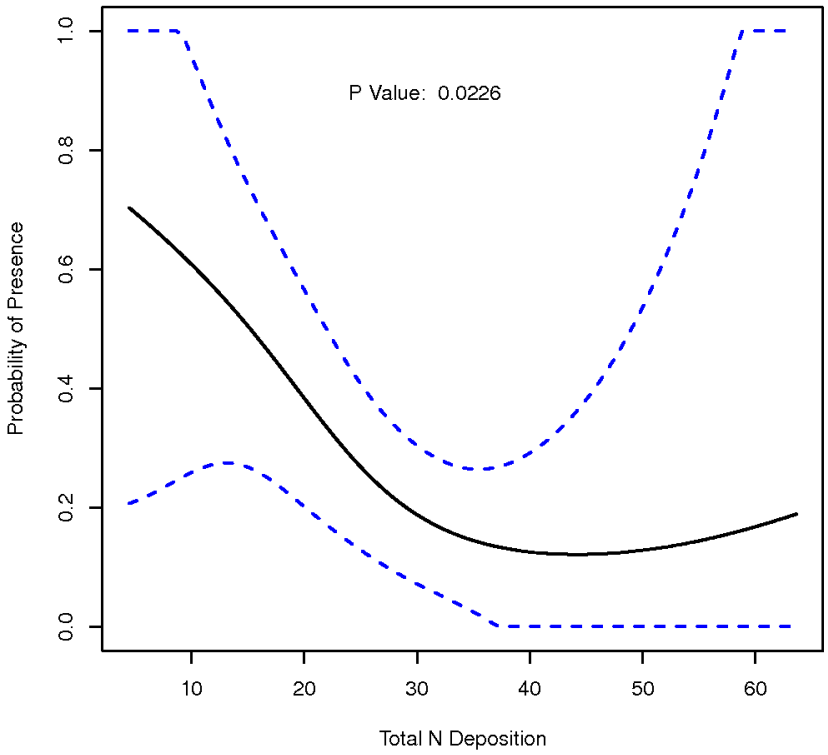

Figure A1.9. Spatial change in the probability of presence of *Carlina vulgaris* in lowland calcareous grassland with increasing total current inorganic N deposition (kg N ha^{-1} yr^{-1}). Data from Vascular Plant Database.

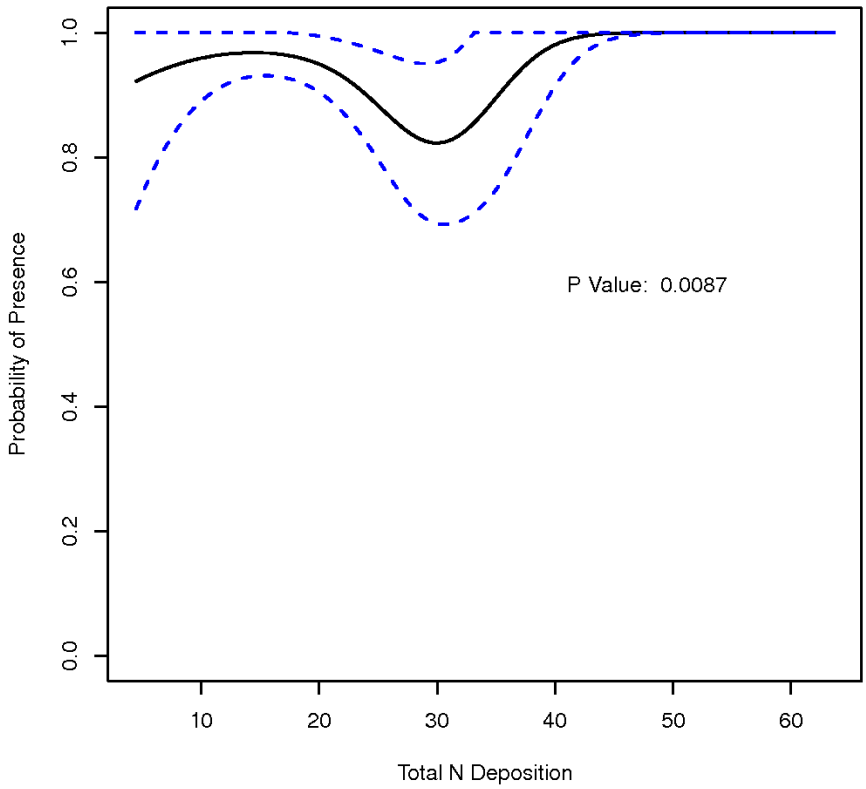

Figure A1.10. Spatial change in the probability of presence of *Centaurium erythraea* in lowland calcareous grassland with increasing total current inorganic N deposition (kg N ha^{-1} yr^{-1}). Data from Vascular Plant Database.

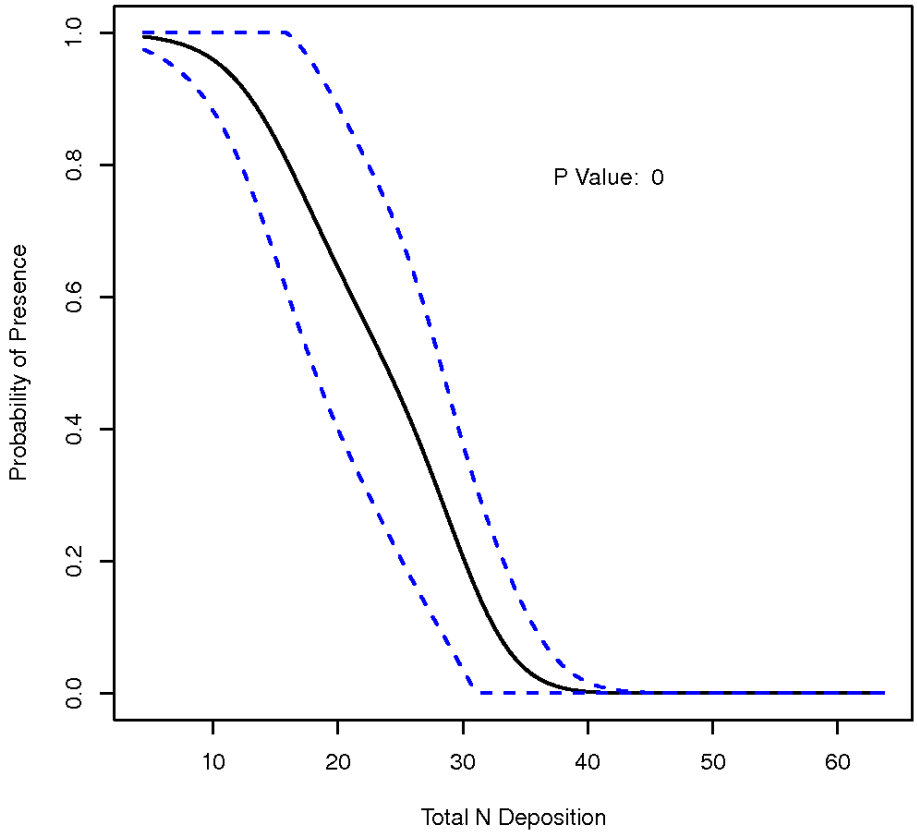

Figure A1.11. Spatial change in the probability of presence of *Cynoglossum officinale* in lowland calcareous grassland with increasing total current inorganic N deposition (kg N ha^{-1} yr^{-1}). Data from Vascular Plant Database.

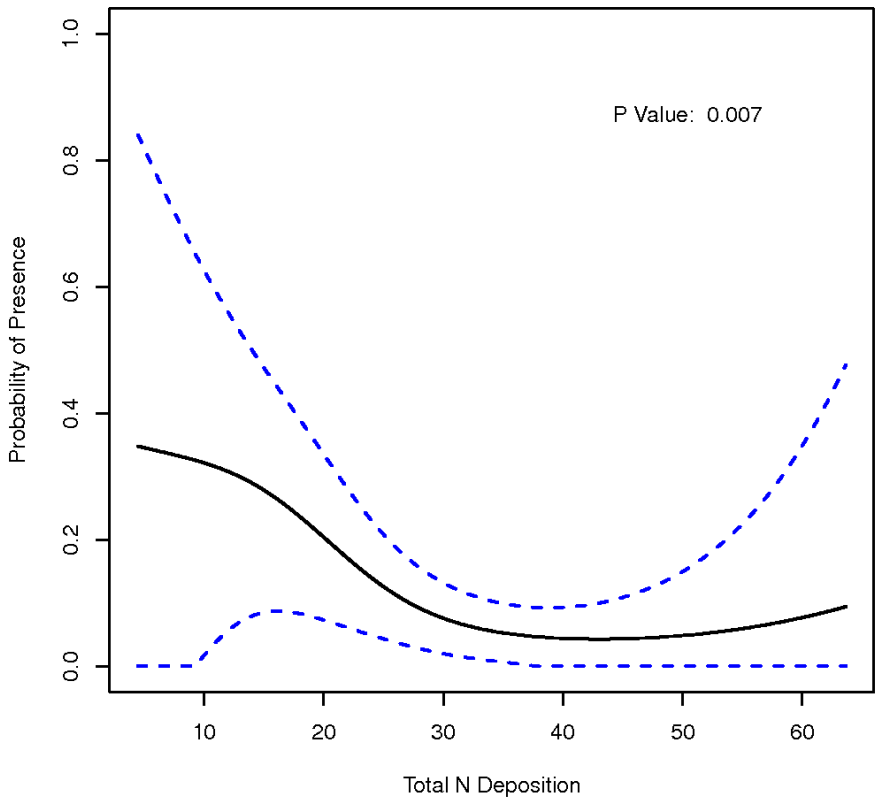

Figure A1.12. Spatial change in the probability of presence of *Echium vulgare* in lowland calcareous grassland with increasing total current inorganic N deposition (kg N ha^{-1} yr^{-1}). Data from Vascular Plant Database.

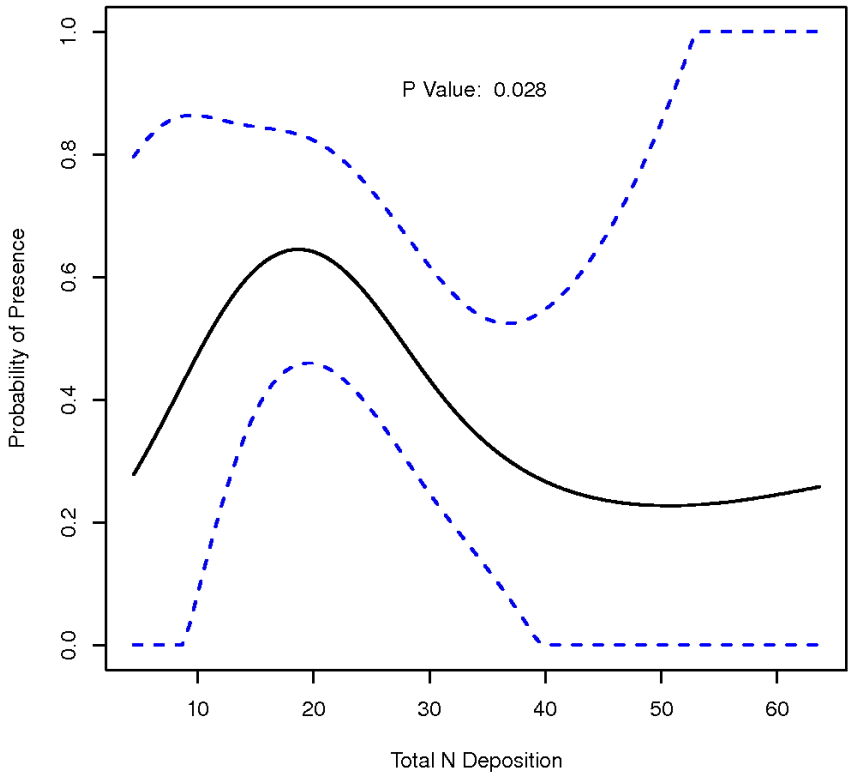

Figure A1.13. Spatial change in the probability of presence of *Epipactis helleborine* in lowland calcareous grassland with increasing total current inorganic N deposition (kg N ha^{-1} yr^{-1}). Data from Vascular Plant Database.

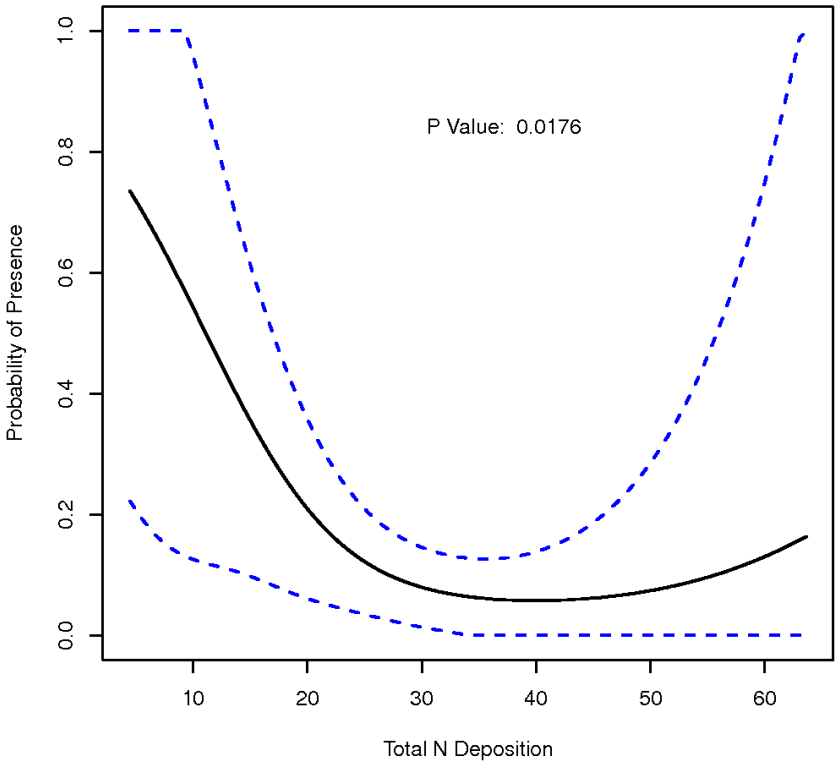

Figure A1.14. Spatial change in the probability of presence of *Geranium columbinum* in lowland calcareous grassland with increasing total current inorganic N deposition (kg N ha^{-1} yr^{-1}). Data from Vascular Plant Database.

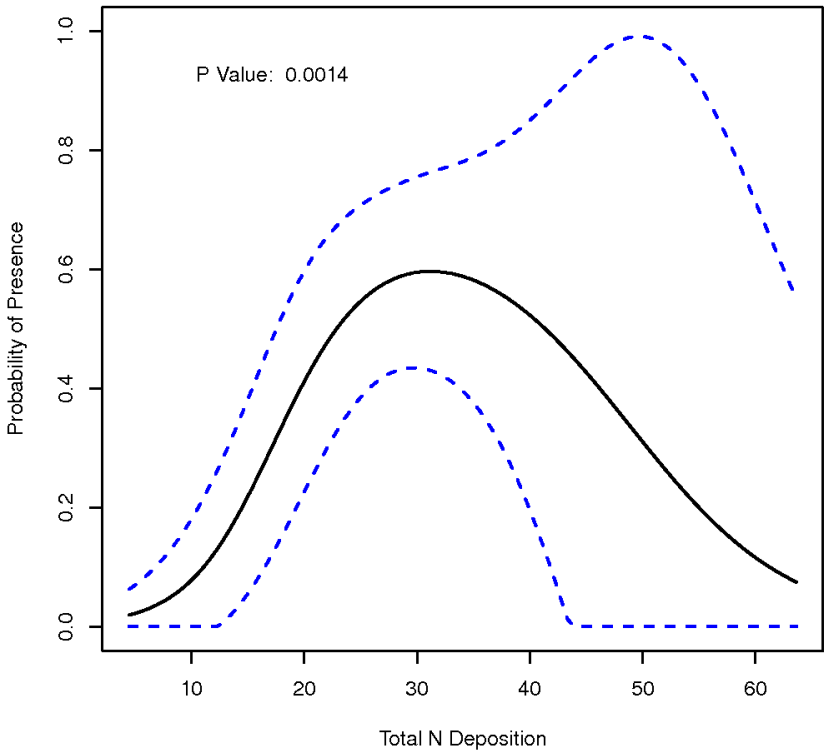

Figure A1.15. Spatial change in the probability of presence of *Knautia arvensis* in lowland calcareous grassland with increasing total current inorganic N deposition (kg N ha^{-1} yr^{-1}). Data from Vascular Plant Database.

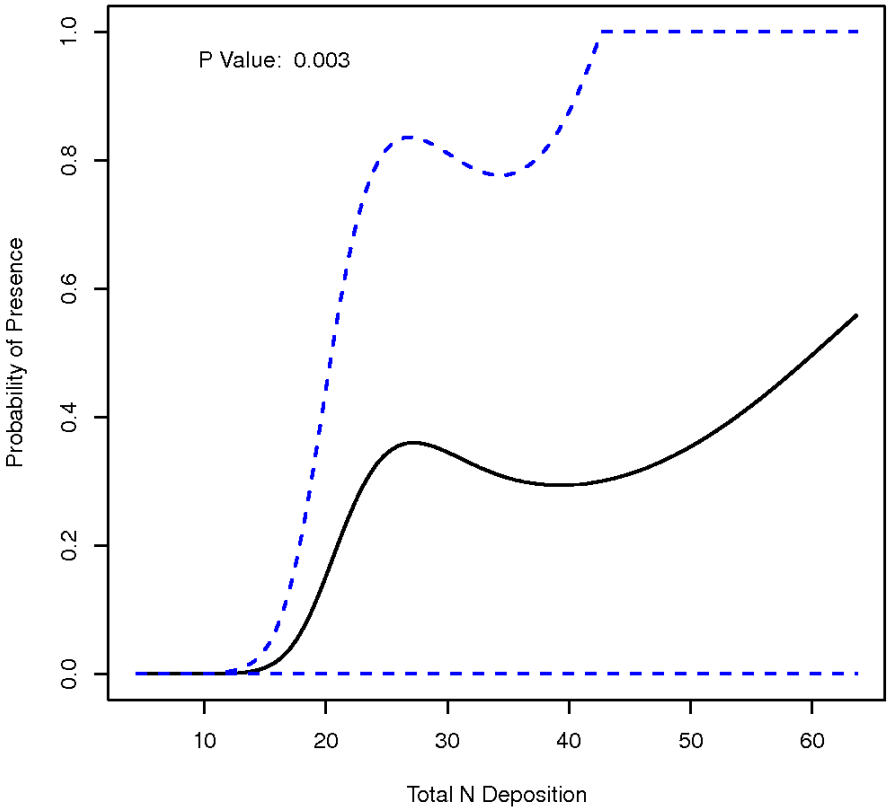

Figure A1.16. Spatial change in the probability of presence of *Lathyrus nissolia* in lowland calcareous grassland with increasing total current inorganic N deposition (kg N ha^{-1} yr^{-1}). Data from Vascular Plant Database.

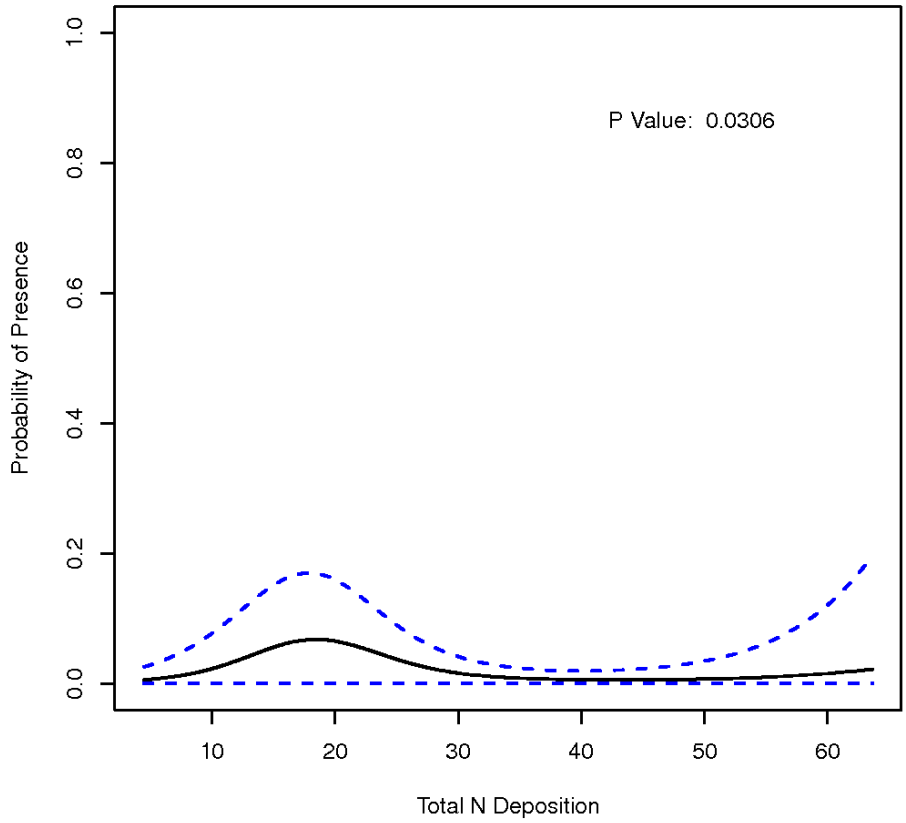

Figure A1.17. Spatial change in the probability of presence of *Linum bienne* in lowland calcareous grassland with increasing total current inorganic N deposition (kg N ha^{-1} yr^{-1}). Data from Vascular Plant Database.

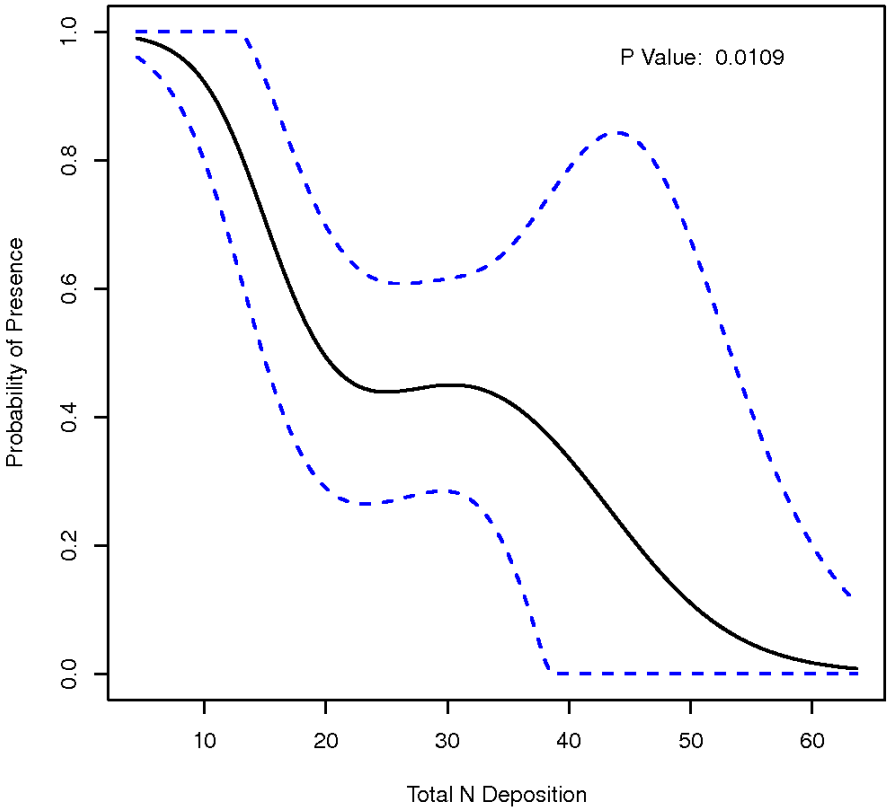

Figure A1.18. Spatial change in the probability of presence of *Ononis repens* in lowland calcareous grassland with increasing total current inorganic N deposition (kg N ha^{-1} yr^{-1}). Data from Vascular Plant Database.

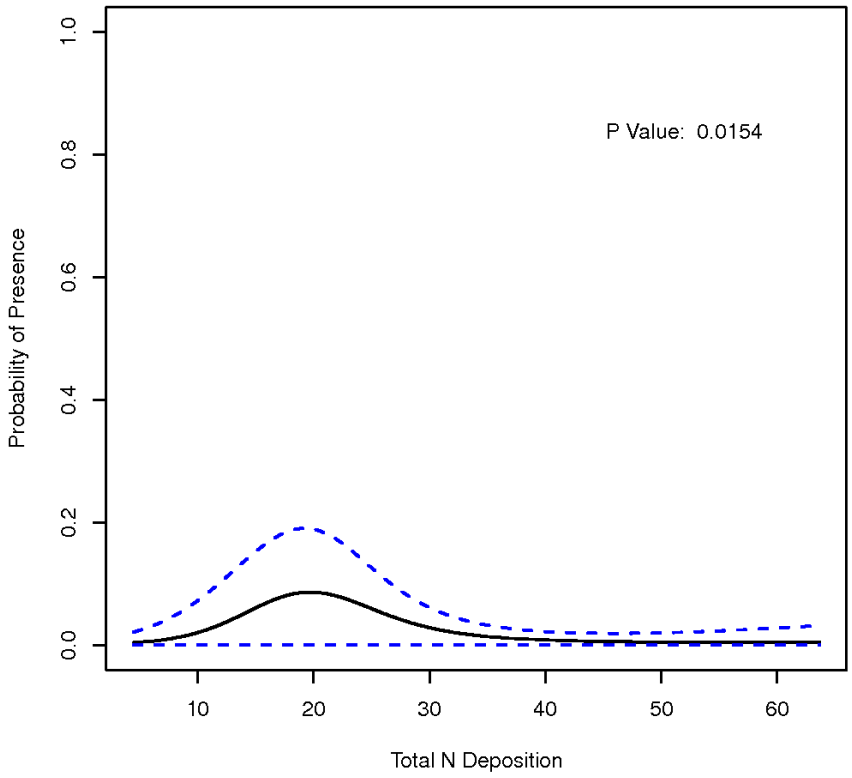

Figure A1.19. Spatial change in the probability of presence of *Pastinaca sativa* in lowland calcareous grassland with increasing total current inorganic N deposition (kg N ha^{-1} yr^{-1}). Data from Vascular Plant Database.

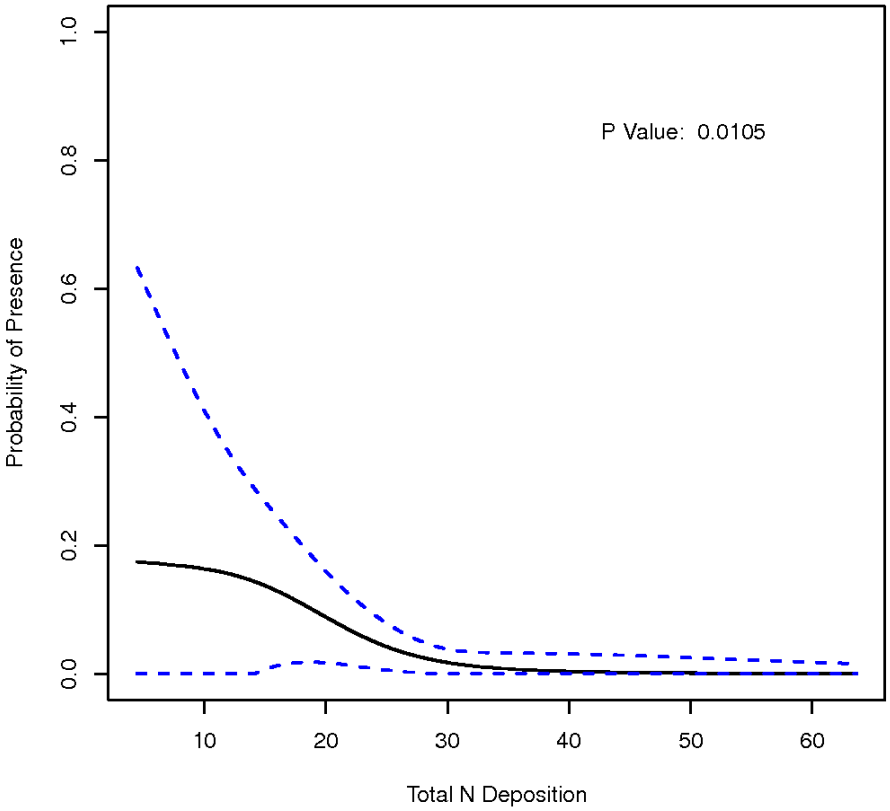

Figure A1.20. Spatial change in the probability of presence of *Rosa micrantha* in lowland calcareous grassland with increasing total current inorganic N deposition (kg N ha^{-1} yr^{-1}). Data from Vascular Plant Database.

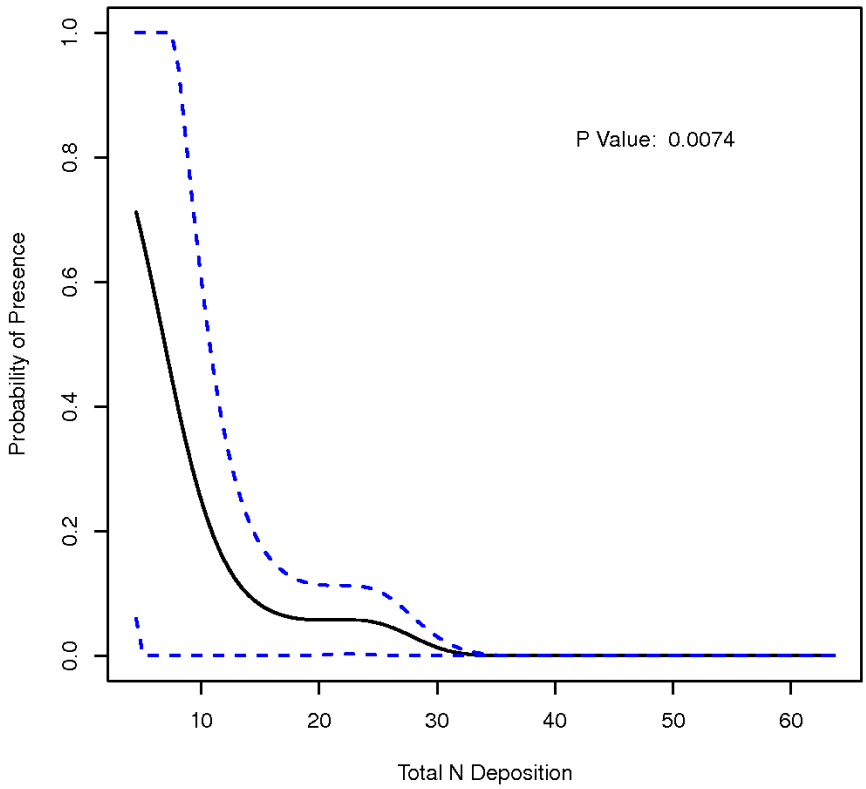

Figure A1.21. Spatial change in the probability of presence of *Spiranthes spiralis* in lowland calcareous grassland with increasing total current inorganic N deposition (kg N ha^{-1} yr^{-1}). Data from Vascular Plant Database.

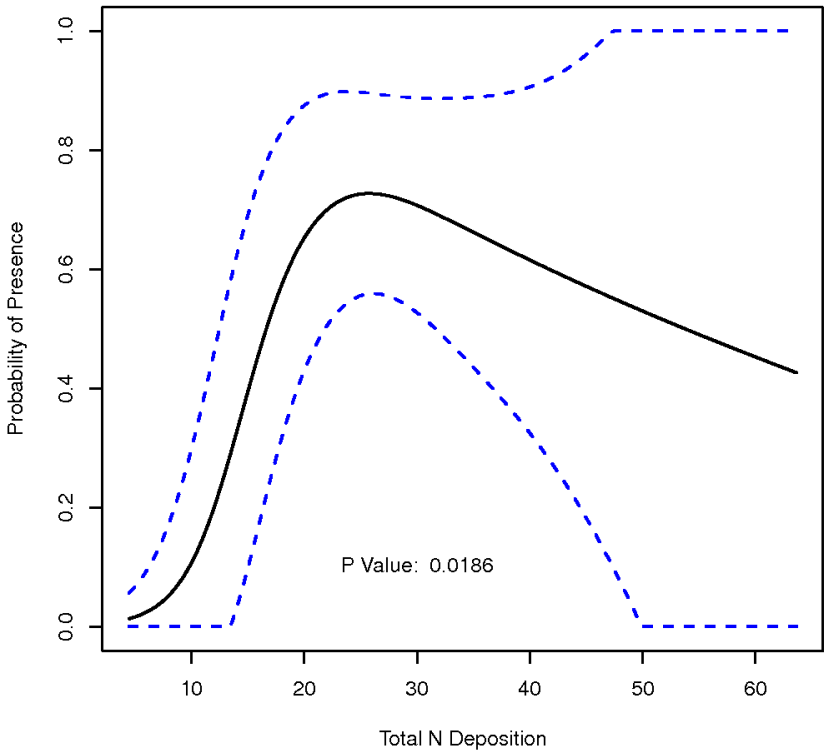

Figure A1.22. Spatial change in the probability of presence of *Stachys officinalis* in lowland calcareous grassland with increasing total current inorganic N deposition (kg N ha^{-1} yr^{-1}). Data from Vascular Plant Database.

Calcareous grassland – upland

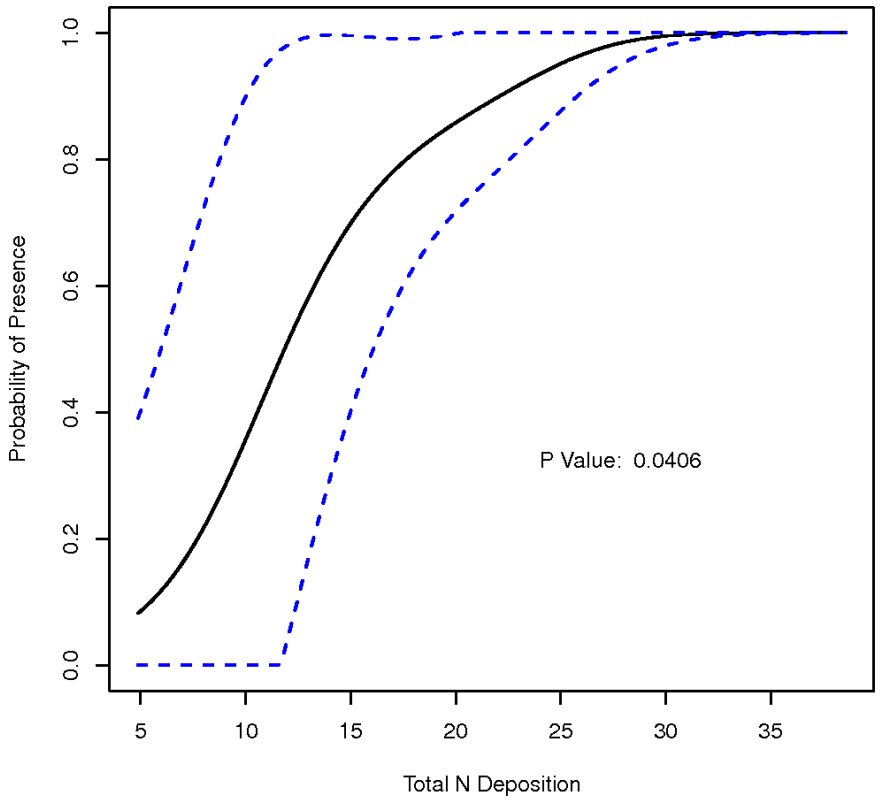

Figure A1.23. Spatial change in the probability of presence of *Alchemilla xanthochlora* in upland calcareous grassland with increasing total current inorganic N deposition (kg N ha^{-1} yr^{-1}). Data from Vascular Plant Database.

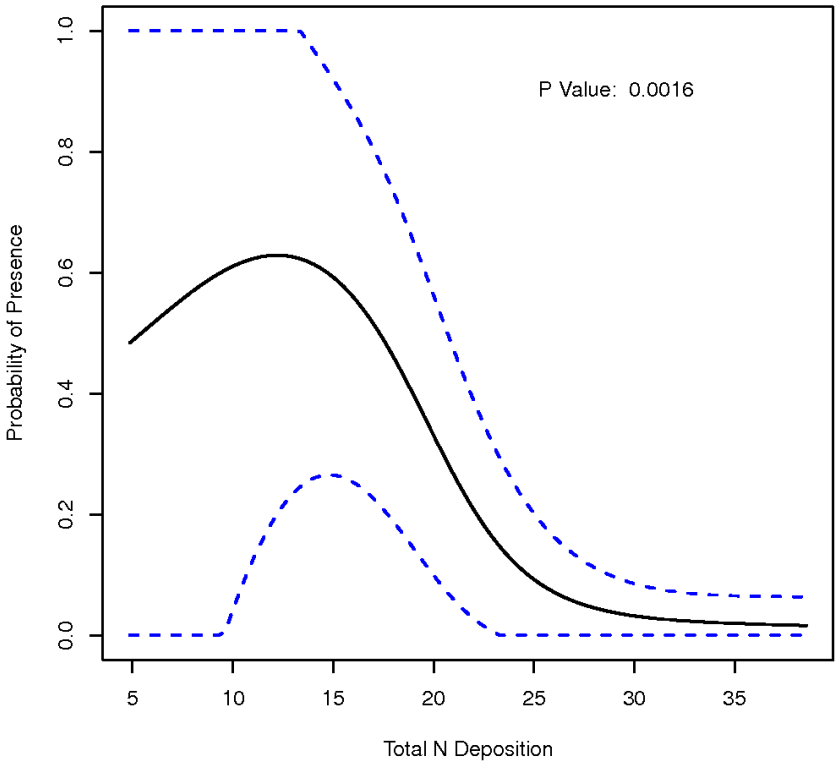

Figure A1.24. Spatial change in the probability of presence of *Melica nutans* in upland calcareous grassland with increasing total current inorganic N deposition (kg N ha^{-1} yr^{-1}). Data from Vascular Plant Database.

Heathland – lowland

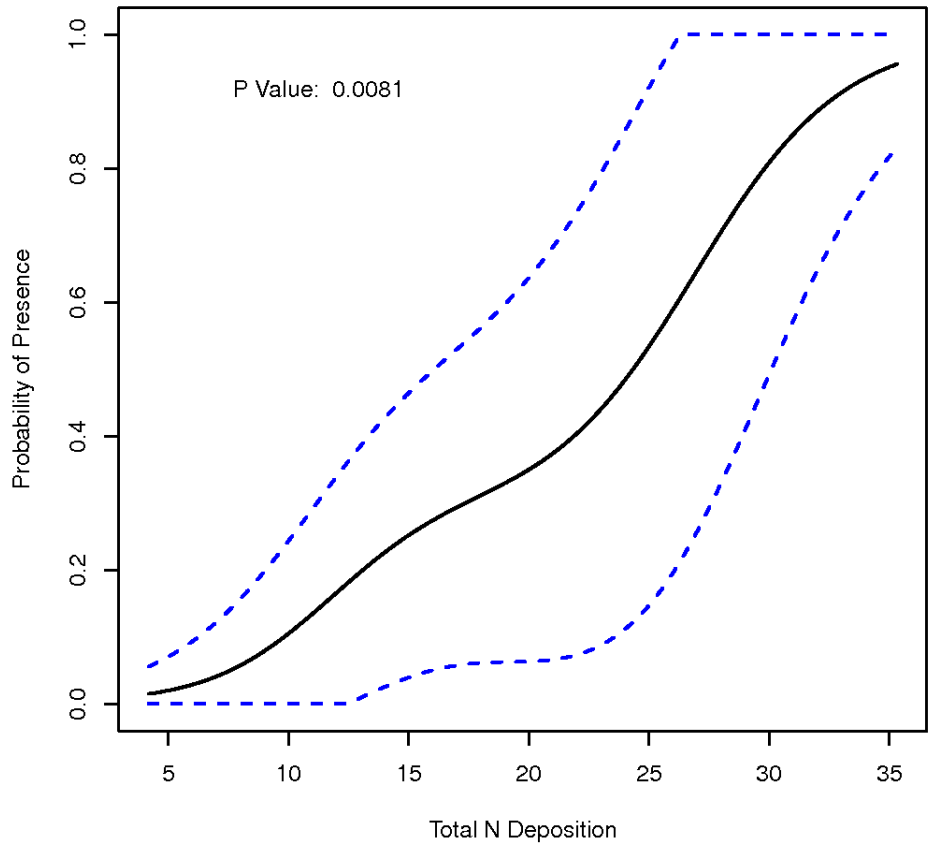

Figure A1.25. Spatial change in the probability of presence of *Platanthera bifolia* in lowland heathland with increasing total current inorganic N deposition (kg N ha^{-1} yr^{-1}). Data from Vascular Plant Database.

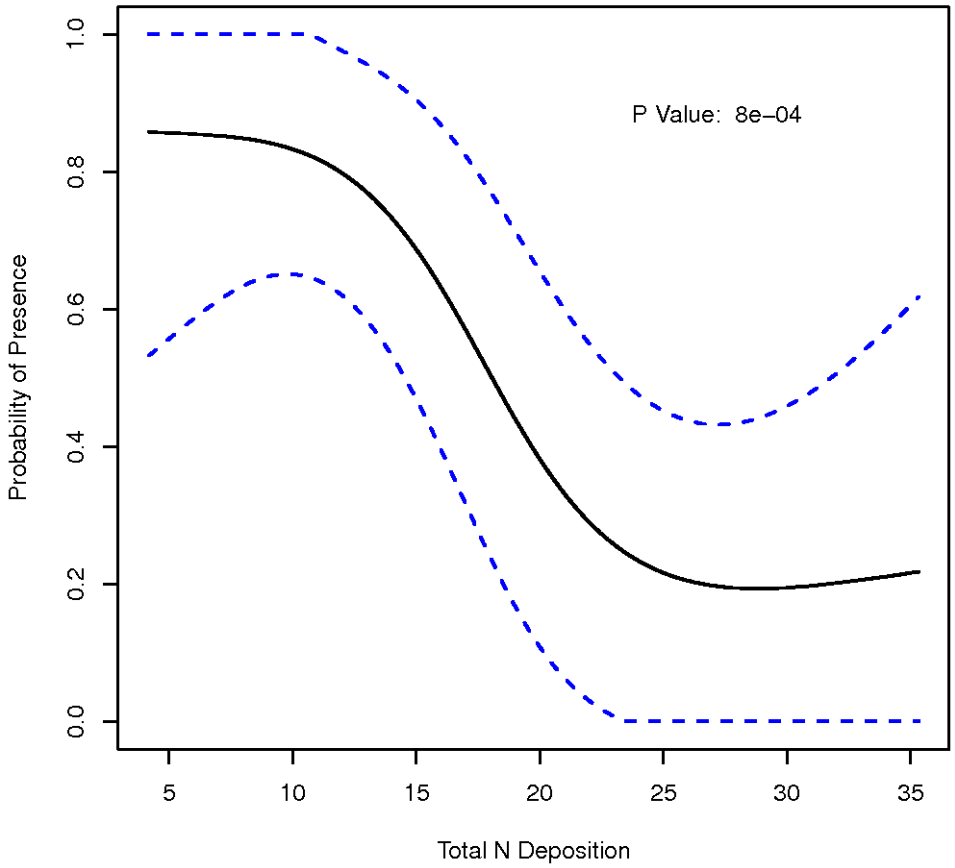

Figure A1.26. Spatial change in the probability of *Viola canina* presence of in lowland heathland with increasing total current inorganic N deposition (kg N ha^{-1} yr^{-1}). Data from Vascular Plant Database.

Heathland – upland

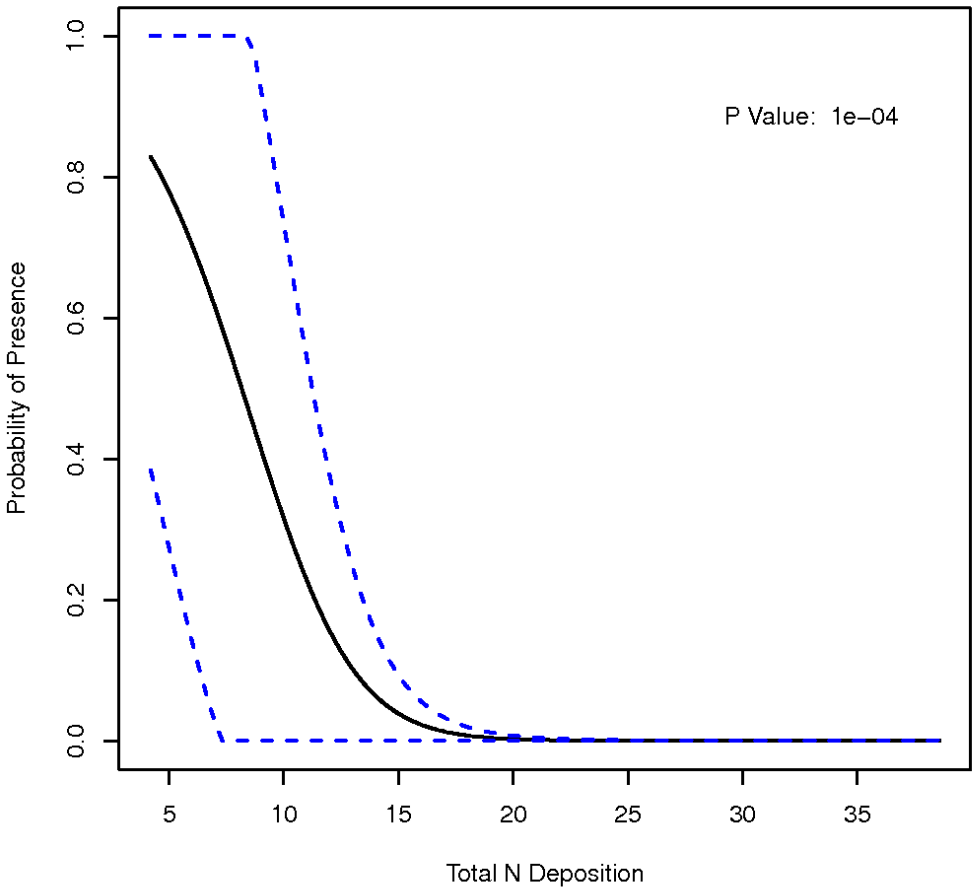

Figure A1.27. Spatial change in the probability of presence of *Arctostaphylos uva-ursi* in upland heathland with increasing total current inorganic N deposition (kg N ha^{-1} yr^{-1}). Data from Vascular Plant Database.

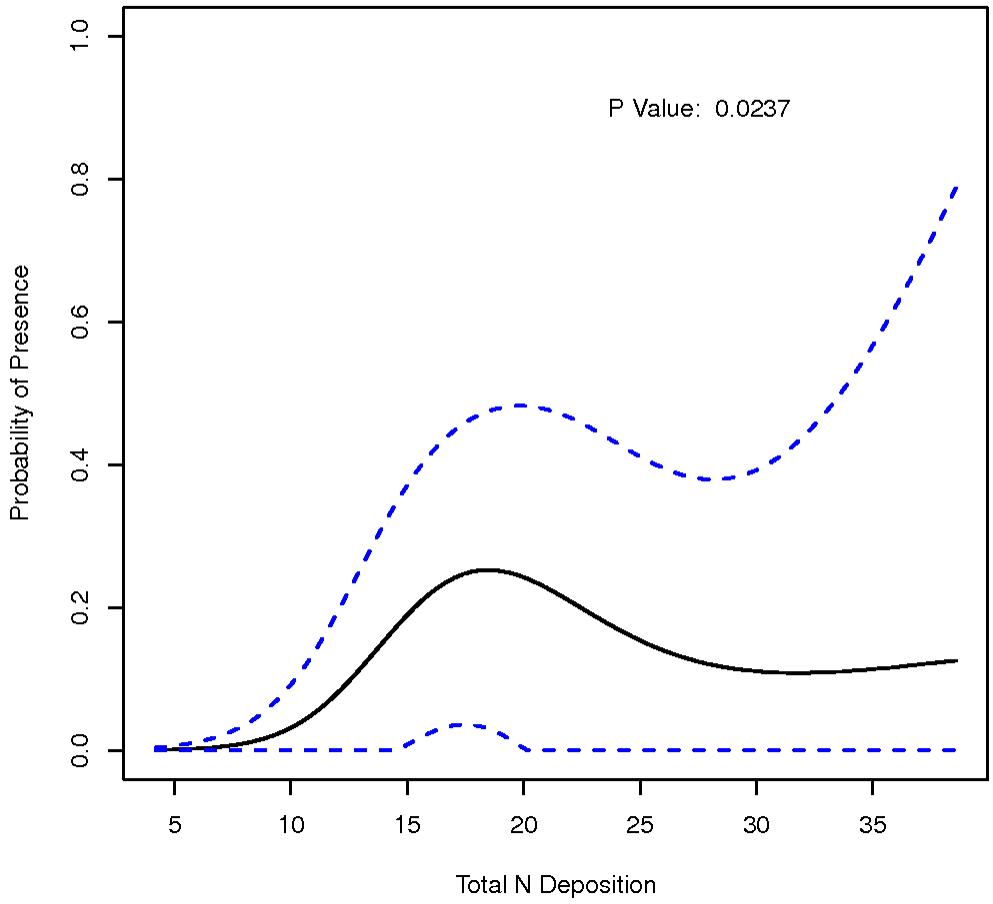

Figure A1.28. Spatial change in the probability of presence of *Trientalis europaea* in upland heathland with increasing total current inorganic N deposition (kg N ha^{-1} yr^{-1}). Data from vascular plant.

Temporal analysis

Acid grassland – lowland

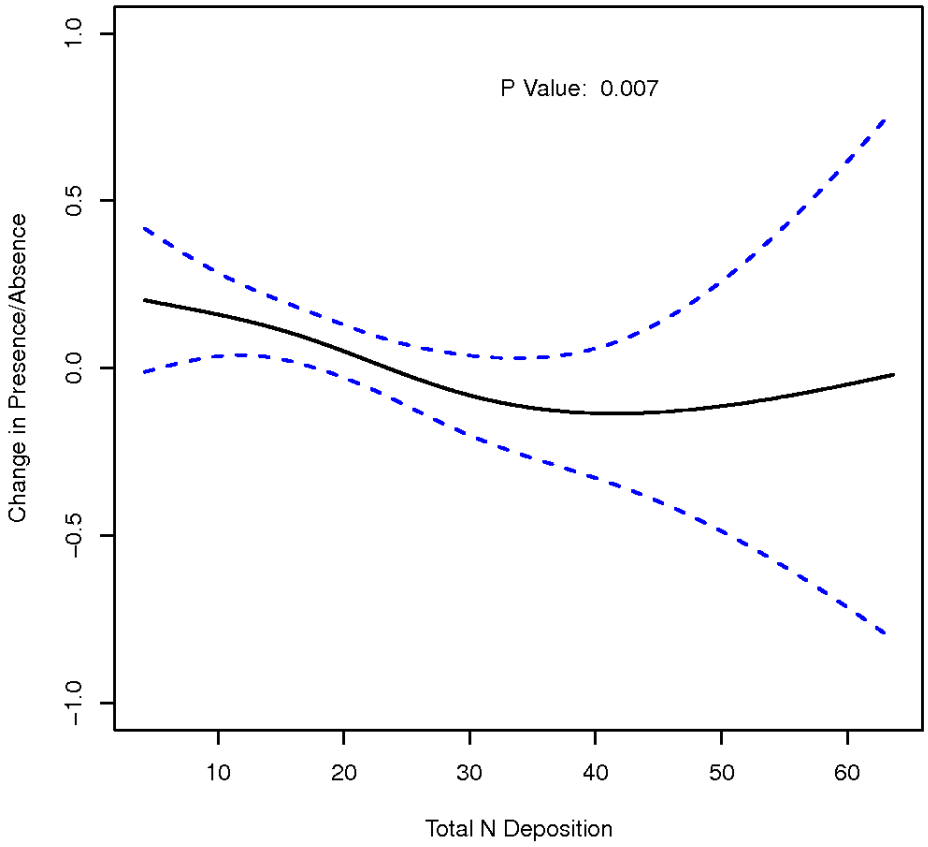

Figure A1.29. Temporal change in the probability of presence of *Cerastium semidecandrum* between survey periods (1930-1969, and 1987-1999) against total current inorganic N deposition (kg N ha^{-1} yr^{-1}) for hectads in lowland acid grassland. Data from Vascular Plant Database.

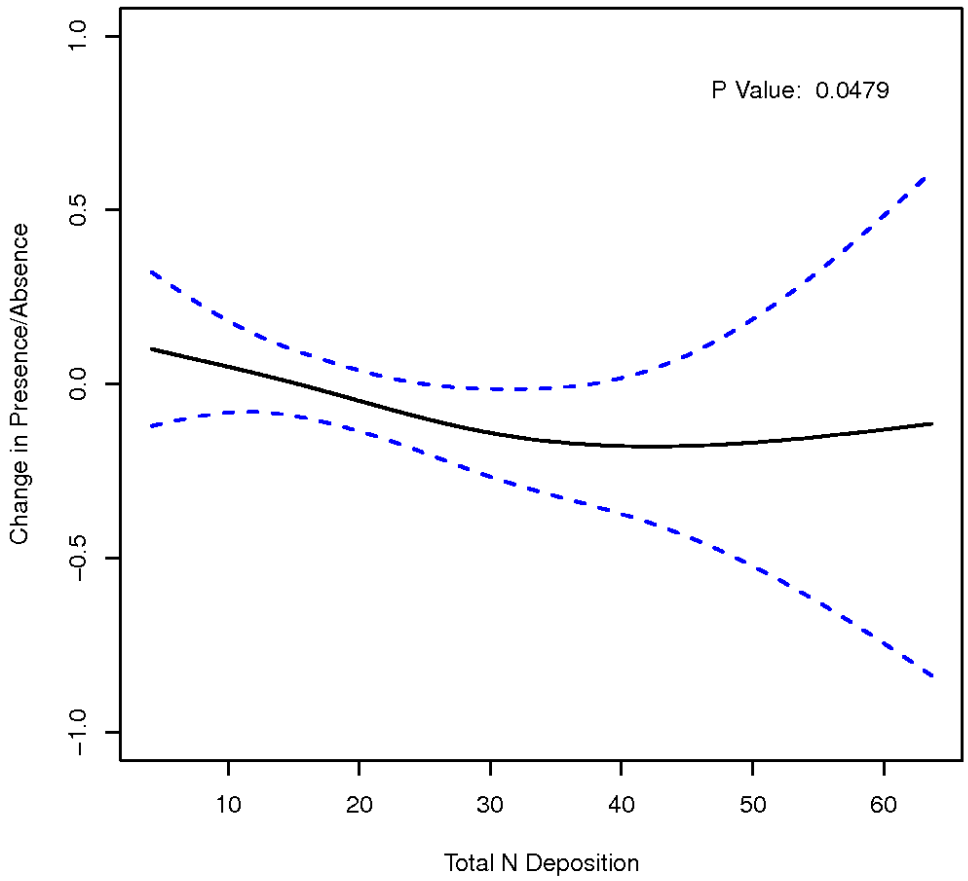

Figure A1.30. Temporal change in the probability of presence of *Myosotis ramosissima* between survey periods (1930-1969, and 1987-1999) against total current inorganic N deposition (kg N ha^{-1} yr^{-1}) for hectads in lowland acid grassland. Data from Vascular Plant Database.

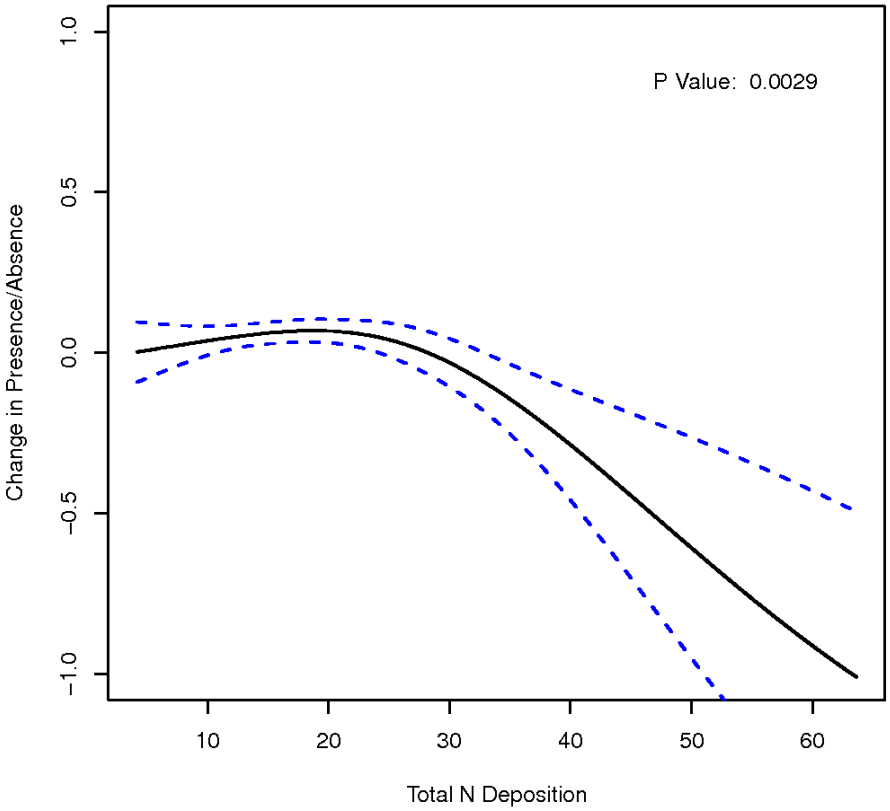

Figure A1.31. Temporal change in the probability of presence of *Ornithopus perpusillus* between survey periods (1930-1969, and 1987-1999) against total current inorganic N deposition (kg N ha^{-1} yr^{-1}) for hectads in lowland acid grassland. Data from Vascular Plant Database.

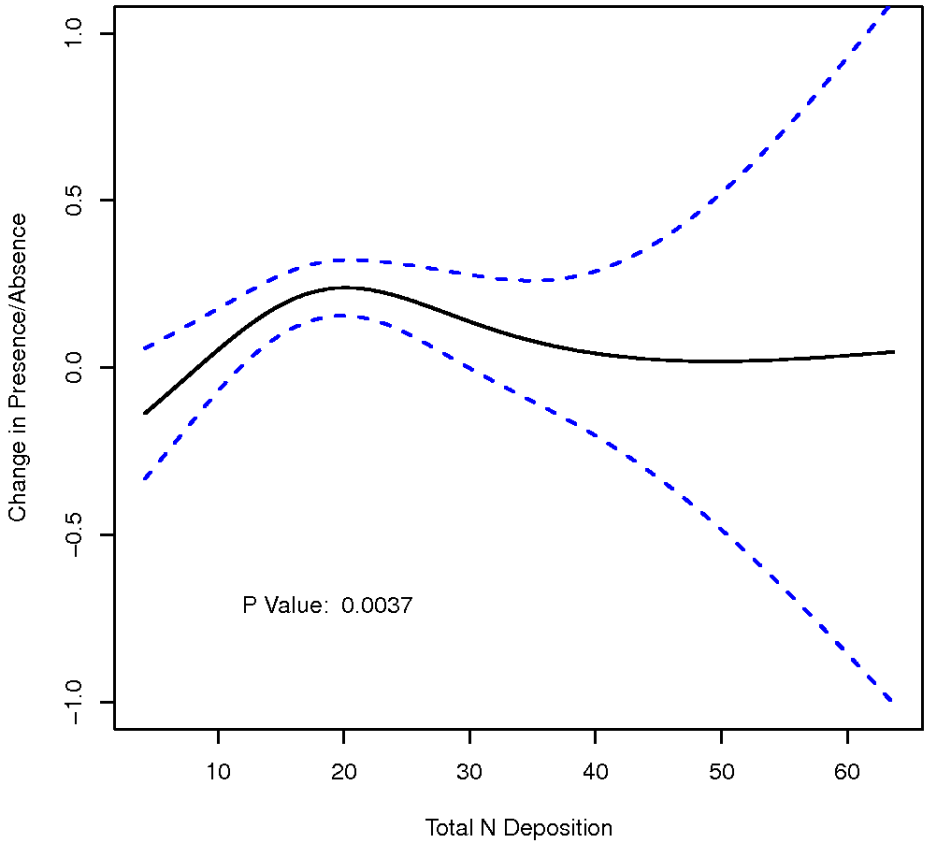

Figure A1.32. Temporal change in the probability of presence of *Senecio sylvaticus* between survey periods (1930-1969, and 1987-1999) against total current inorganic N deposition (kg N ha^{-1} yr^{-1}) for hectads in lowland acid grassland. Data from Vascular Plant Database.

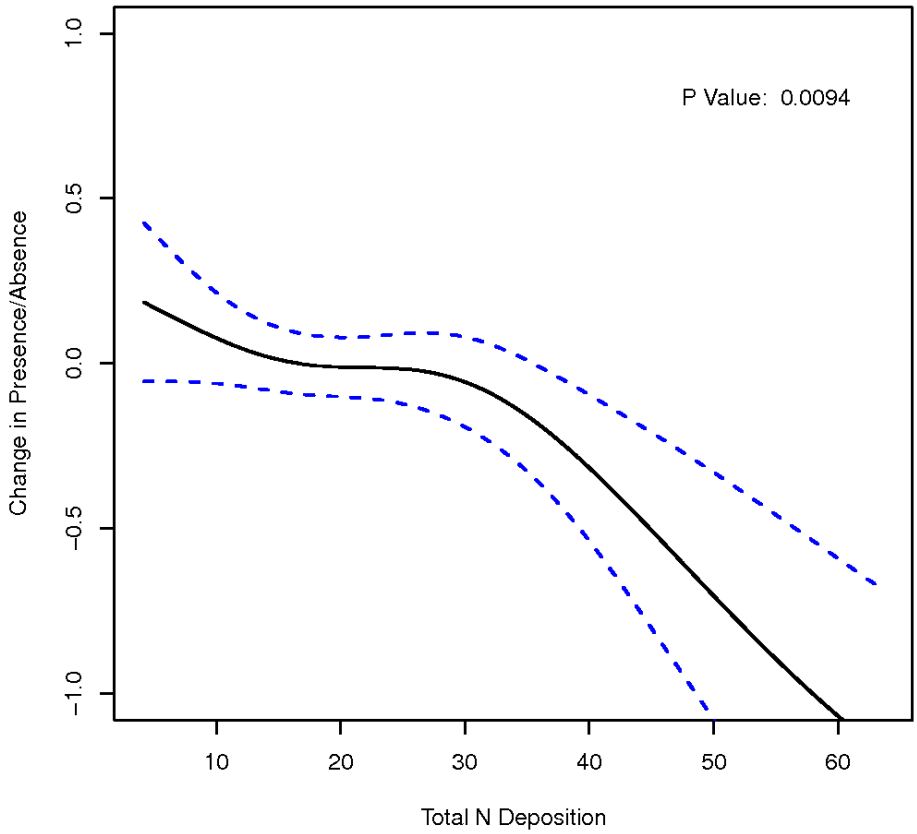

Figure A1.33. Temporal change in the probability of presence of *Trifolium arvense* between survey periods (1930-1969, and 1987-1999) against total current inorganic N deposition (kg N ha^{-1} yr^{-1}) for hectads in lowland acid grassland. Data from Vascular Plant Database.

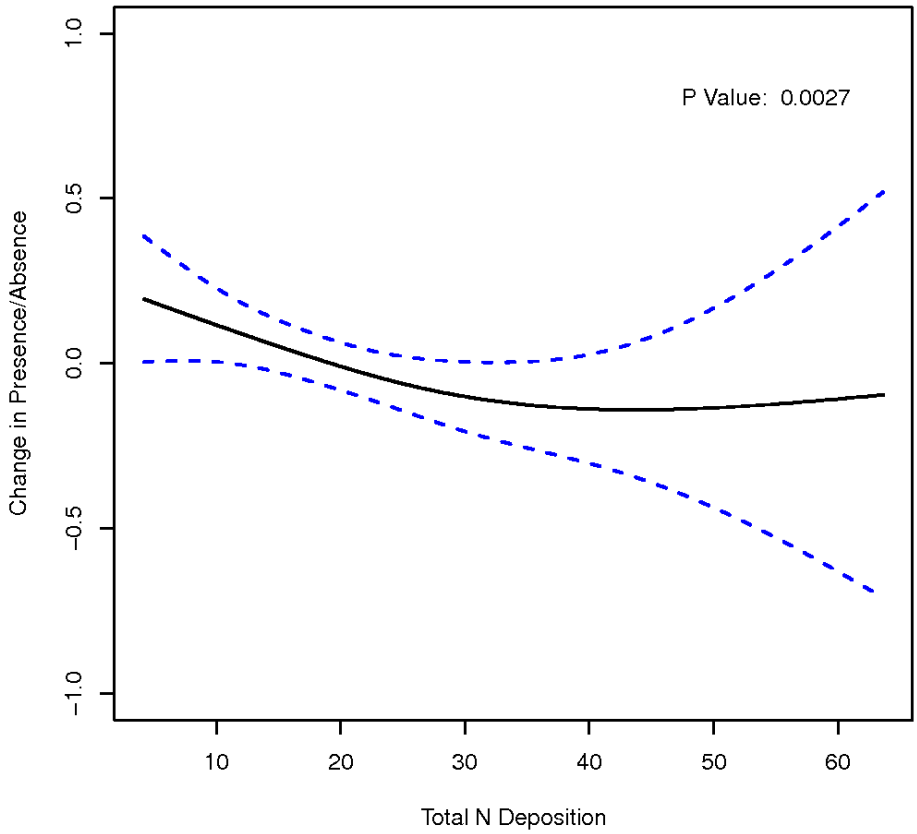

Figure A1.34. Temporal change in the probability of presence of *Trifolium micranthum* between survey periods (1930-1969, and 1987-1999) against total current inorganic N deposition (kg N ha^{-1} yr^{-1}) for hectads in lowland acid grassland. Data from Vascular Plant Database.

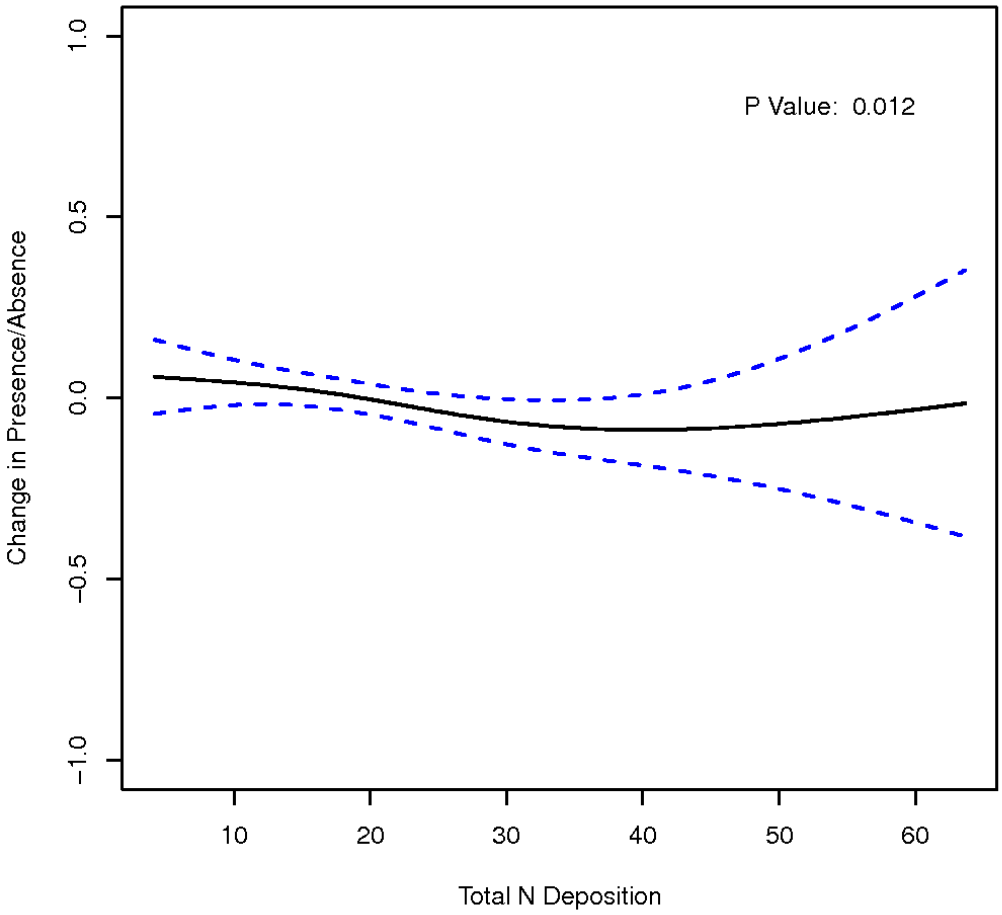

Figure A1.35. Temporal change in the probability of presence of *Trifolium ornithopodioides* between survey periods (1930-1969, and 1987-1999) against total current inorganic N deposition (kg N ha^{-1} yr^{-1}) for hectads in lowland acid grassland. Data from Vascular Plant Database.

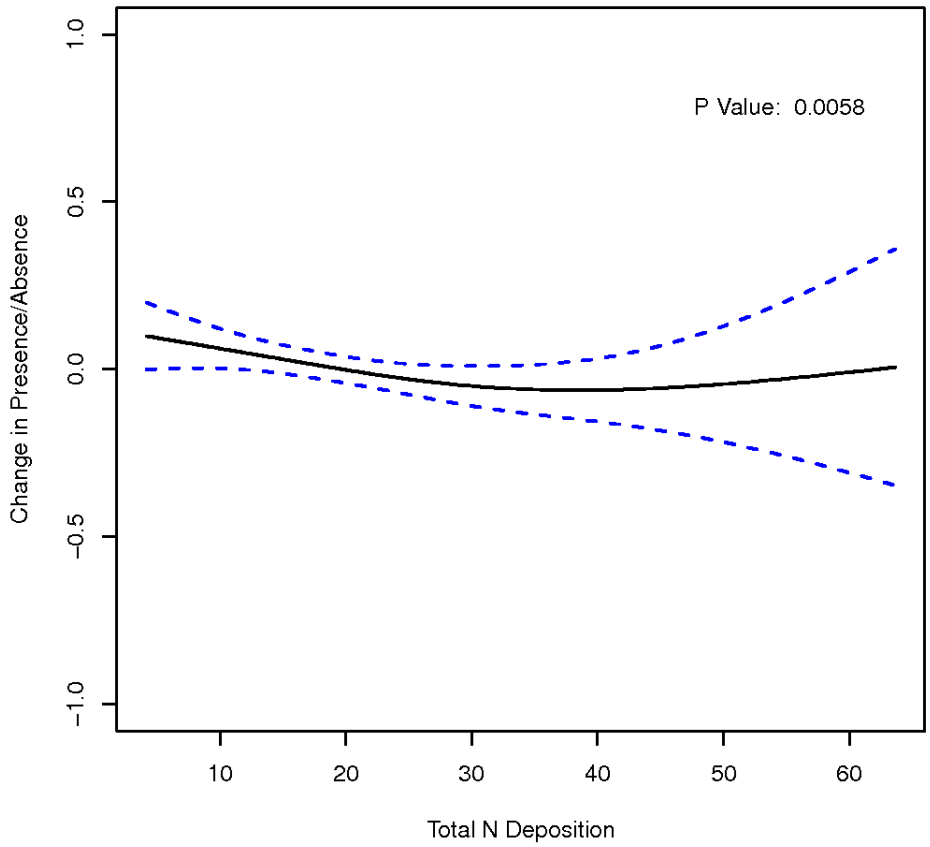

Figure A1.36. Temporal change in the probability of presence of *Trifolium subterraneum* between survey periods (1930-1969, and 1987-1999) against total current inorganic N deposition (kg N ha^{-1} yr^{-1}) for hectads in lowland acid grassland. Data from Vascular Plant Database.

Calcareous grassland – lowland

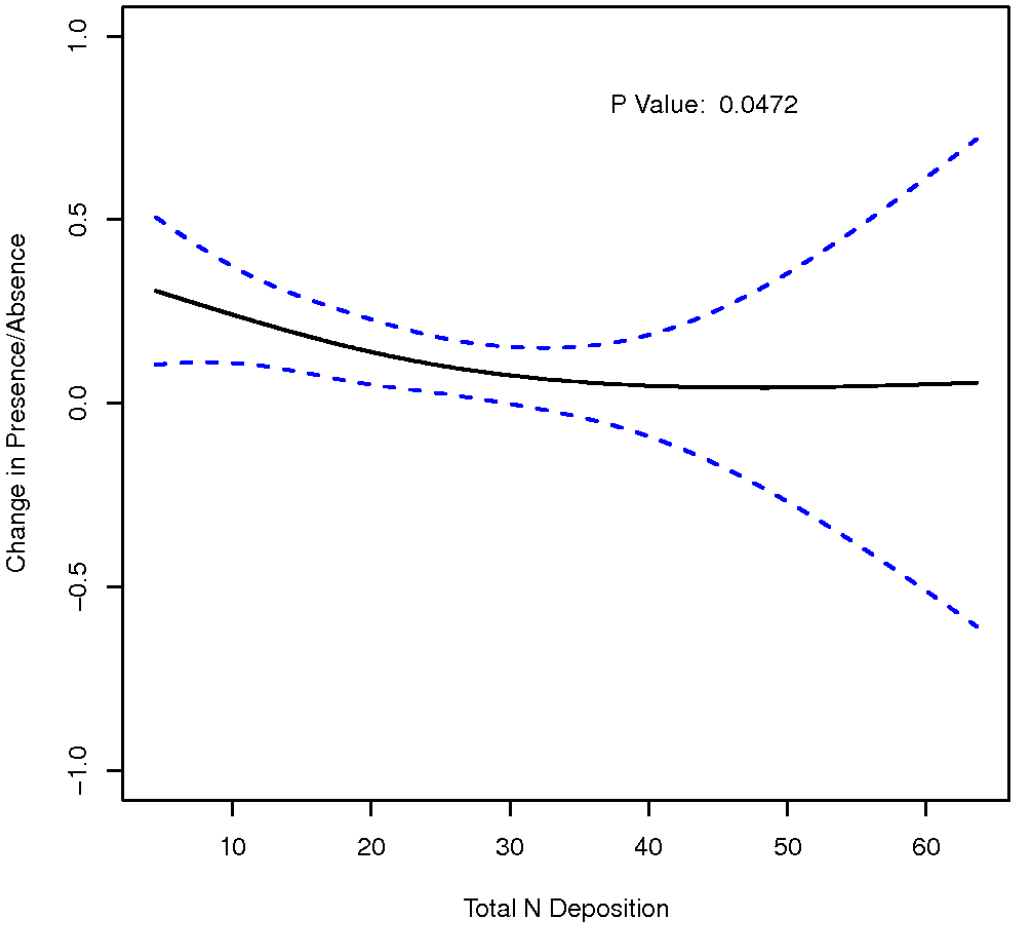

Figure A1.37. Temporal change in the probability of presence of *Anacamptis pyramidalis* between survey periods (1930-1969, and 1987-1999) against total current inorganic N deposition (kg N ha^{-1} yr^{-1}) for hectads in lowland calcareous grassland. Data from Vascular Plant Database.

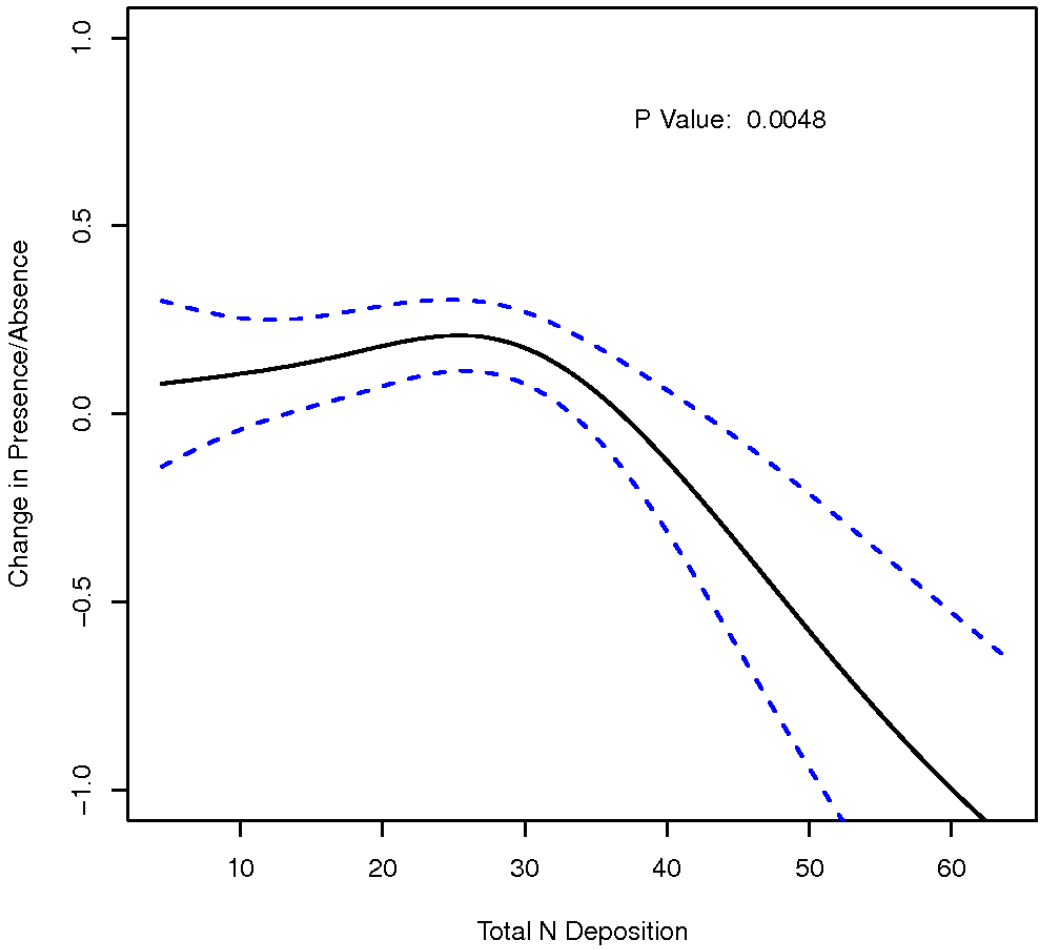

Figure A1.38. Temporal change in the probability of presence of *Carex spicata* between survey periods (1930-1969, and 1987-1999) against total current inorganic N deposition (kg N ha^{-1} yr^{-1}) for hectads in lowland calcareous grassland. Data from Vascular Plant Database.

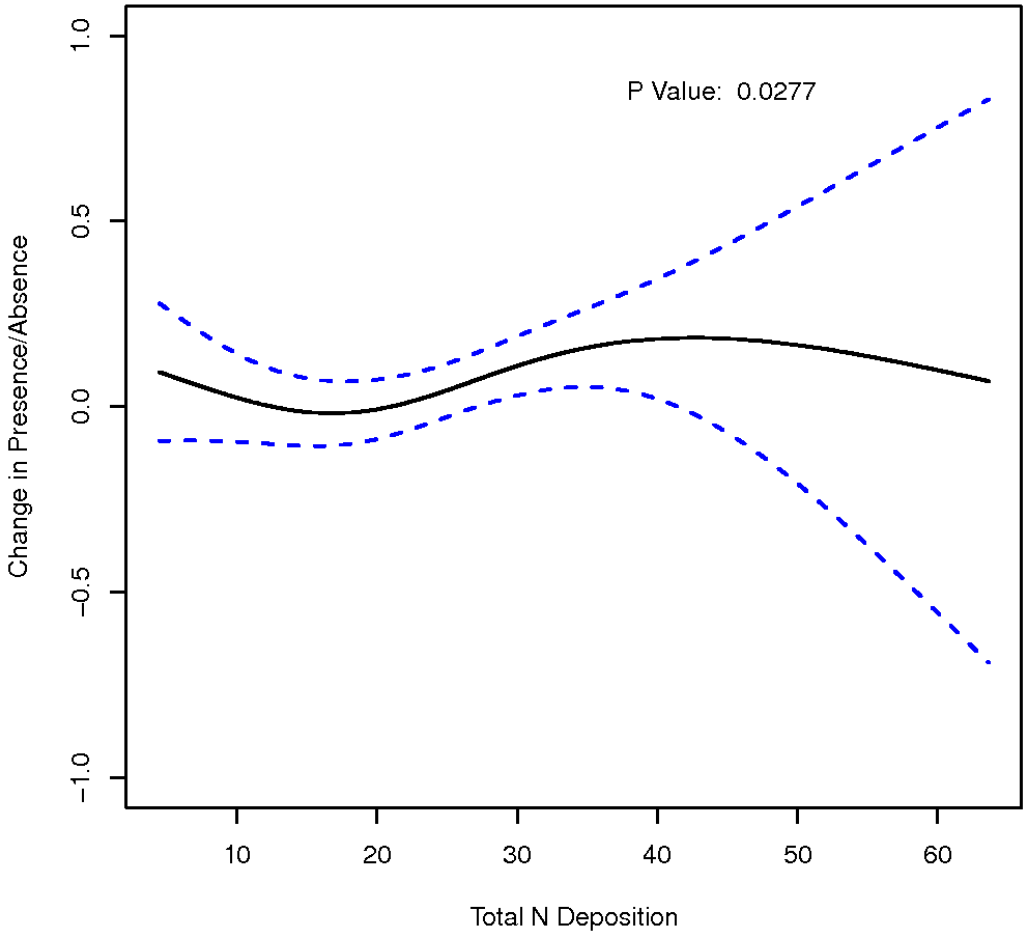

Figure A1.39. Temporal change in the probability of presence of *Centaurea scabiosa* between survey periods (1930-1969, and 1987-1999) against total current inorganic N deposition (kg N ha^{-1} yr^{-1}) for hectads in lowland calcareous grassland. Data from Vascular Plant Database.

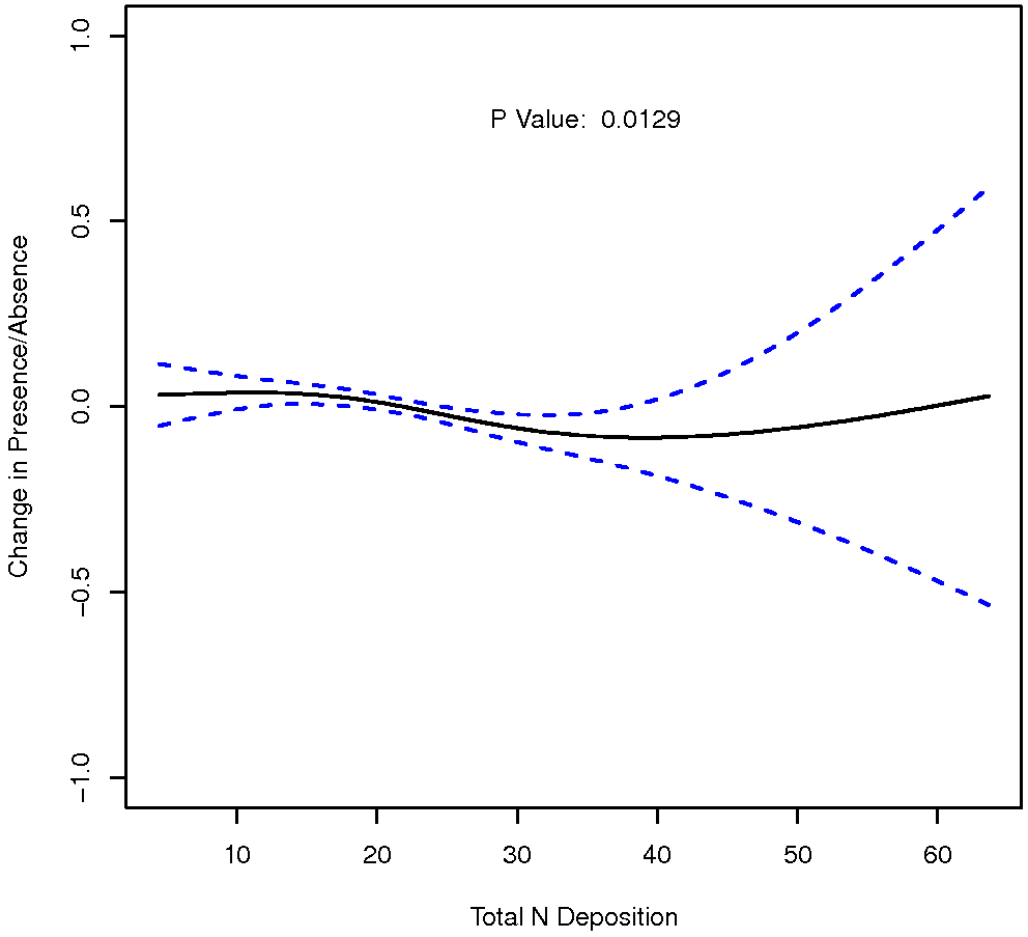

Figure A1.40. Temporal change in the probability of presence of *Convallaria majalis* between survey periods (1930-1969, and 1987-1999) against total current inorganic N deposition (kg N ha^{-1} yr^{-1}) for hectads in lowland calcareous grassland. Data from Vascular Plant Database.

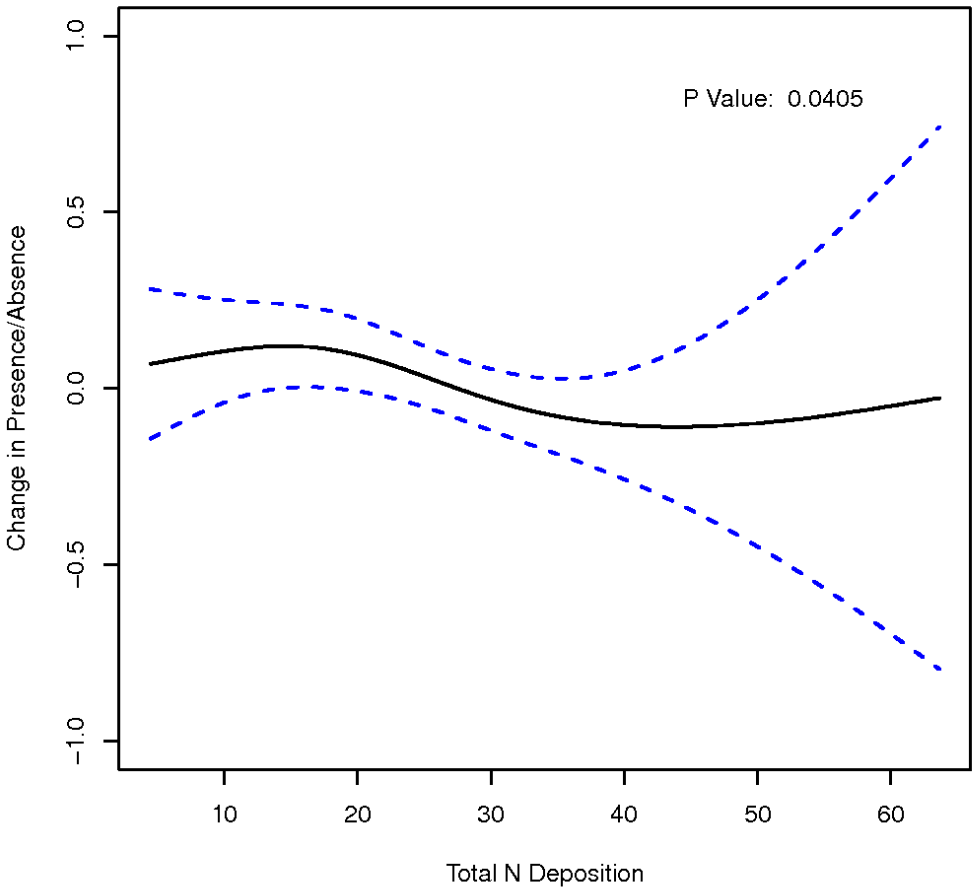

Figure A1.41. Temporal change in the probability of presence of *Orchis morio* between survey periods (1930-1969, and 1987-1999) against total current inorganic N deposition (kg N ha^{-1} yr^{-1}) for hectads in lowland calcareous grassland. Data from Vascular Plant Database.

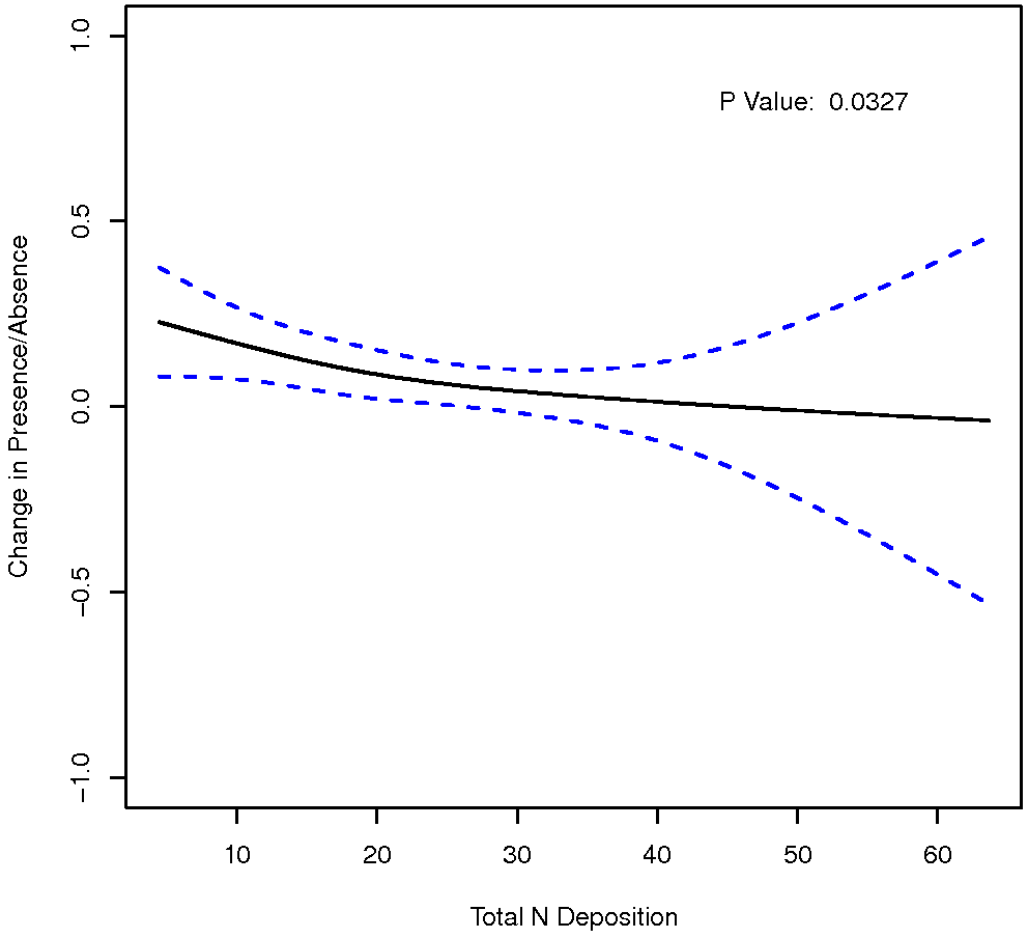

Figure A1.42. Temporal change in the probability of presence of *Rosa rubiginosa* between survey periods (1930-1969, and 1987-1999) against total current inorganic N deposition (kg N ha^{-1} yr^{-1}) for hectads in lowland calcareous grassland. Data from Vascular Plant Database.

Calcareous grassland – upland

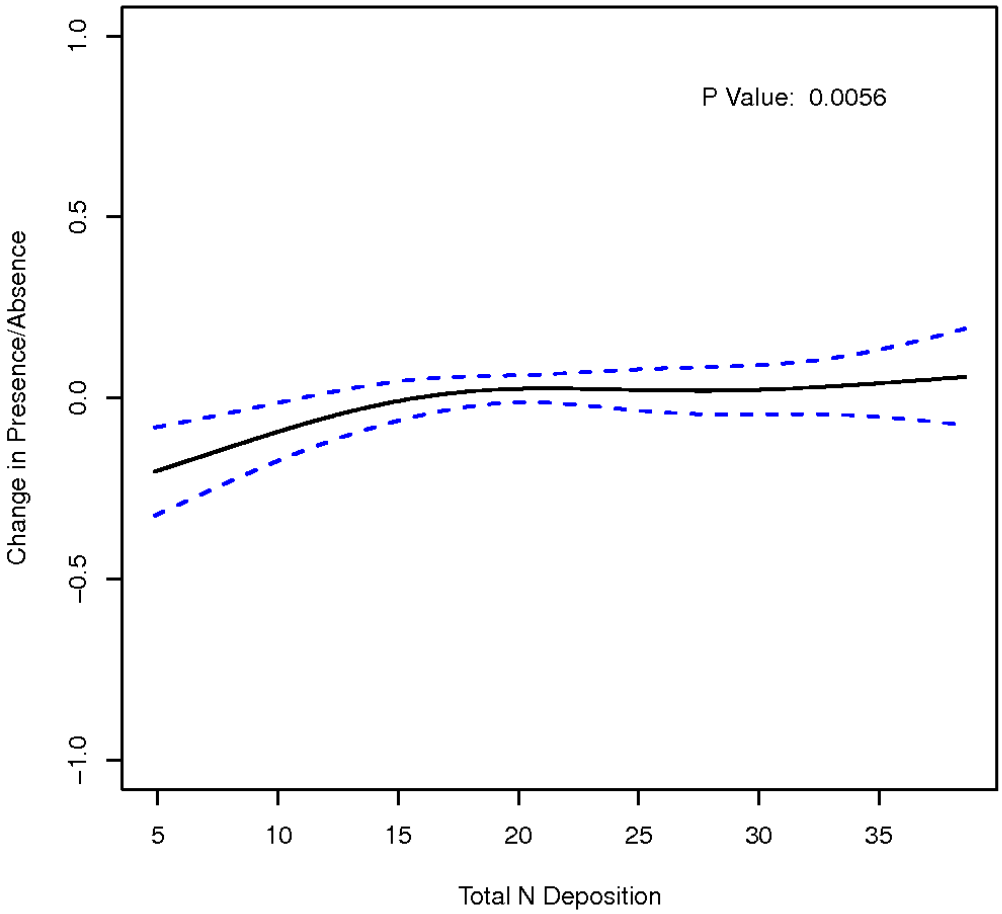

Figure A1.43. Temporal change in the probability of presence of *Alchemilla alpina* between survey periods (1930-1969, and 1987-1999) against total current inorganic N deposition (kg N ha^{-1} yr^{-1}) for hectads in upland calcareous grassland. Data from Vascular Plant Database.

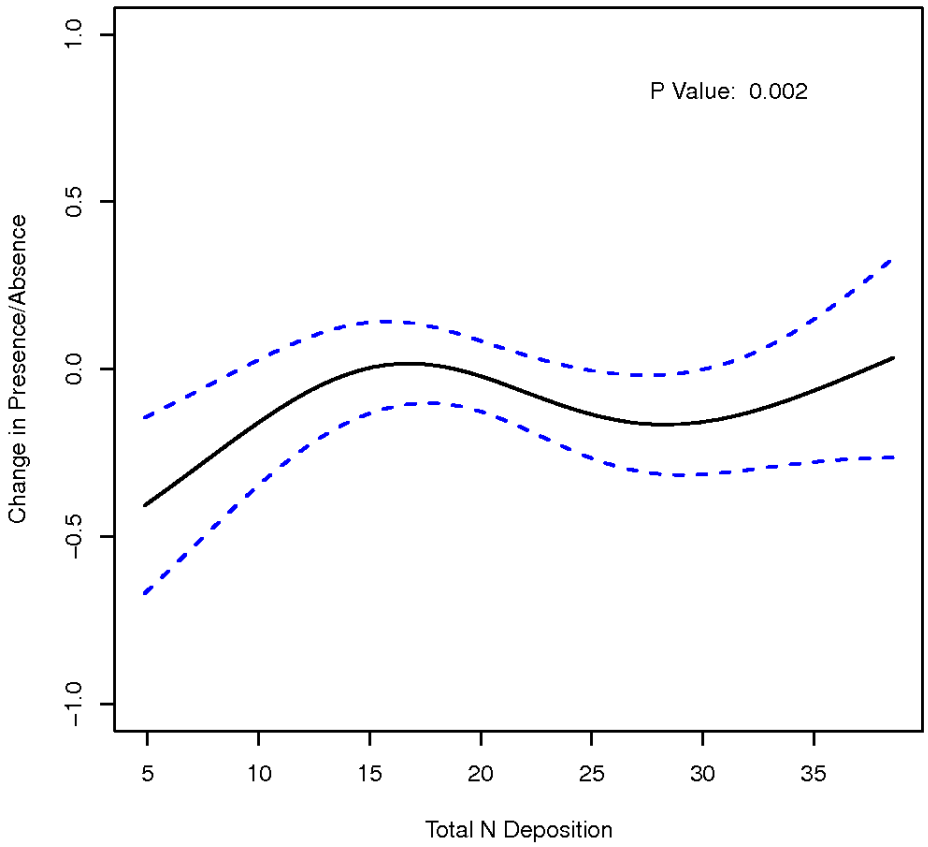

Figure A1.44. Temporal change in the probability of presence of *Melica nutans* between survey periods (1930-1969, and 1987-1999) against total current inorganic N deposition (kg N ha^{-1} yr^{-1}) for hectads in upland calcareous grassland. Data from Vascular Plant Database.

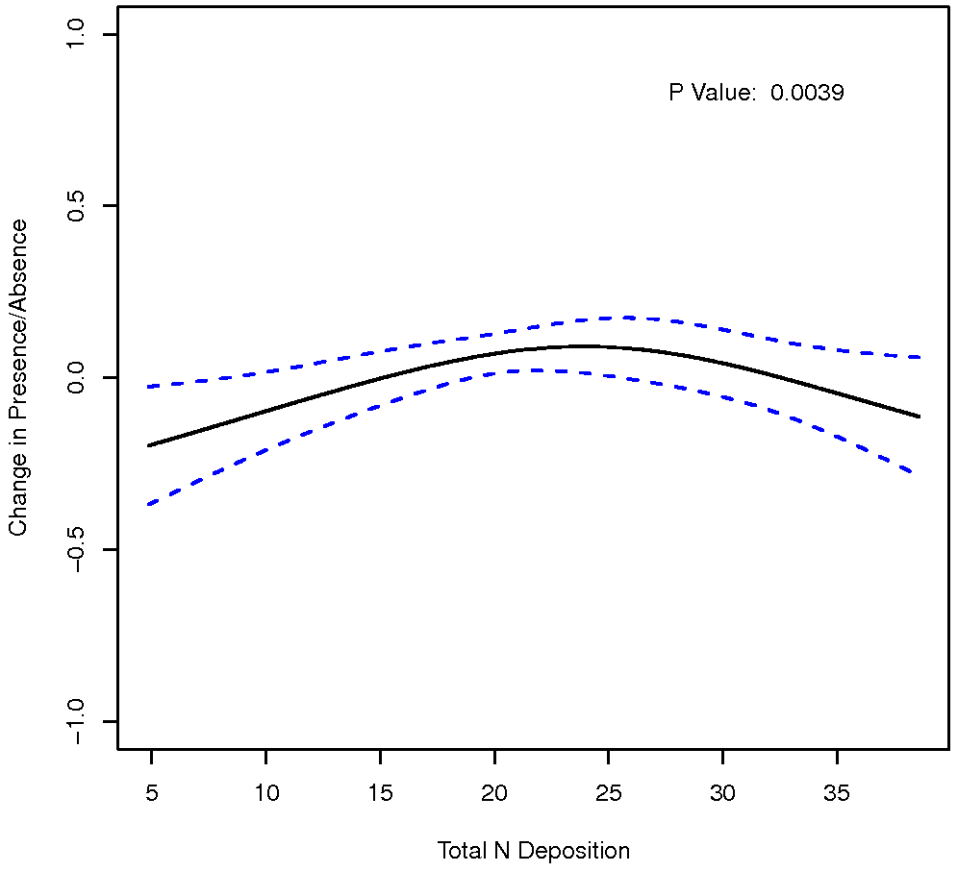

Figure A1.45. Temporal change in the probability of presence of *Persicaria vivipara* between survey periods (1930-1969, and 1987-1999) against total current inorganic N deposition (kg N ha^{-1} yr^{-1}) for hectads in upland calcareous grassland. Data from Vascular Plant Database.

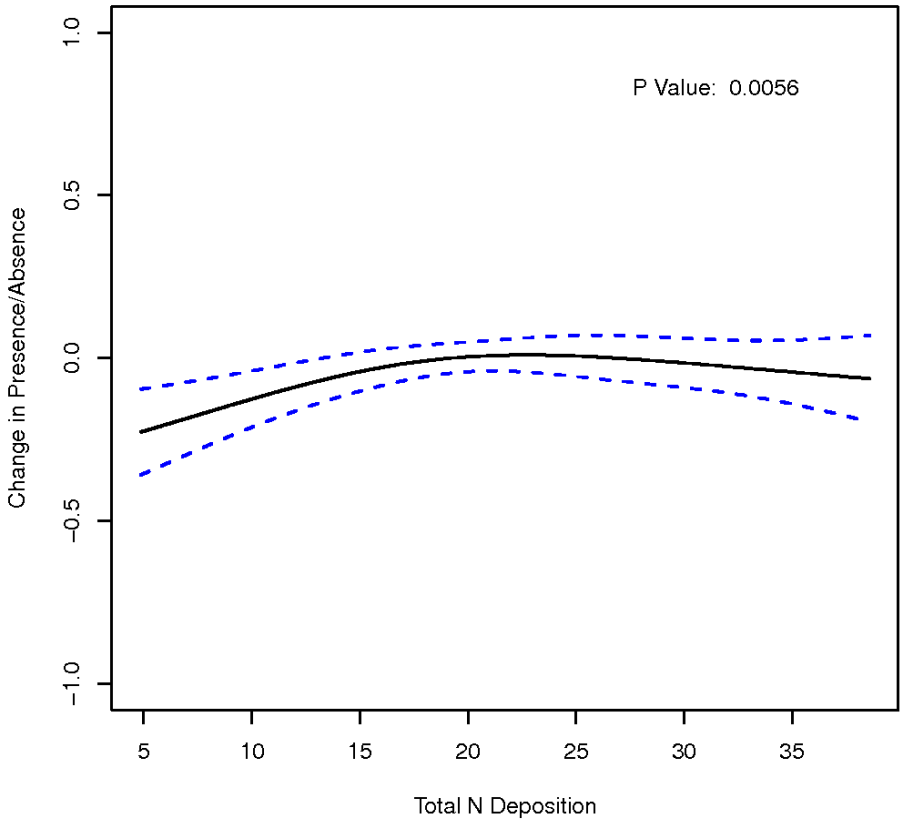

Figure A1.46. Temporal change in the probability of presence of *Saussurea alpina* between survey periods (1930-1969, and 1987-1999) against total current inorganic N deposition (kg N ha^{-1} yr^{-1}) for hectads in upland calcareous grassland. Data from Vascular Plant Database.

Bogs – upland

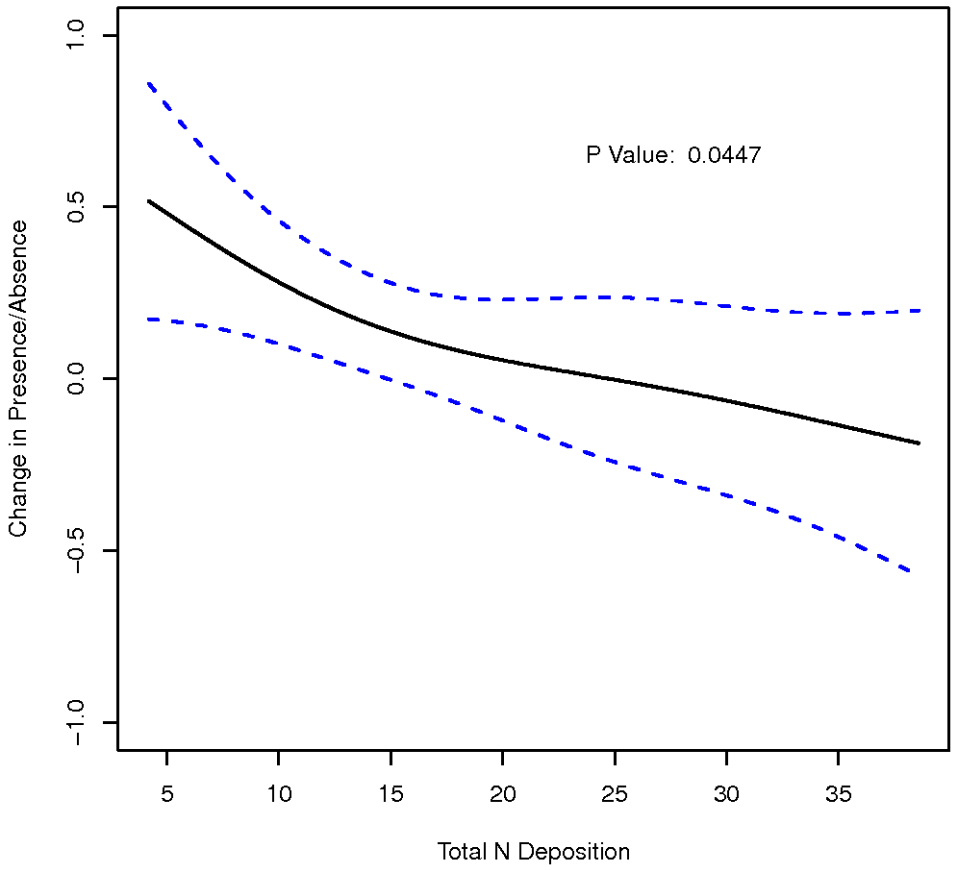

Figure A1.47. Temporal change in the probability of presence of *Carex limosa* between survey periods (1930-1969, and 1987-1999) against total current inorganic N deposition (kg N ha^{-1} yr^{-1}) for hectads in upland bog. Data from Vascular Plant Database.

Heathland – upland

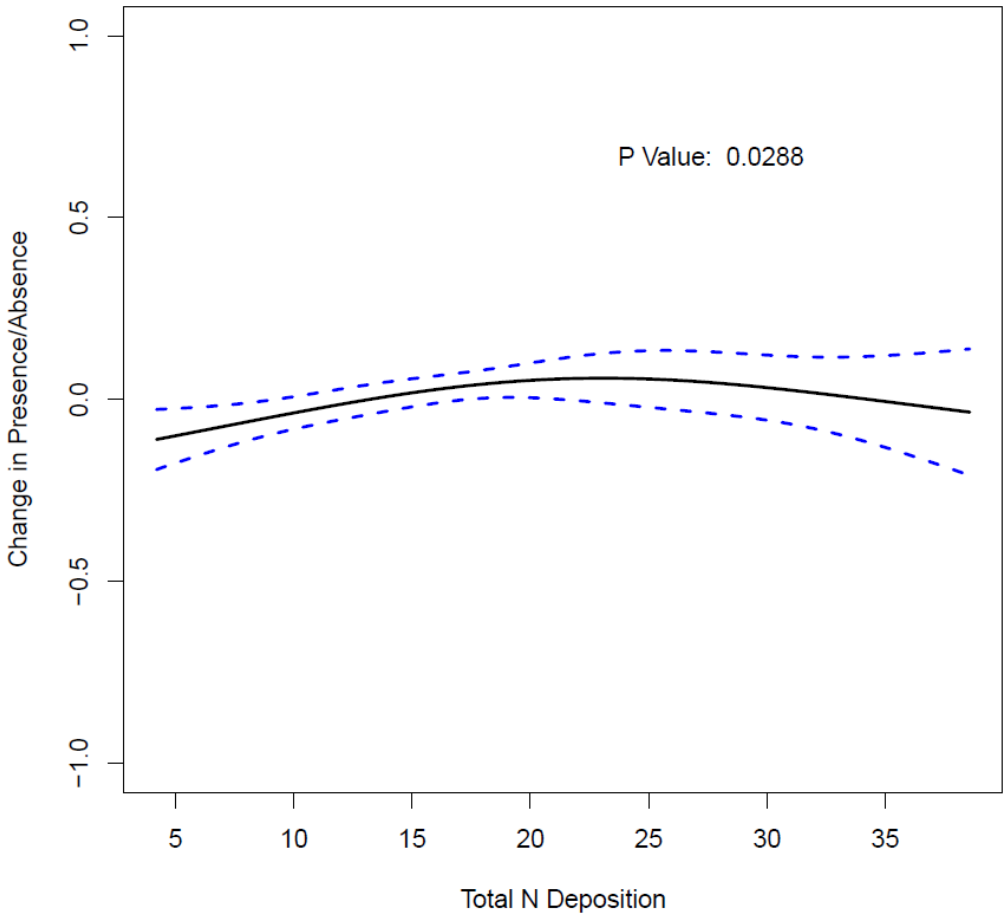

Figure A1.48. Temporal change in the probability of presence of *Cryptogramma crispa* between survey periods (1930-1969, and 1987-1999) against total current inorganic N deposition (kg N ha^{-1} yr^{-1}) for hectads in upland heathland. Data from Vascular Plant Database.

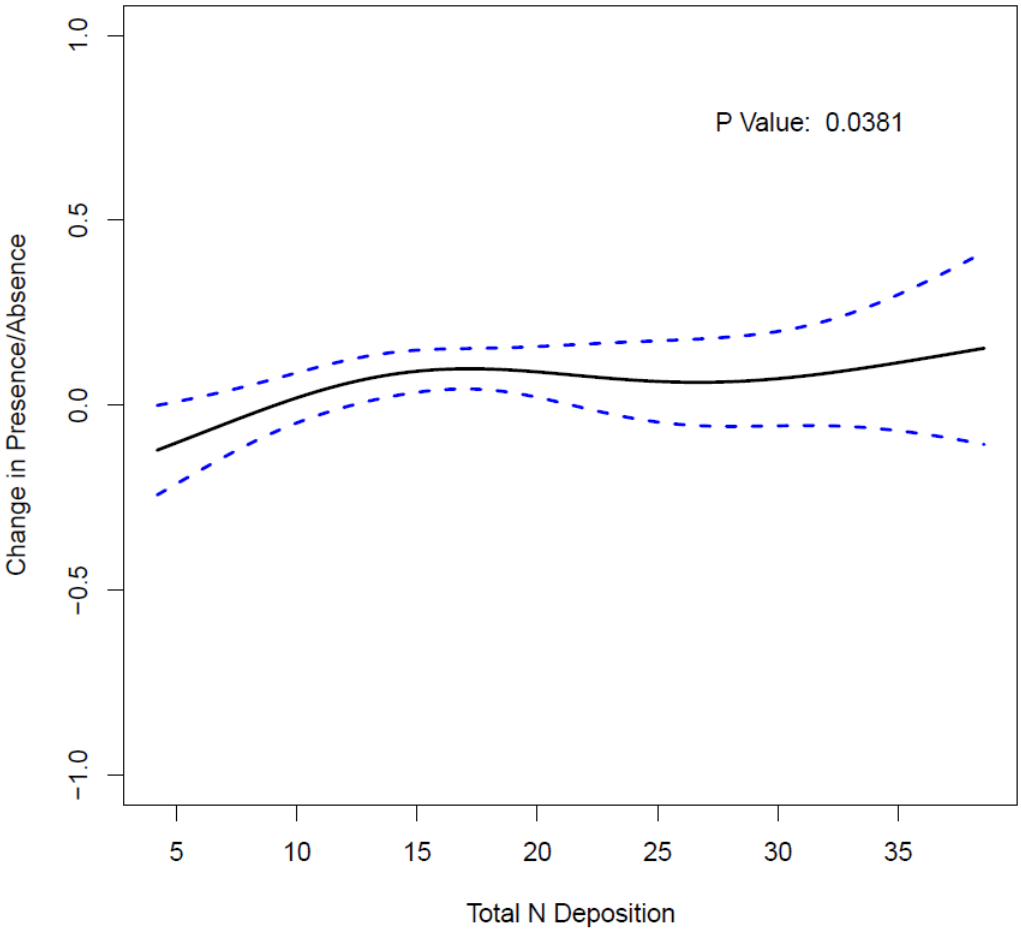

Figure A1.49. Temporal change in the probability of presence of *Lycopodium clavatum* between survey periods (1930-1969, and 1987-1999) against total current inorganic N deposition (kg N ha^{-1} yr^{-1}) for hectads in upland heathland. Data from Vascular Plant Database.

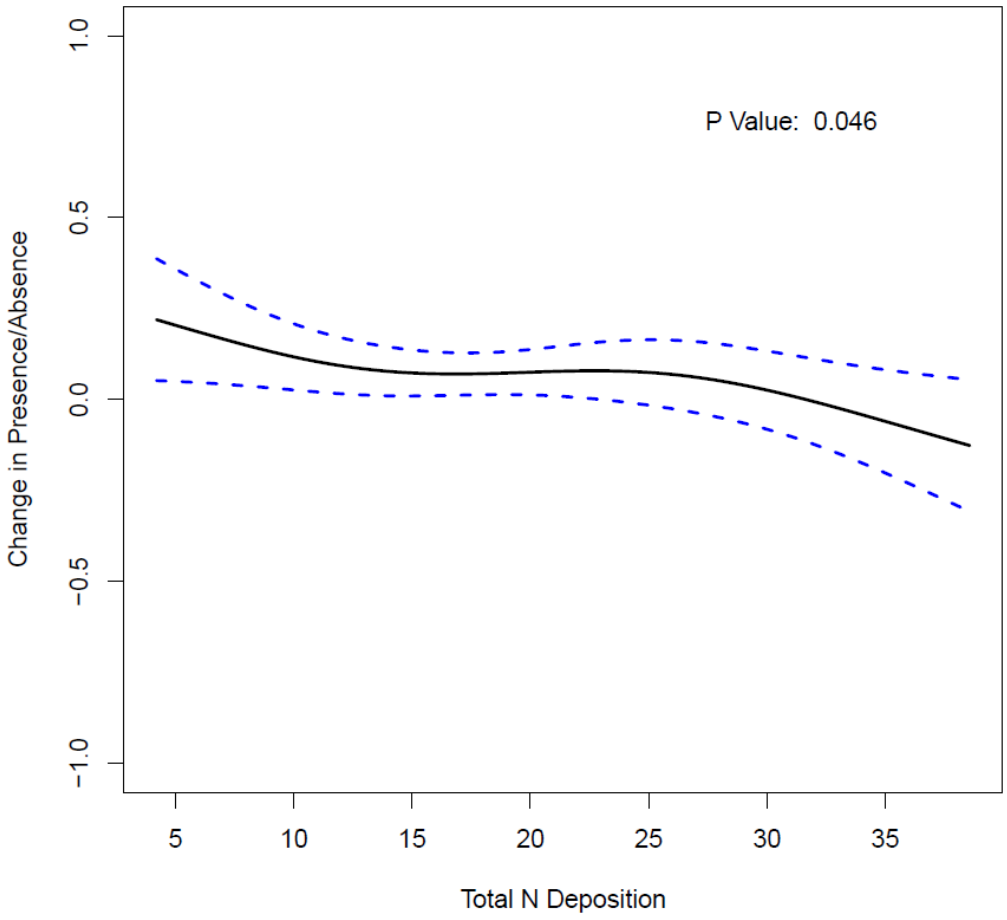

Figure A1.50. Temporal change in the probability of presence of *Rubus chamaemorus* between survey periods (1930-1969, and 1987-1999) against total current inorganic N deposition (kg N ha^{-1} yr^{-1}) for hectads in upland heathland. Data from Vascular Plant Database.

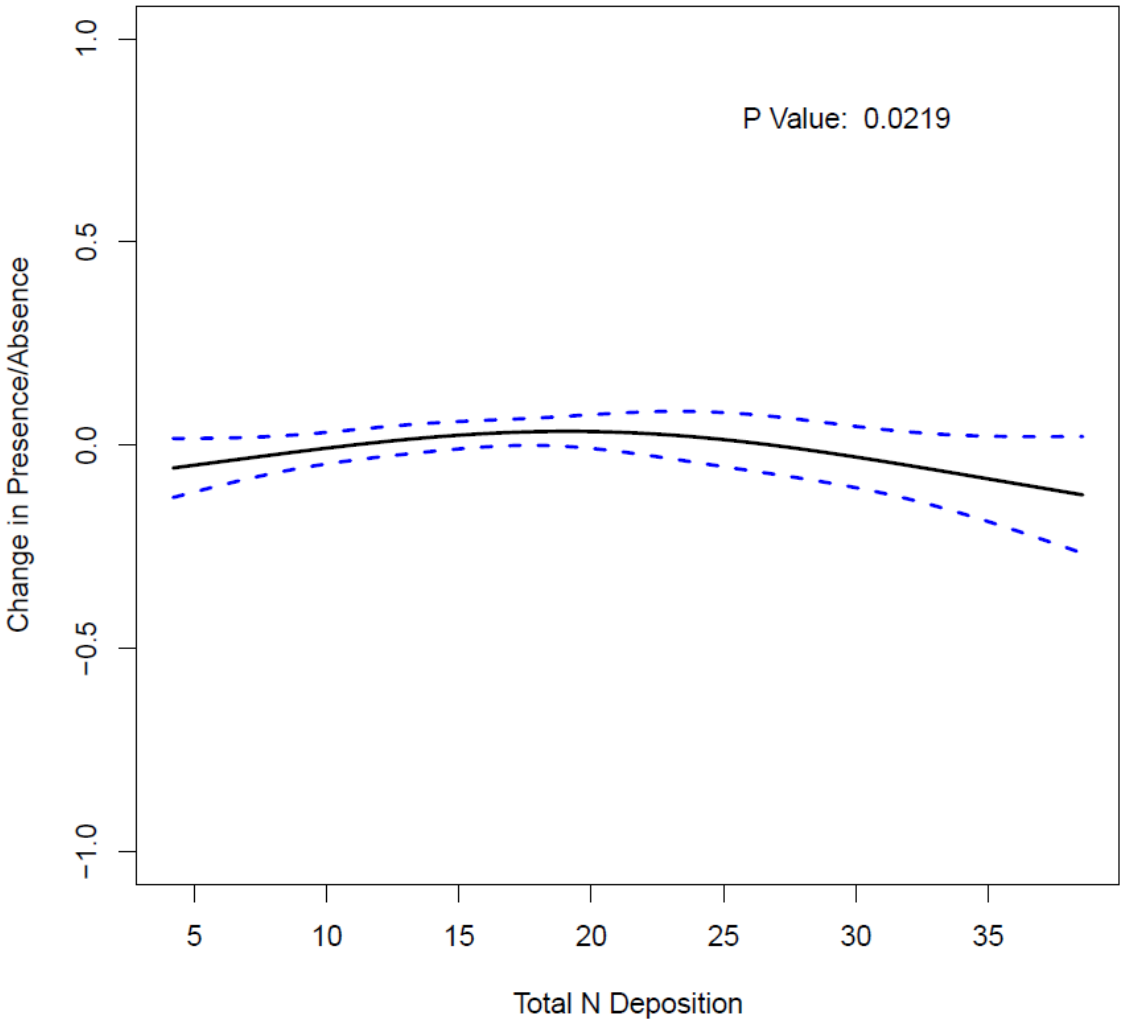

Figure A1.51. Temporal change in the probability of presence of *Trientalis europaea* between survey periods (1930-1969, and 1987-1999) against total current inorganic N deposition (kg N ha^{-1} yr^{-1}) for hectads in upland heathland. Data from Vascular Plant Database.

Electronic appendix 2

BSBI Local Change survey

Spatial analysis

Acid grassland - upland

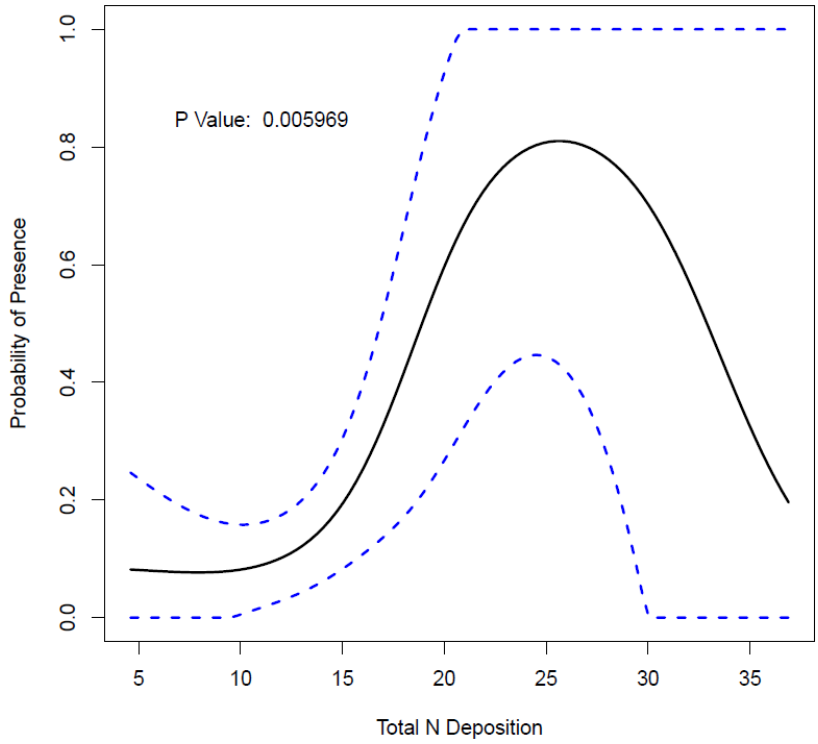

Figure A2.1. Spatial change in the probability of presence of *Agrostis vinealis* in upland acid grassland with increasing total current inorganic N deposition (kg N ha^{-1} yr^{-1}). Data from BSBI Local Change.

Calcareous grassland - lowland

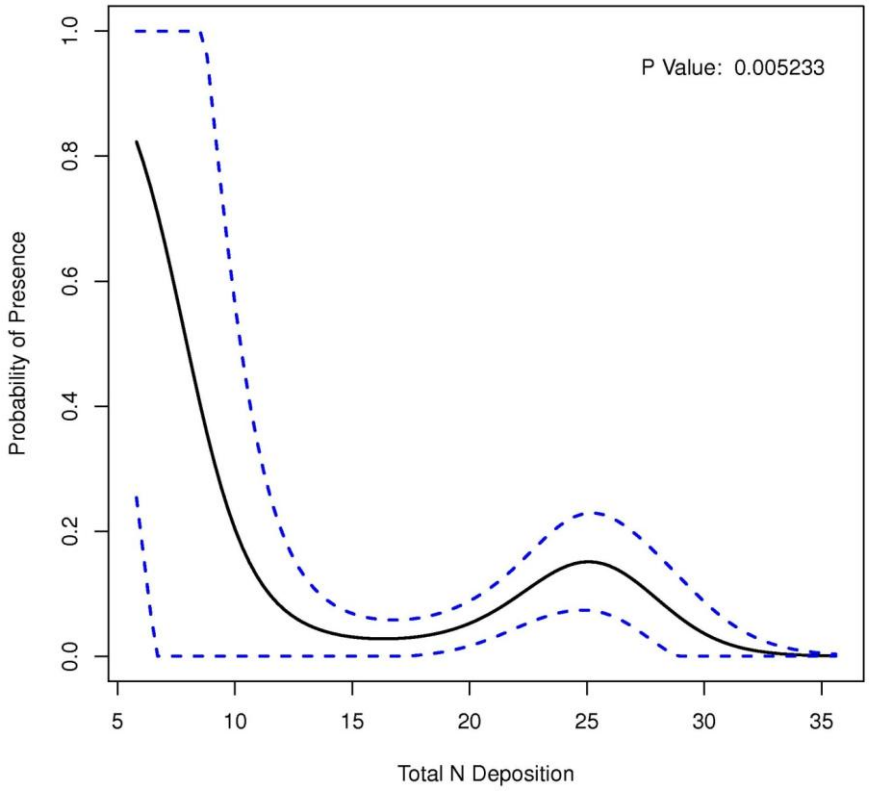

Figure A2.2. Spatial change in the probability of presence of *Bromopsis erecta* in lowland calcareous grassland with increasing total current inorganic N deposition (kg N ha^{-1} yr^{-1}). Data from BSBI Local Change.

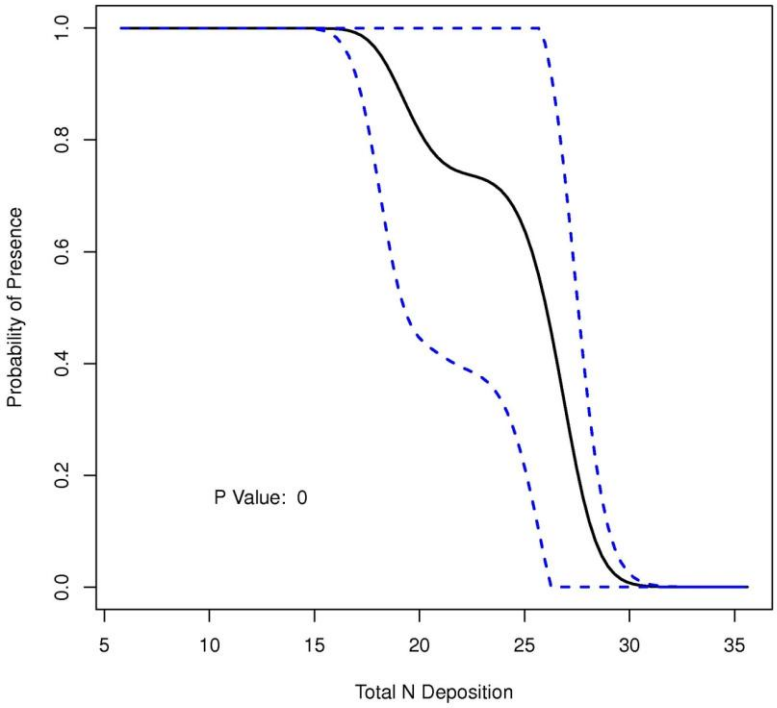

Figure A2.3. Spatial change in the probability of presence of *Campanula glomerata* in lowland calcareous grassland with increasing total current inorganic N deposition (kg N ha^{-1} yr^{-1}). Data from BSBI Local Change.

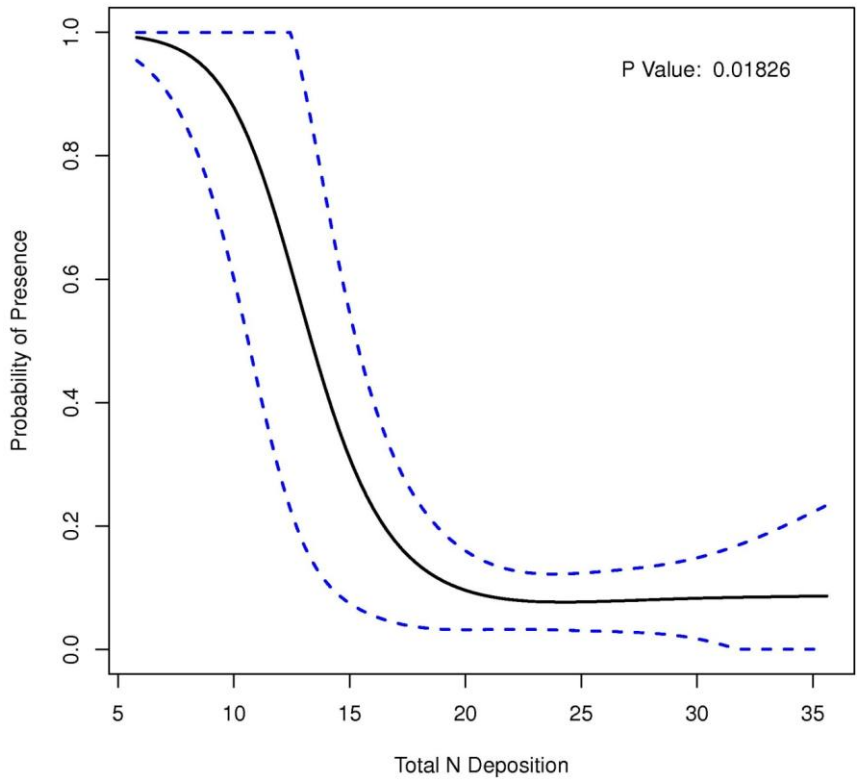

Figure A2.4. Spatial change in the probability of presence of *Carex spicata* in lowland calcareous grassland with increasing total current inorganic N deposition (kg N ha^{-1} yr^{-1}). Data from BSBI Local Change.

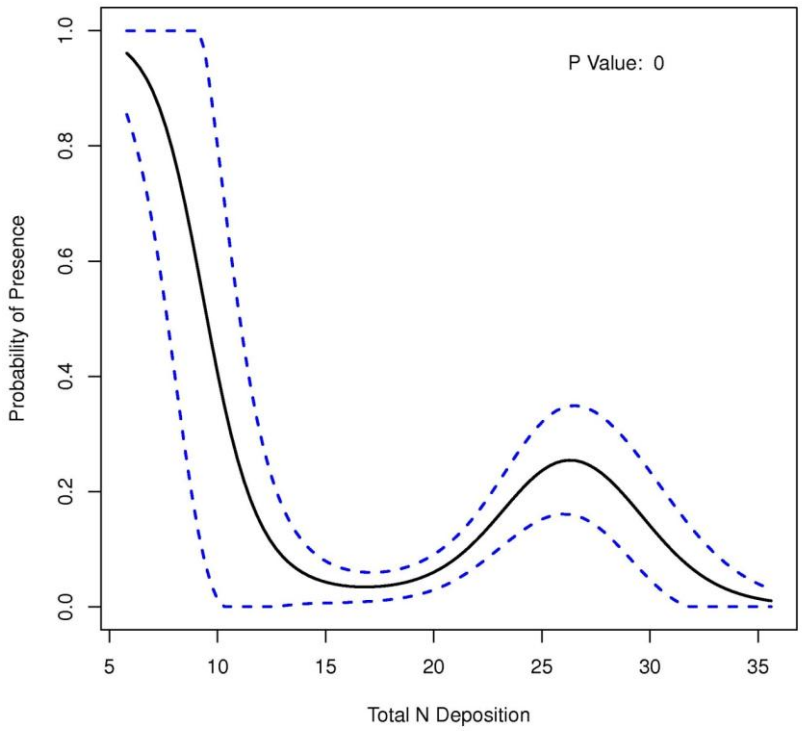

Figure A2.5. Spatial change in the probability of presence of *Centaurea scabiosa* in lowland calcareous grassland with increasing total current inorganic N deposition (kg N ha^{-1} yr^{-1}). Data from BSBI Local Change.

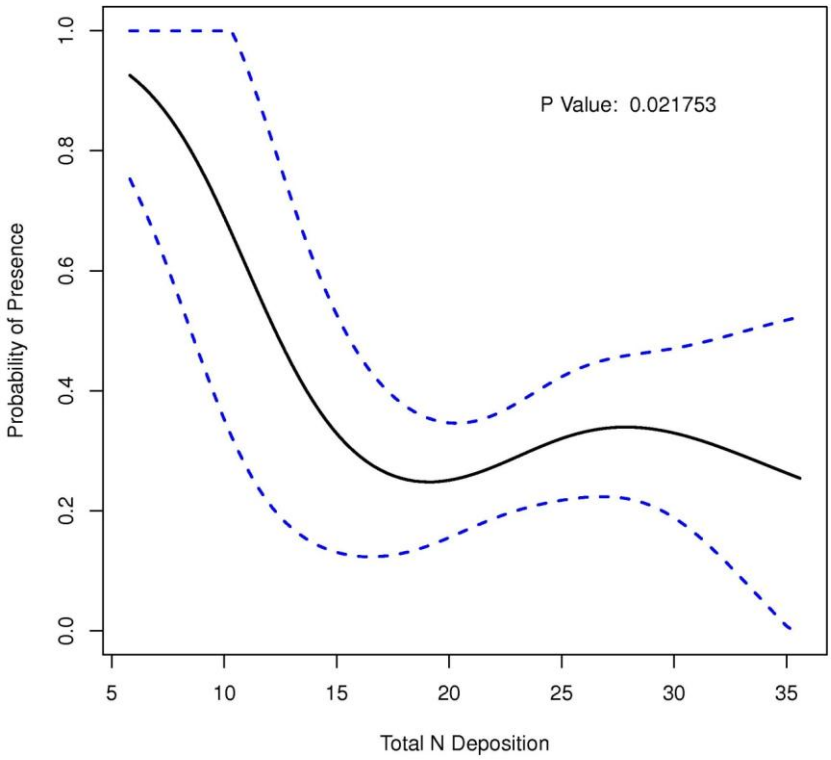

Figure A2.6. Spatial change in the probability of presence of *Daucus carota* in lowland calcareous grassland with increasing total current inorganic N deposition (kg N ha^{-1} yr^{-1}). Data from BSBI Local Change.

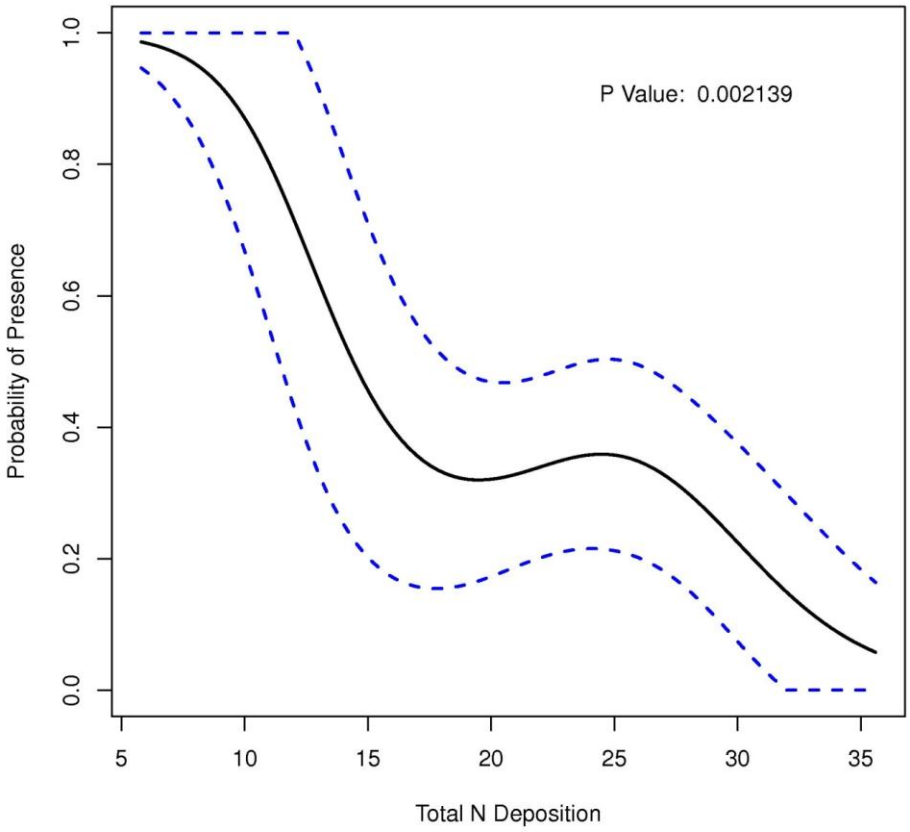

Figure A2.7. Spatial change in the probability of presence of *Ononis repens* in lowland calcareous grassland with increasing total current inorganic N deposition (kg N ha^{-1} yr^{-1}). Data from BSBI Local Change.

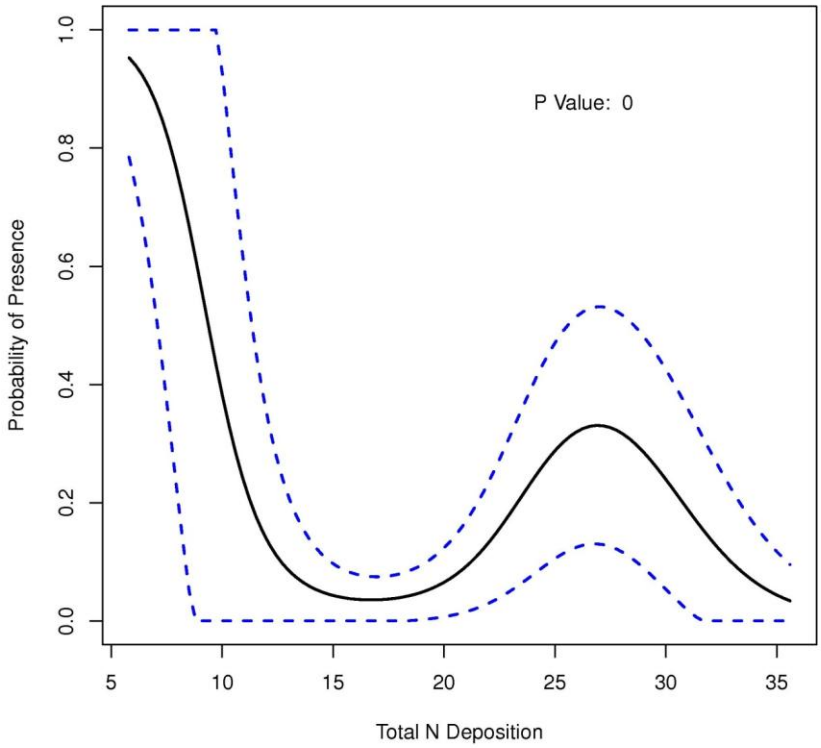

Figure A2.8. Spatial change in the probability of presence of *Sanguisorba minor* in lowland calcareous grassland with increasing total current inorganic N deposition (kg N ha^{-1} yr^{-1}). Data from BSBI Local Change.

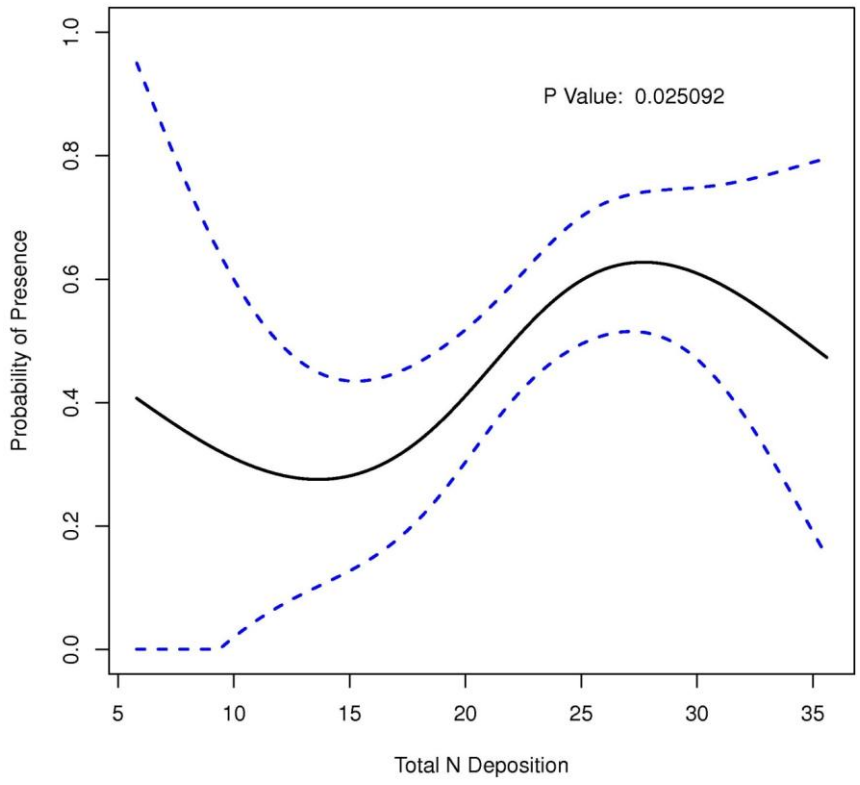

Figure A2.9. Spatial change in the probability of presence of *Viola odorata* in lowland calcareous grassland with increasing total current inorganic N deposition (kg N ha^{-1} yr^{-1}). Data from BSBI Local Change.

Calcareous grassland - upland

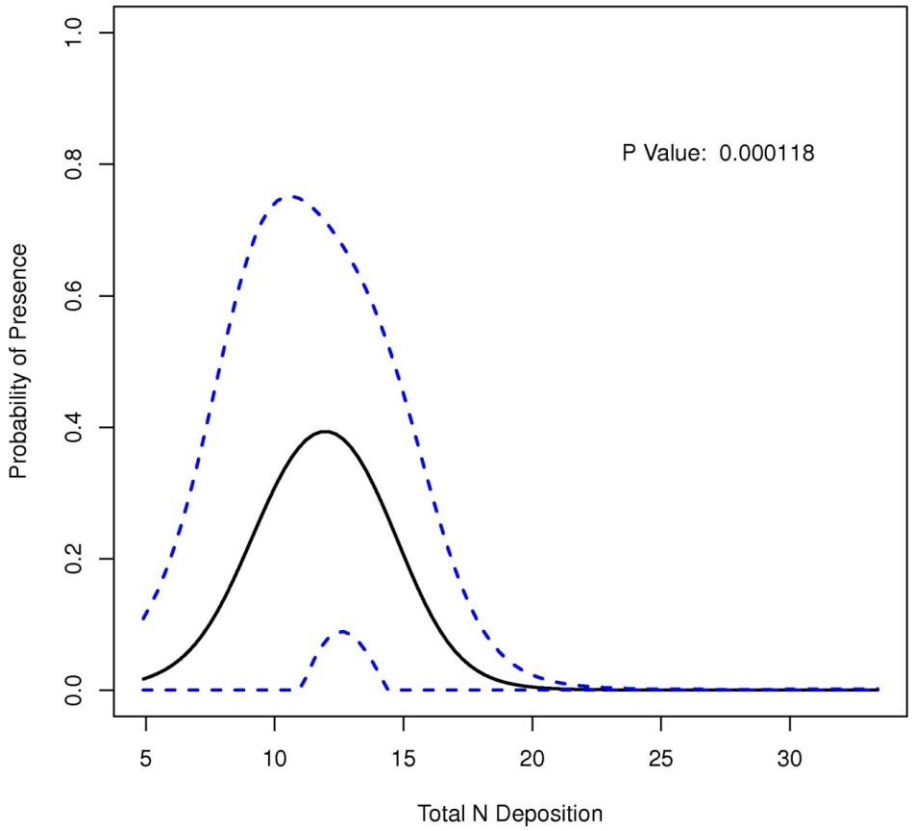

Figure A2.10. Spatial change in the probability of presence of *Persicaria vivipara* in upland calcareous grassland with increasing total current inorganic N deposition (kg N ha^{-1} yr^{-1}). Data from BSBI Local Change.

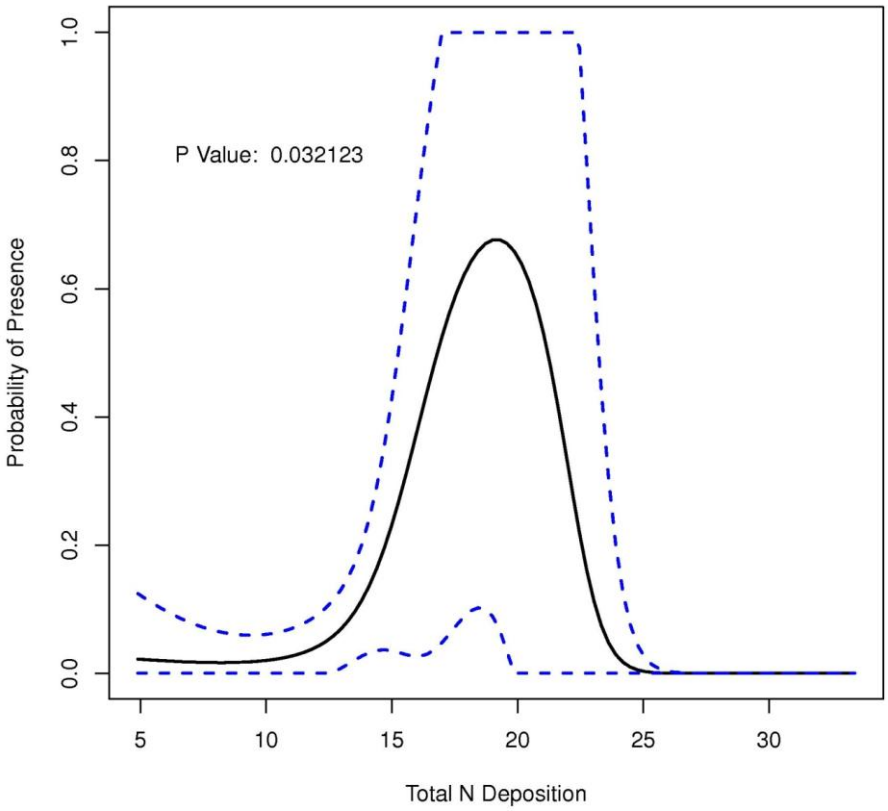

Figure A2.11. Spatial change in the probability of presence of *Rubus saxatilis* in upland calcareous grassland with increasing total current inorganic N deposition (kg N ha^{-1} yr^{-1}). Data from BSBI Local Change.

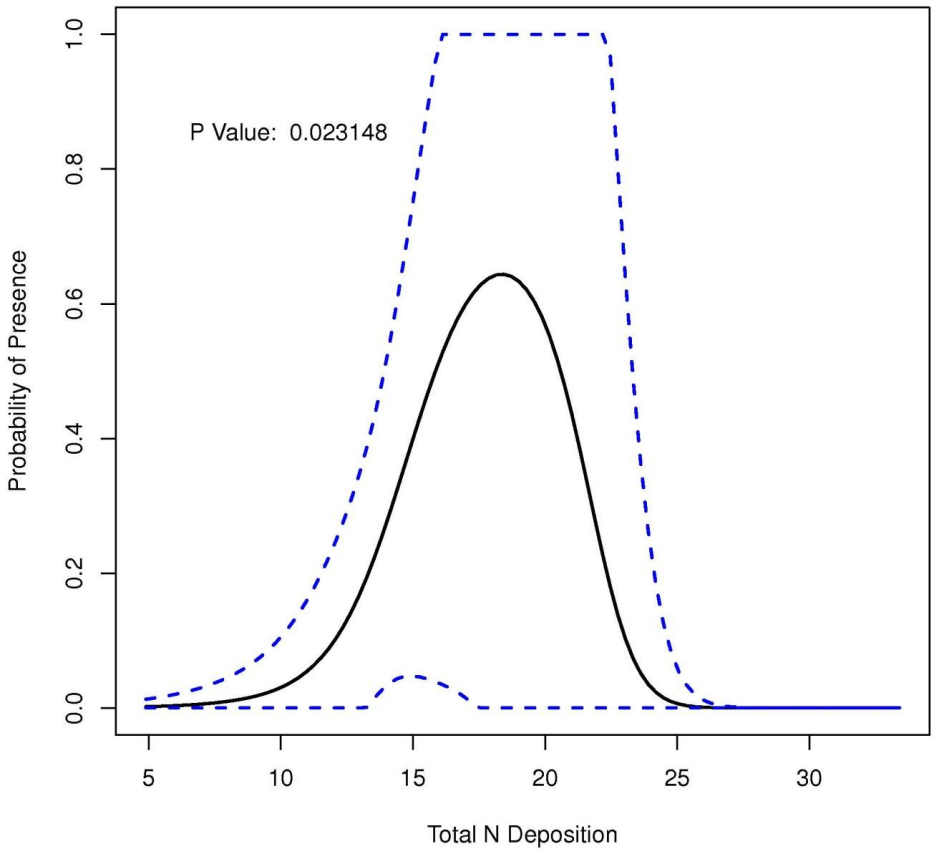

Figure A2.12. Spatial change in the probability of presence of *Thalictrum alpinum* in upland calcareous grassland with increasing total current inorganic N deposition (kg N ha^{-1} yr^{-1}). Data from BSBI Local Change.

Heathland - upland

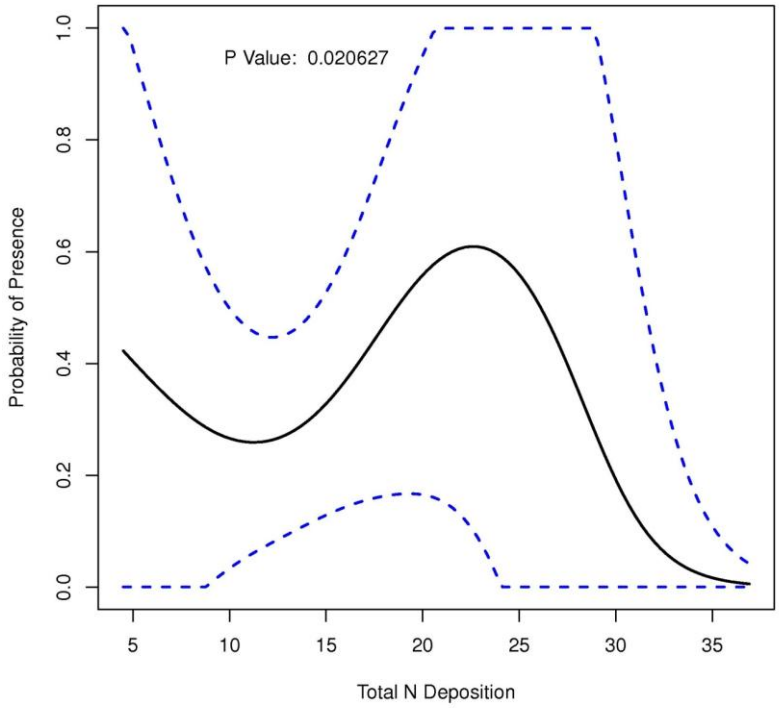

Figure A2.13. Spatial change in the probability of presence of *Agrostis vinealis* in upland heathland with increasing total current inorganic N deposition (kg N ha^{-1} yr^{-1}). Data from BSBI Local Change.

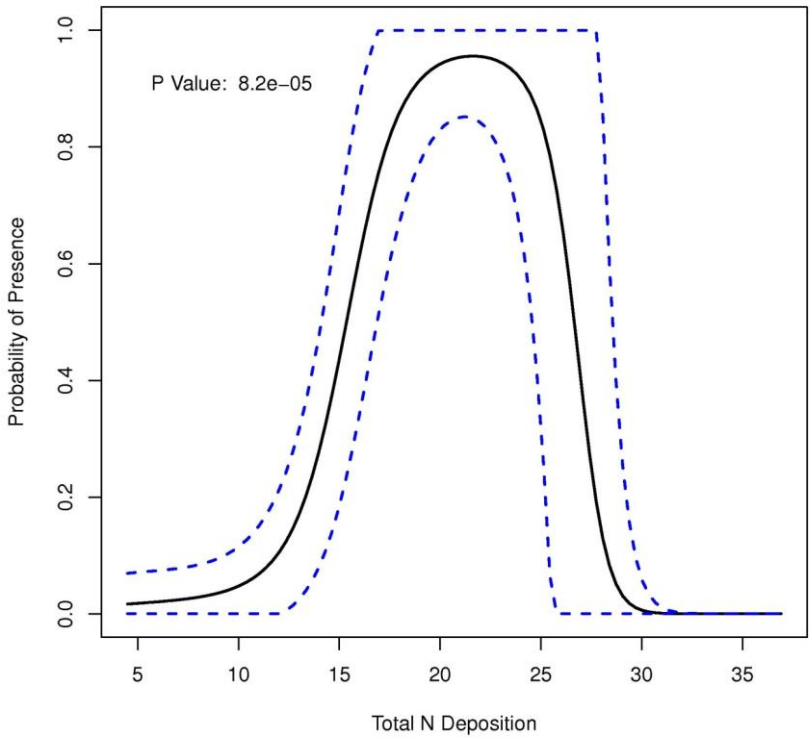

Figure A2.14. Spatial change in the probability of presence of *Listera cordata* in upland heathland with increasing total current inorganic N deposition (kg N ha^{-1} yr^{-1}). Data from BSBI Local Change.

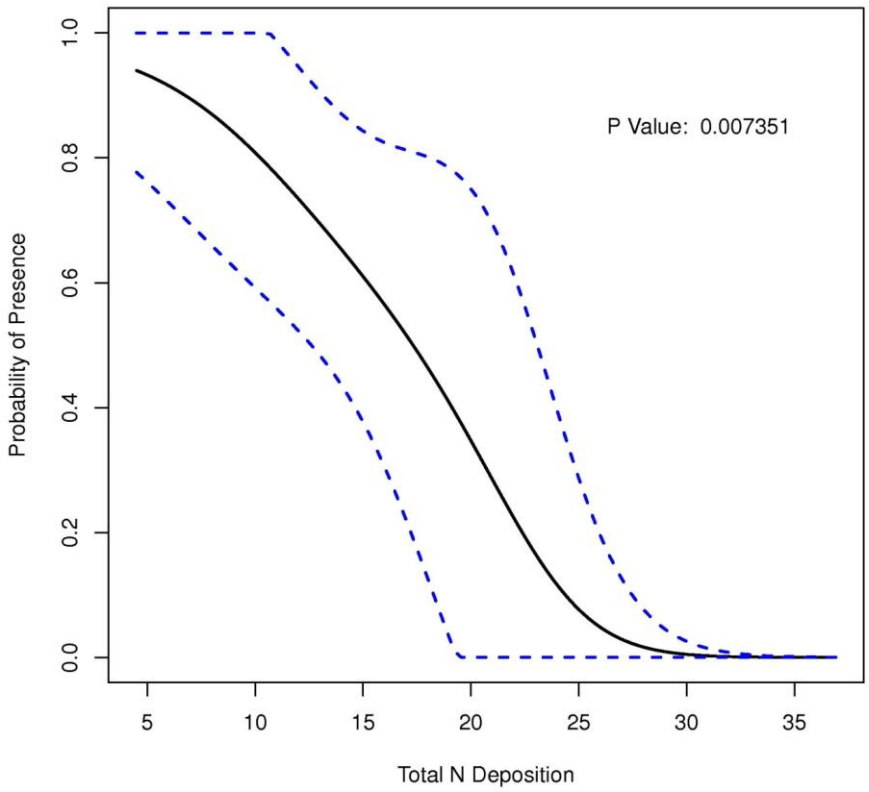

Figure A2.15. Spatial change in the probability of presence of *Vaccinium vitis-idaea* in upland heathland with increasing total current inorganic N deposition (kg N ha^{-1} yr^{-1}). Data from BSBI Local Change.

Temporal analysis

Heathlands – lowland

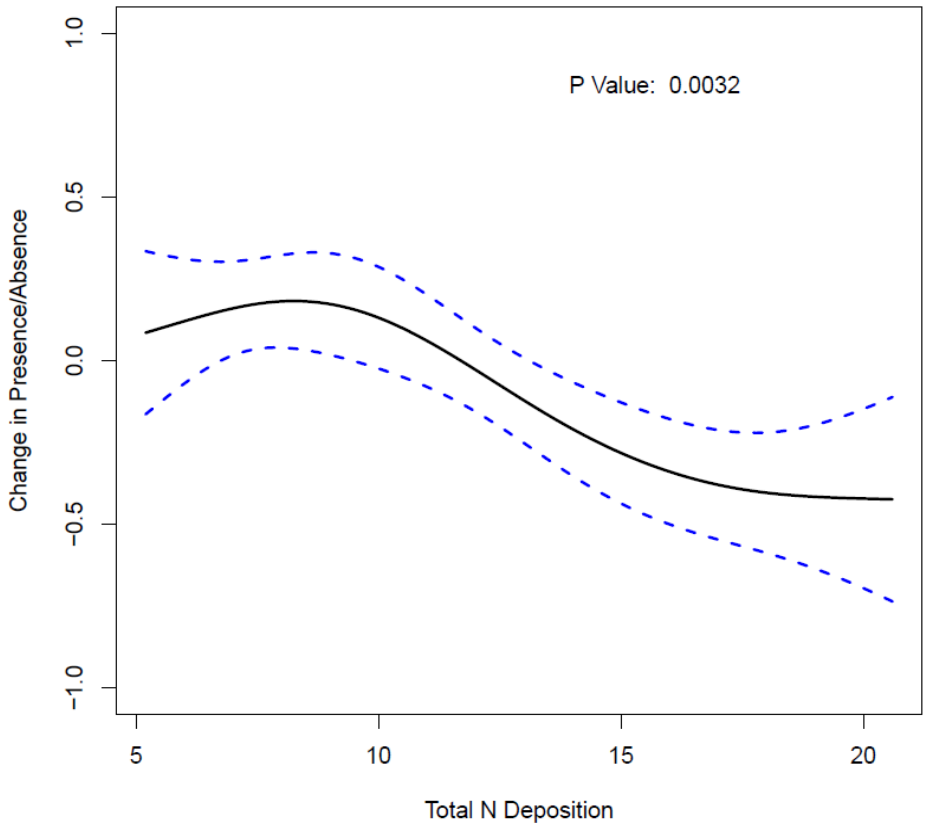

Figure A2.16. Temporal change in the probability of presence of *Scleranthus annuus* between survey periods (1987-1988, and 2003-2004) against total current inorganic N deposition (kg N ha^{-1} yr^{-1}) for hectads in lowland heathland. Data from BSBI Local Change.

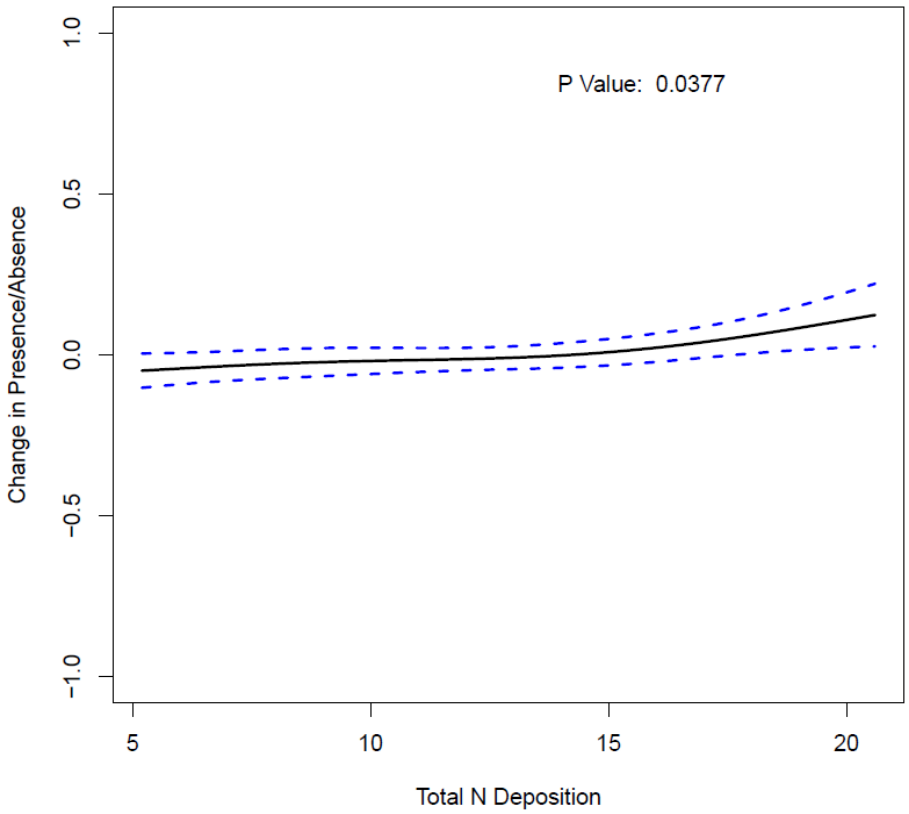

Figure A2.17. Temporal change in the probability of presence of *Viola lactea* between survey periods (1987-1988, and 2003-2004) against total current inorganic N deposition (kg N ha^{-1} yr^{-1}) for hectads in lowland heathland. Data from BSBI Local Change.

Heathlands – upland

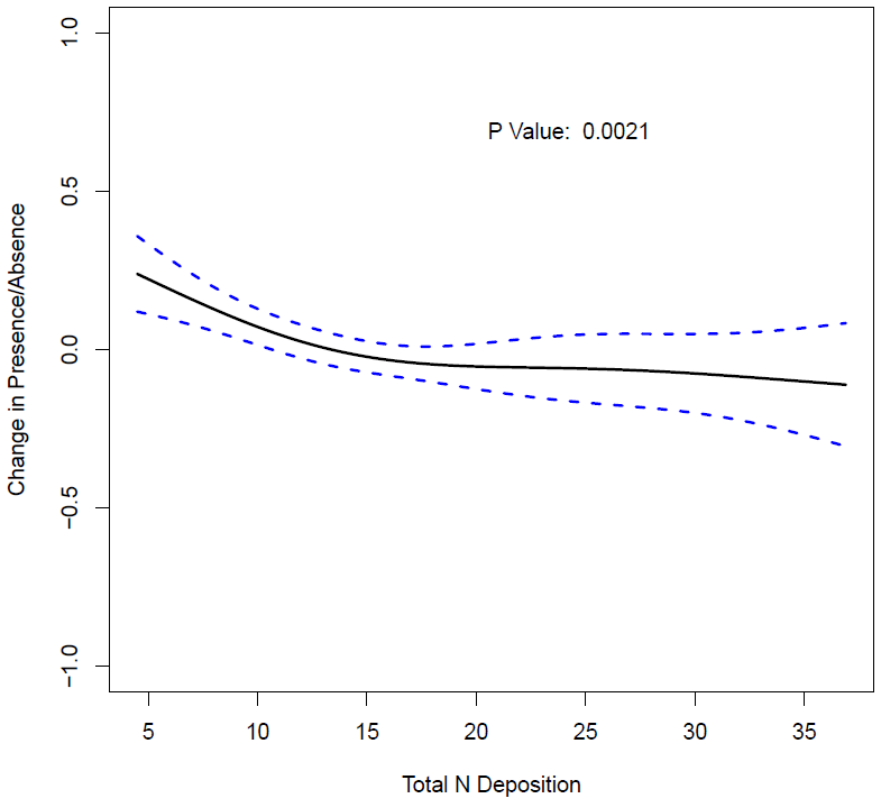

Figure A2.18. Temporal change in the probability of presence of *Lycopodium annotinum* between survey periods (1987-1988, and 2003-2004) against total current inorganic N deposition (kg N ha^{-1} yr^{-1}) for hectads in upland heathland. Data from BSBI Local Change.

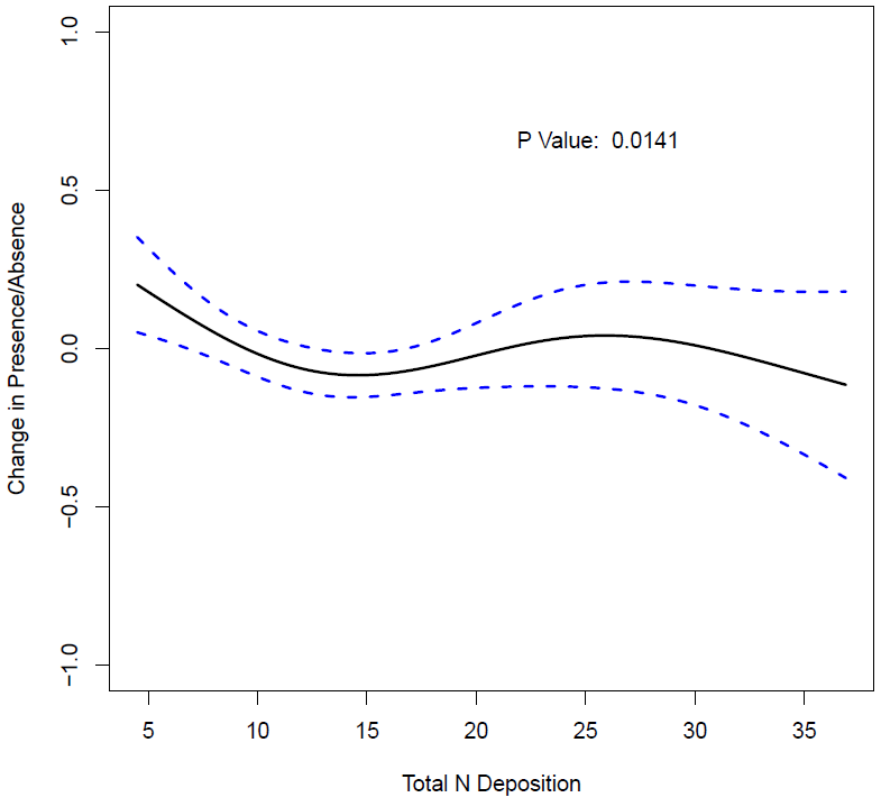

Figure A2.19. Temporal change in the probability of presence of *Trientalis europaea* between survey periods (1987-1988, and 2003-2004) against total current inorganic N deposition (kg N ha^{-1} yr^{-1}) for hectads in upland heathland. Data from BSBI Local Change.

Electronic appendix 3

British Lichen Society data analysis results

Acid grassland

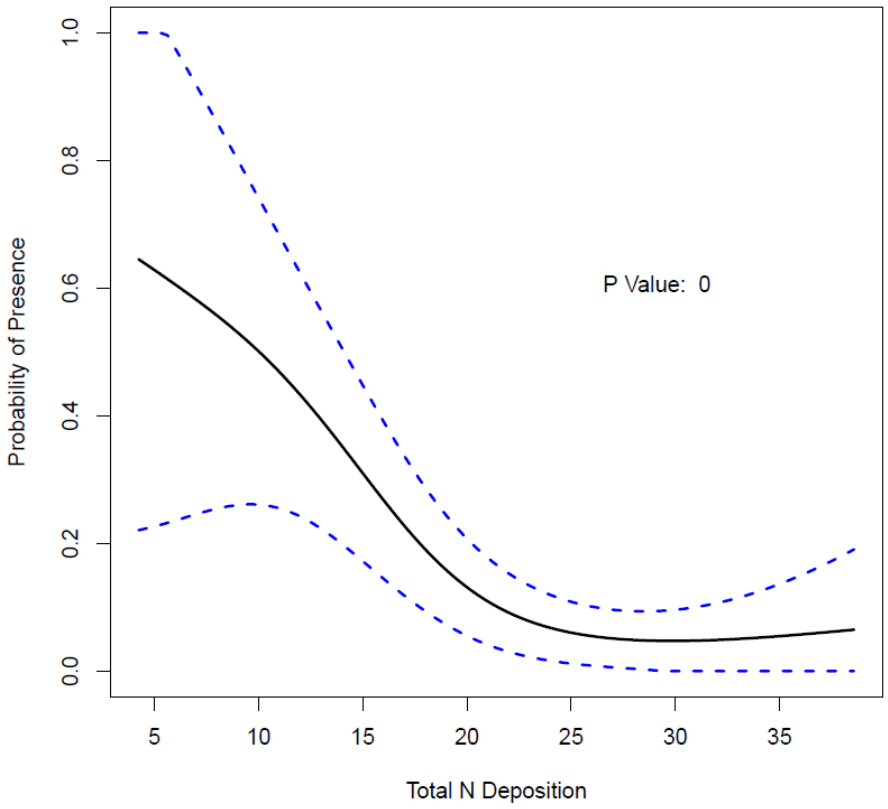

Figure A3.1. Spatial change in the probability of presence of *Cetraria aculeata* in acid grassland with increasing total current inorganic N deposition (kg N ha^{-1} yr^{-1}). Data from BLS.

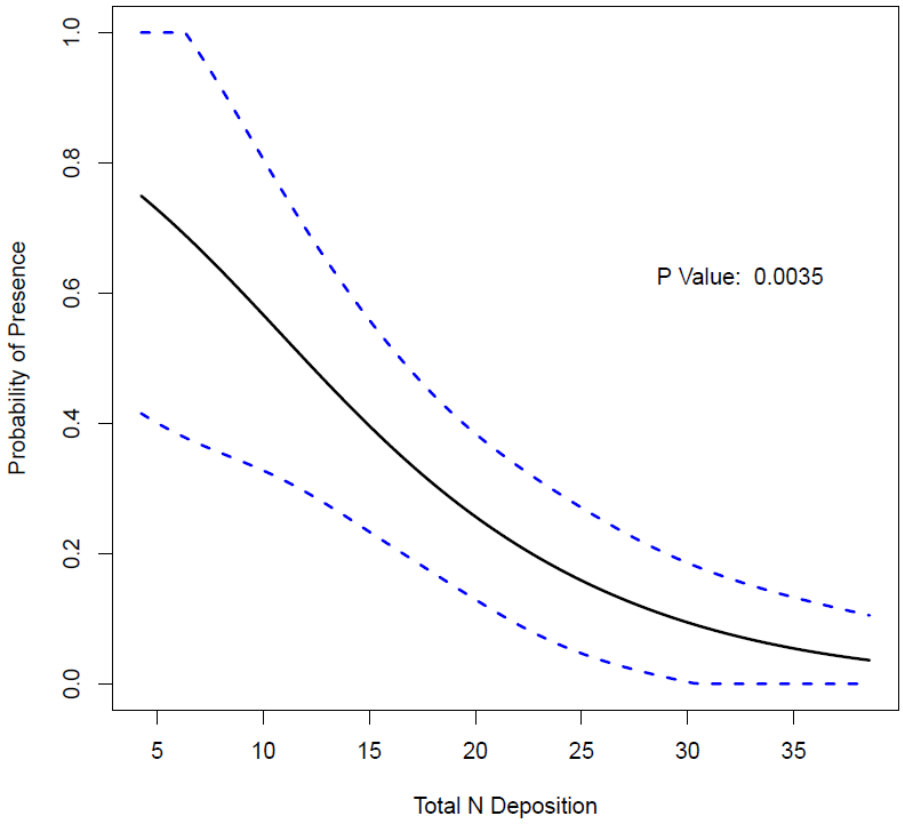

Figure A3.2. Spatial change in the probability of presence of *Peltigera didactyla* in acid grassland with increasing total current inorganic N deposition (kg N ha^{-1} yr^{-1}). Data from BLS.

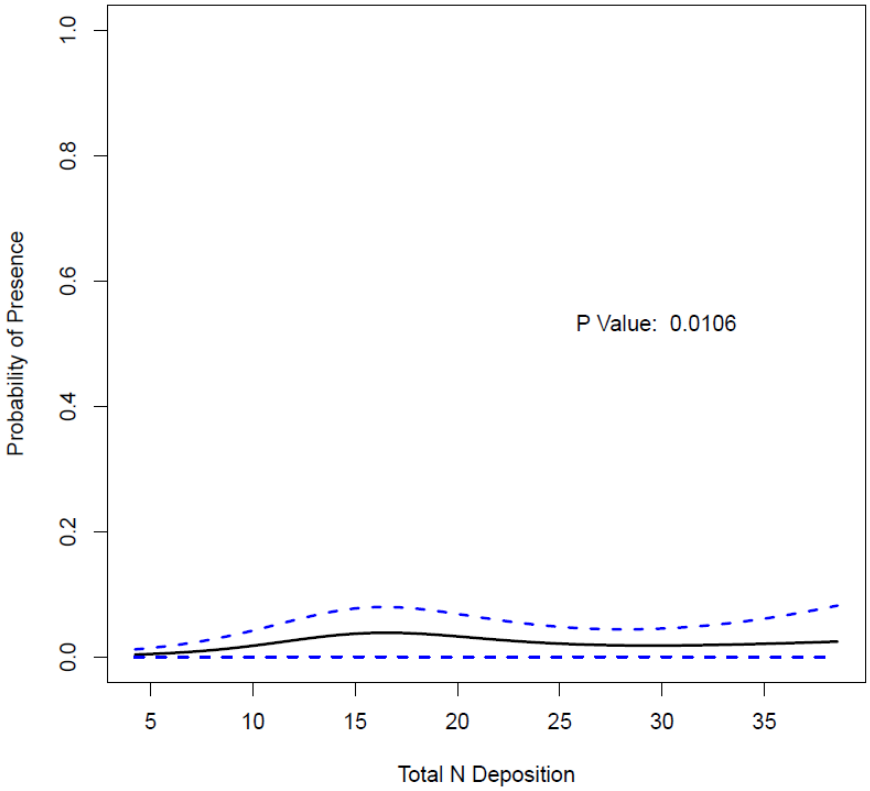

Figure A3.3. Spatial change in the probability of presence of *Catapyreneum lachneum* in acid grassland with increasing total current inorganic N deposition (kg N ha^{-1} yr^{-1}). Data from BLS.

Calcareous grassland

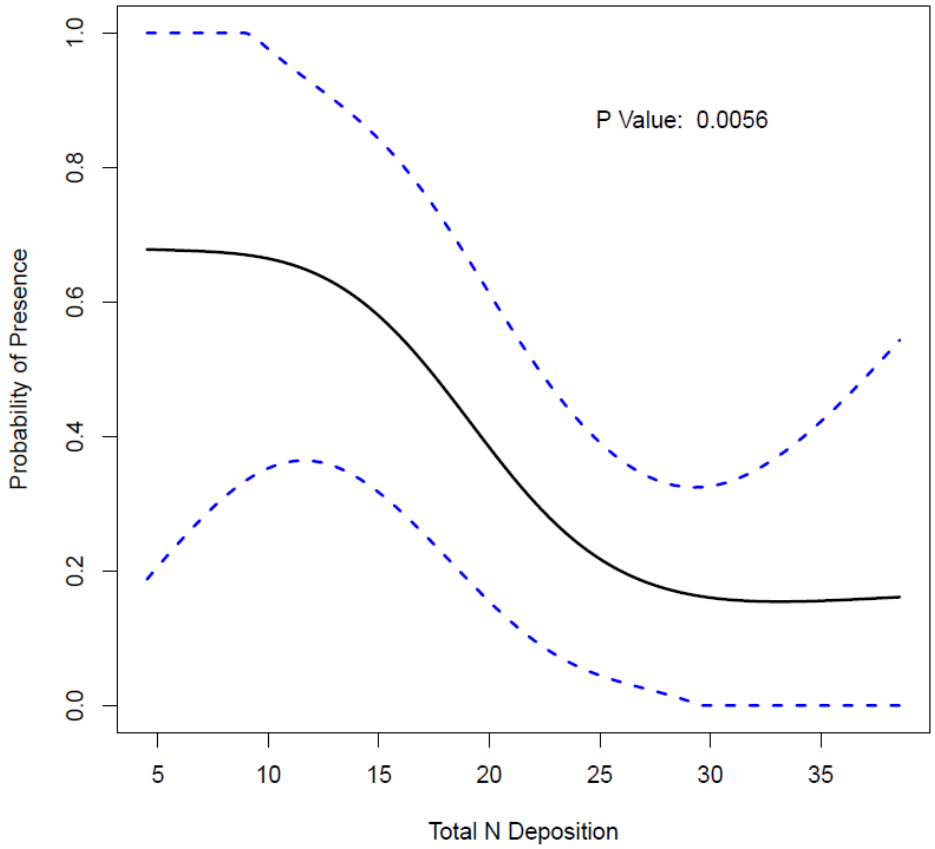

Figure A3.4. Spatial change in the probability of presence of *Cladonia foliacea* in calcareous grassland with increasing total current inorganic N deposition (kg N ha^{-1} yr^{-1}). Data from BLS.

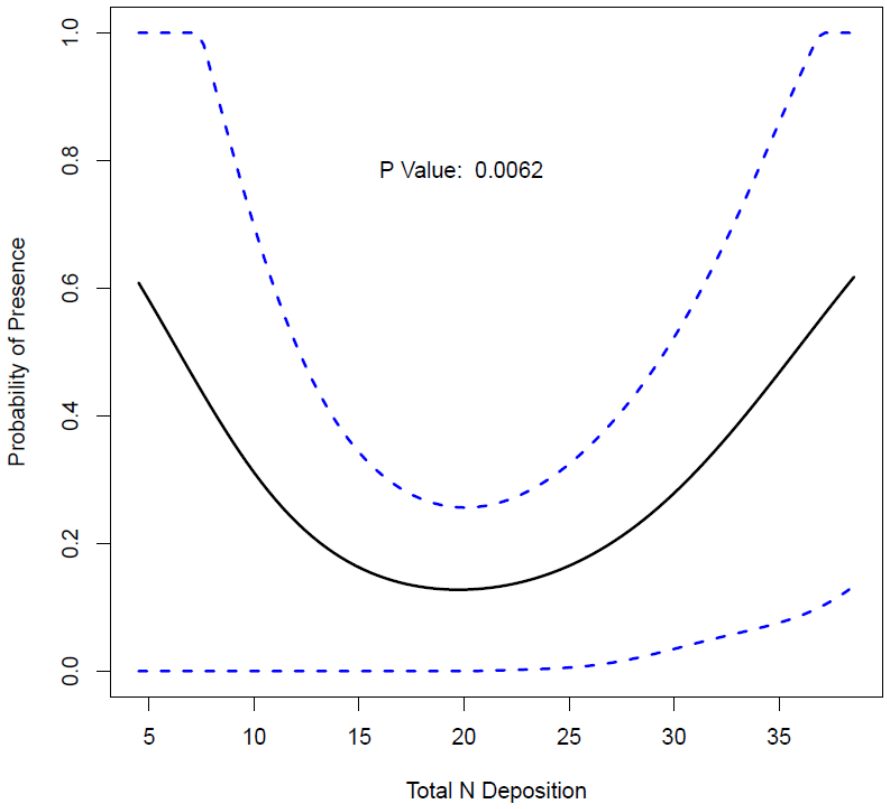

Figure A3.5. Spatial change in the probability of presence of *Diploschistes muscorum* in calcareous grassland with increasing total current inorganic N deposition (kg N ha^{-1} yr^{-1}). Data from BLS.

Bog

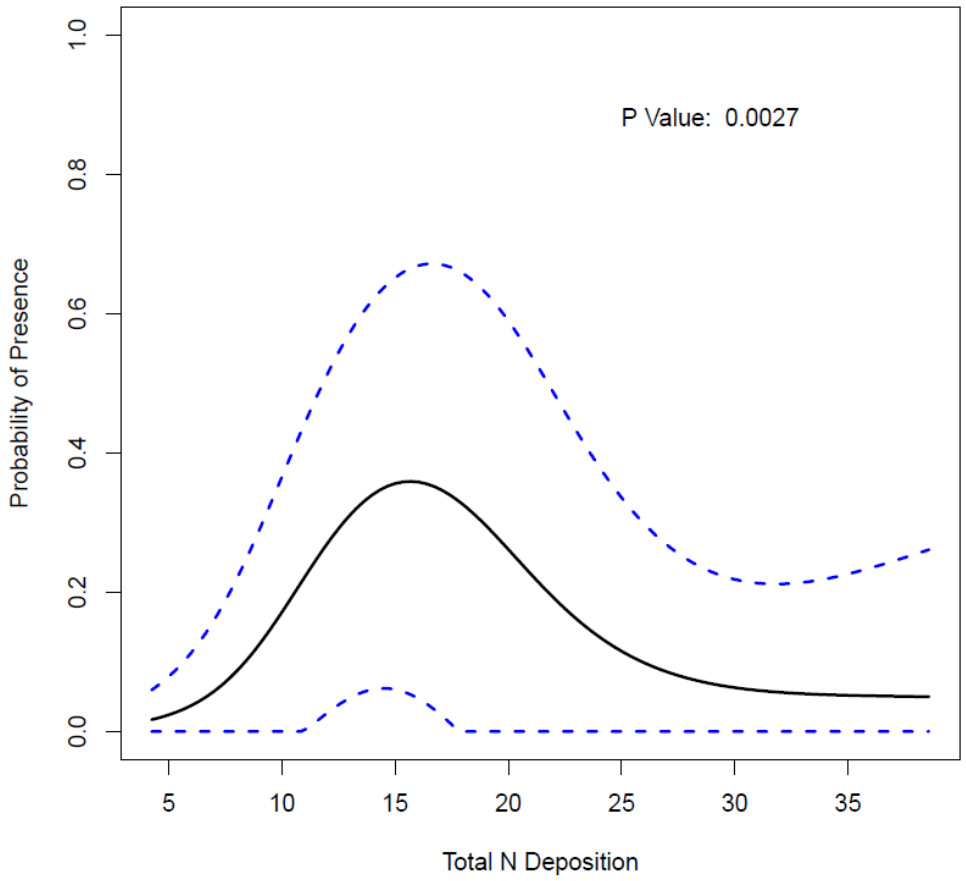

Figure A3.6. Spatial change in the probability of presence of *Cladonia arbuscula squarrosa* in bog with increasing total current inorganic N deposition (kg N ha^{-1} yr^{-1}). Data from BLS.

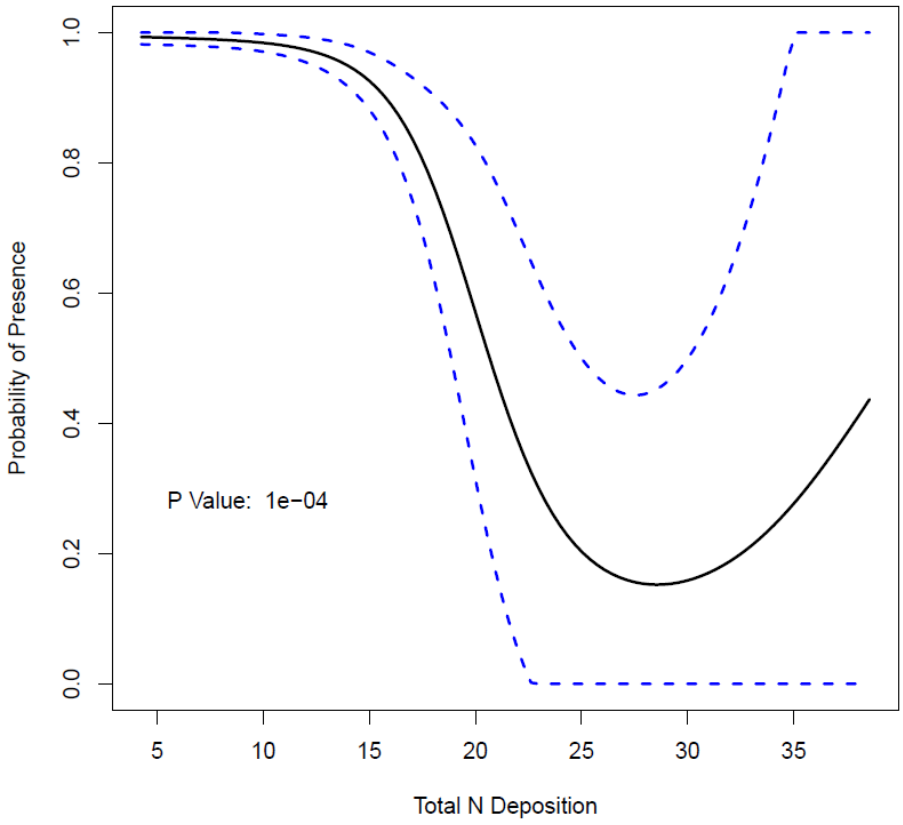

Figure A3.7. Spatial change in the probability of presence of *Cladonia portentosa* in bog with increasing total current inorganic N deposition (kg N ha^{-1} yr^{-1}). Data from BLS.

Heathland

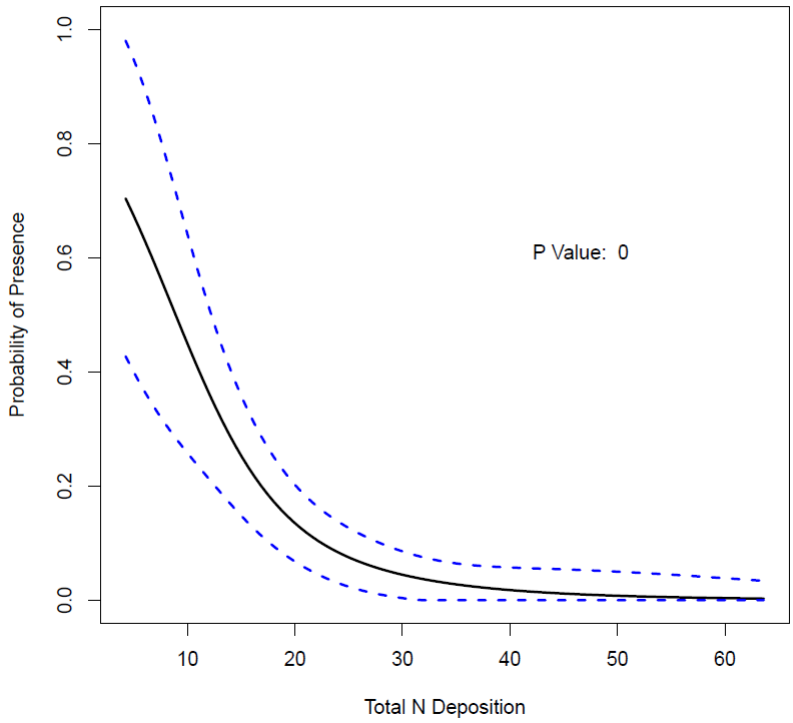

Figure A3.8. Spatial change in the probability of presence of *Cetraria aculeata* in heathland with increasing total current inorganic N deposition (kg N ha^{-1} yr^{-1}). Data from BLS.

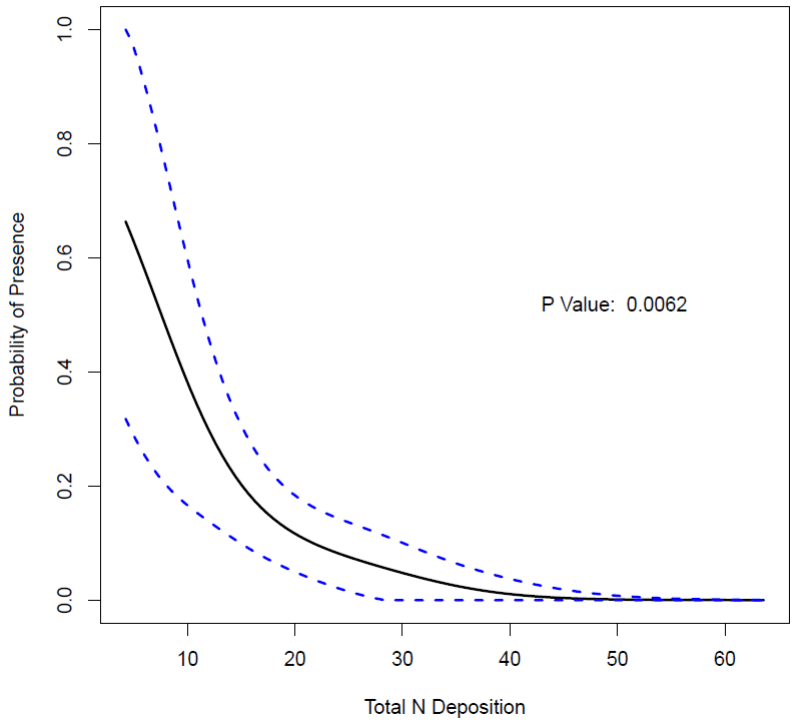

Figure A3.9. Spatial change in the probability of presence of *Cetraria muricata* in heathland with increasing total current inorganic N deposition (kg N ha^{-1} yr^{-1}). Data from BLS.

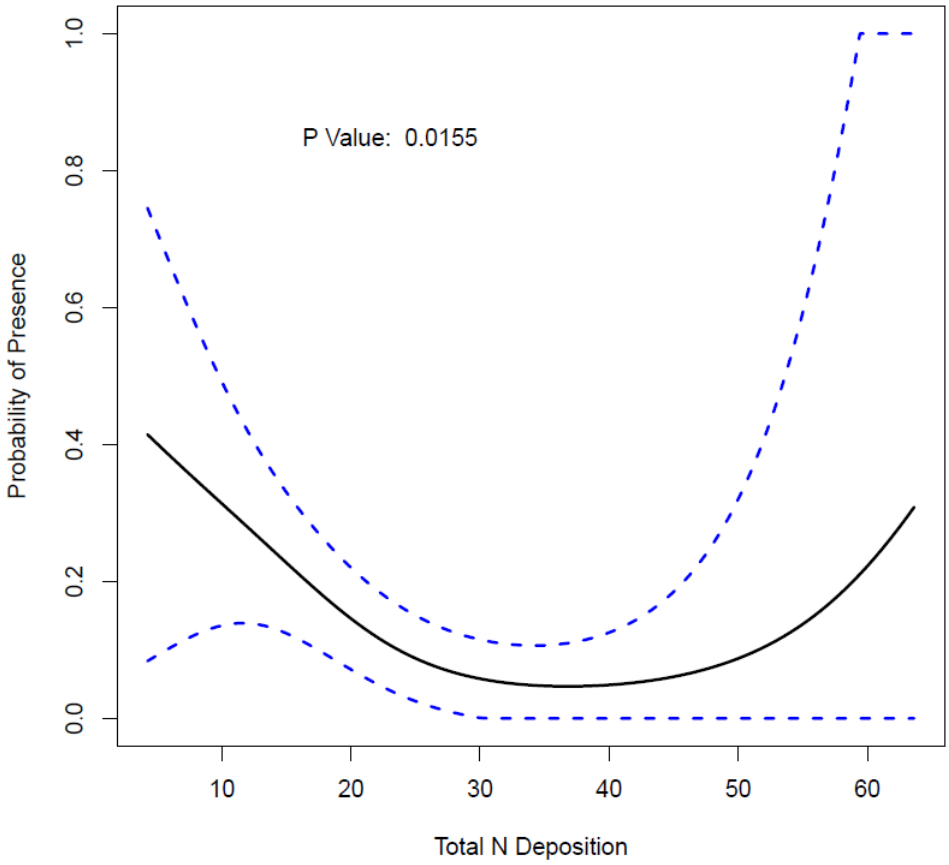

Figure A3.10. Spatial change in the probability of presence of *Cladonia arbuscula squarrosa* in heathland with increasing total current inorganic N deposition (kg N ha^{-1} yr^{-1}). Data from BLS.

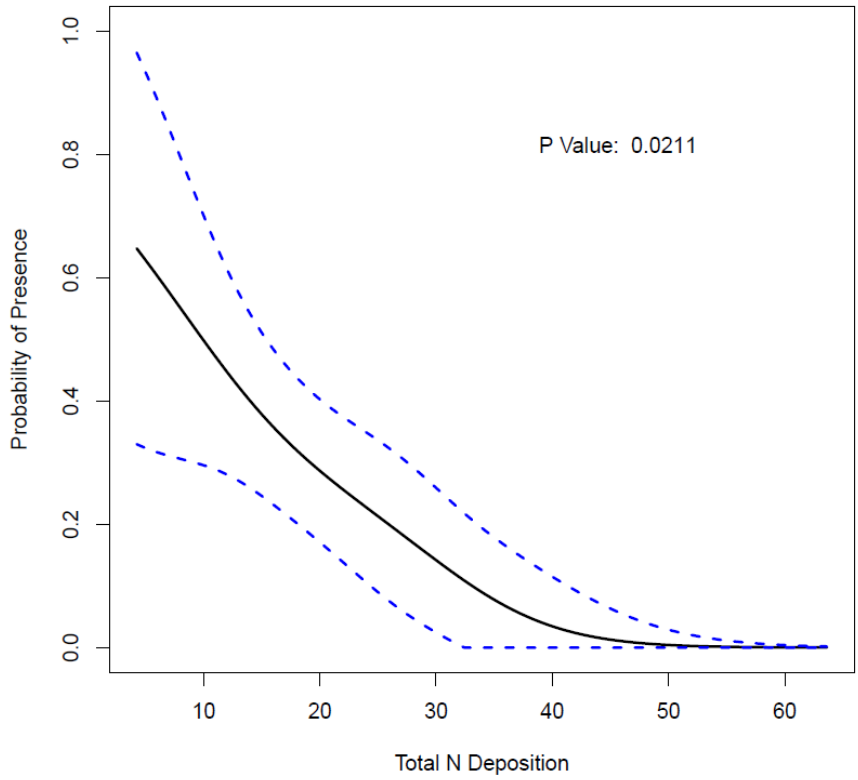

Figure A3.11. Spatial change in the probability of presence of *Cladonia cervicornis cervicornis* in heathland with increasing total current inorganic N deposition (kg N ha^{-1} yr^{-1}). Data from BLS.

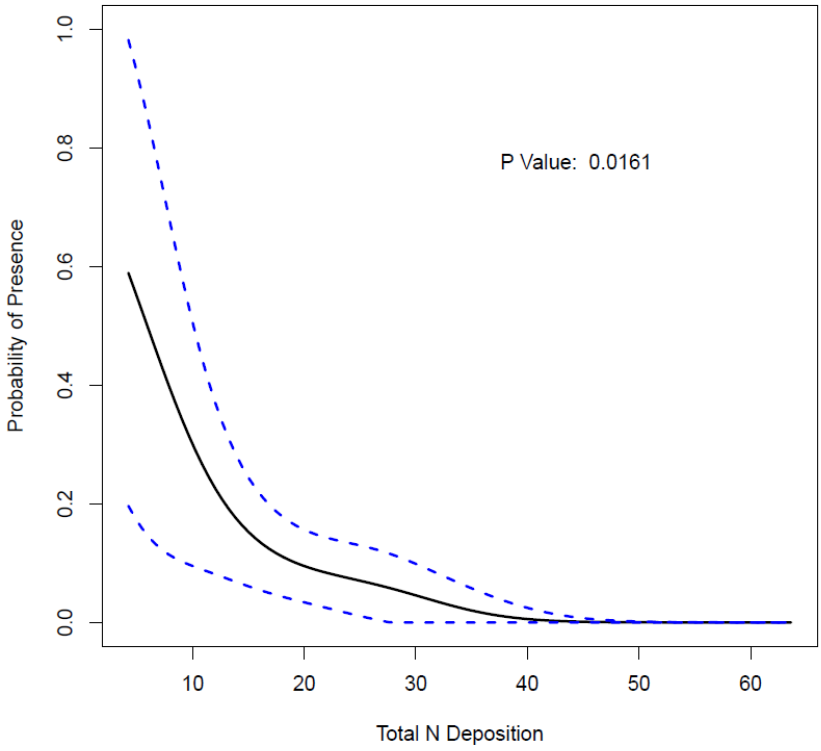

Figure A3.12. Spatial change in the probability of presence of *Cladonia cervicornis verticillata* in heathland with increasing total current inorganic N deposition (kg N ha^{-1} yr^{-1}). Data from BLS.

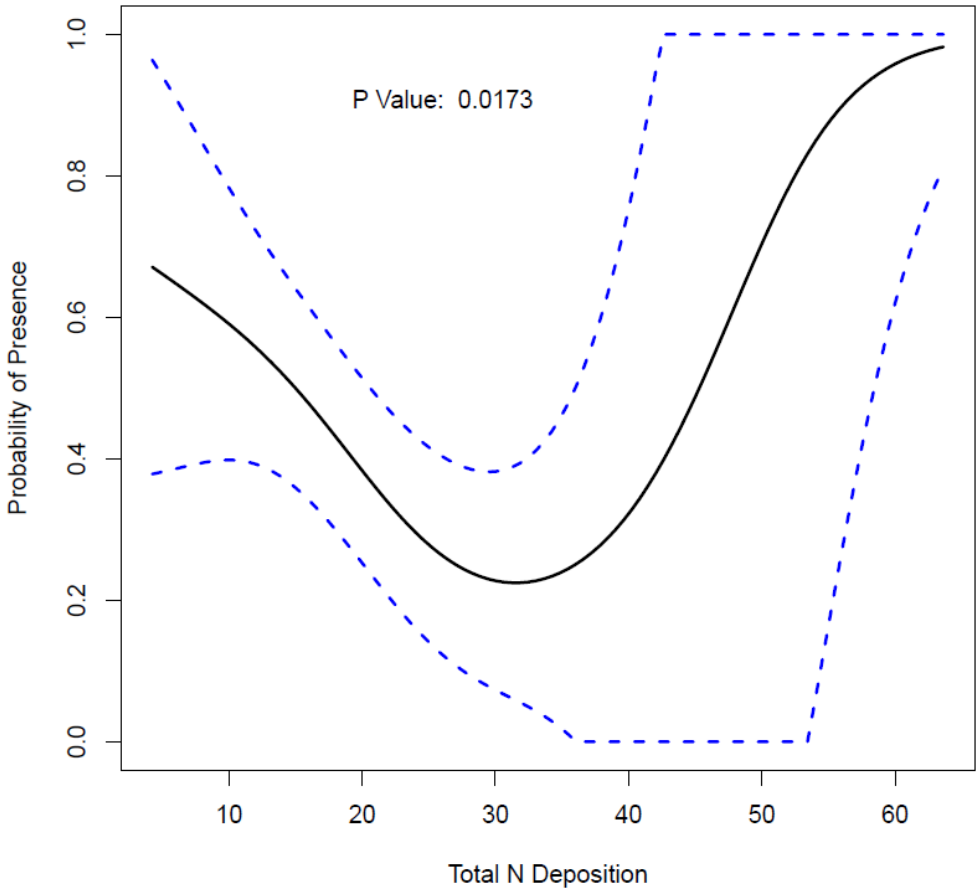

Figure A3.13. Spatial change in the probability of presence of *Cladonia floerkeana* in heathland with increasing total current inorganic N deposition (kg N ha^{-1} yr^{-1}). Data from BLS.

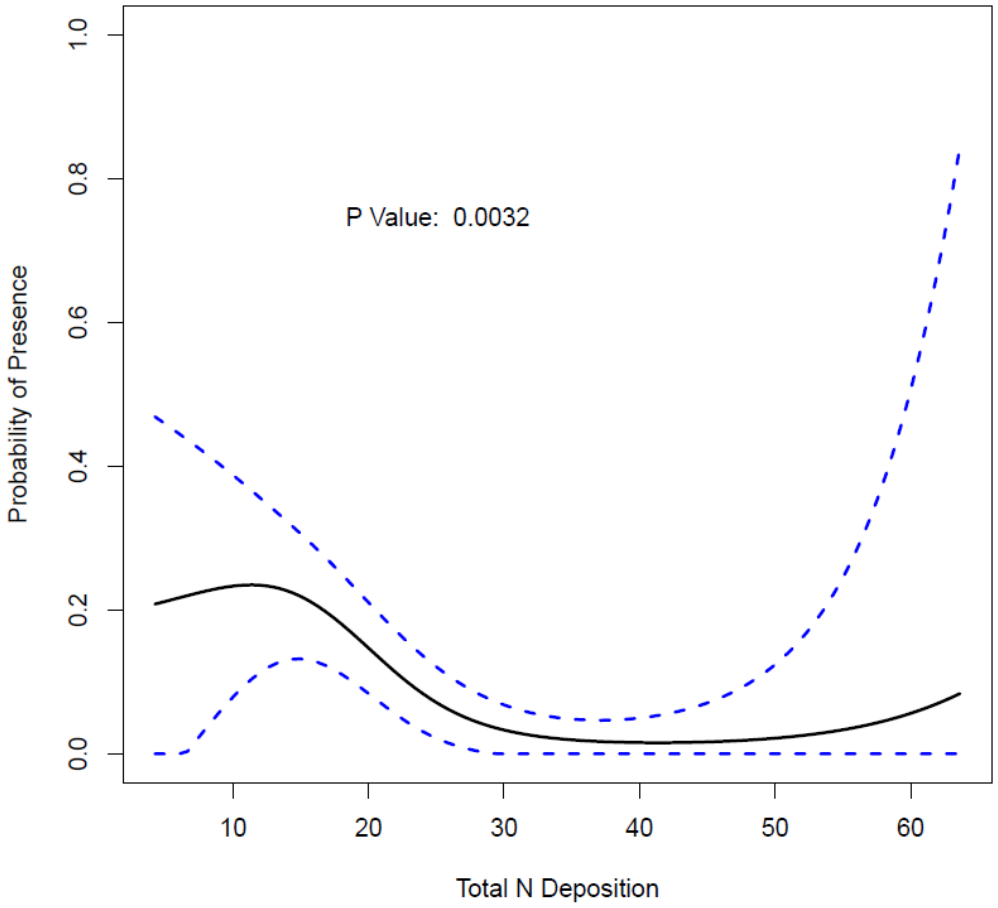

Figure A3.14. Spatial change in the probability of presence of *Cladonia glauca* in heathland with increasing total current inorganic N deposition (kg N ha^{-1} yr^{-1}). Data from BLS.

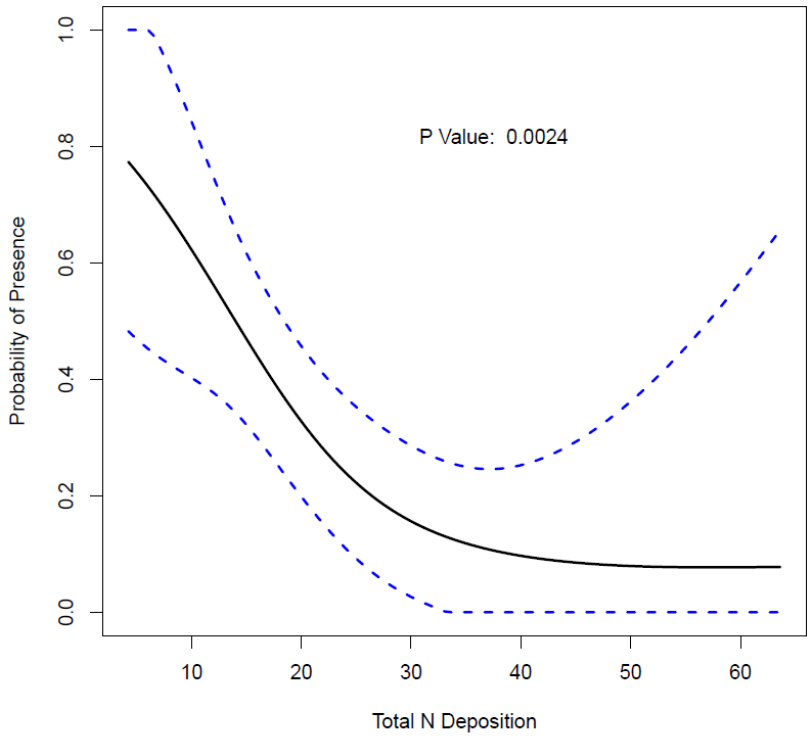

Figure A3.15. Spatial change in the probability of presence of *Cladonia portentosa* in heathland with increasing total current inorganic N deposition (kg N ha^{-1} yr^{-1}). Data from BLS.

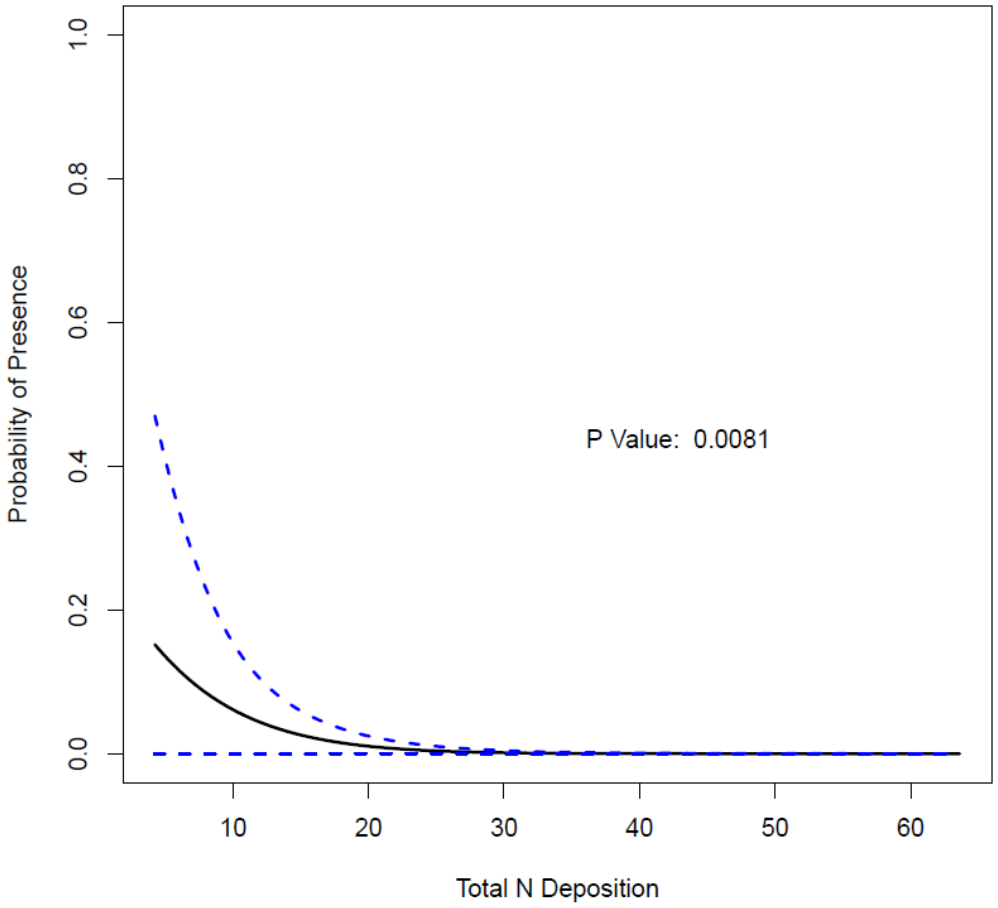

Figure A3.16. Spatial change in the probability of presence of *Cladonia strepsilis* in heathland with increasing total current inorganic N deposition (kg N ha^{-1} yr^{-1}). Data from BLS.

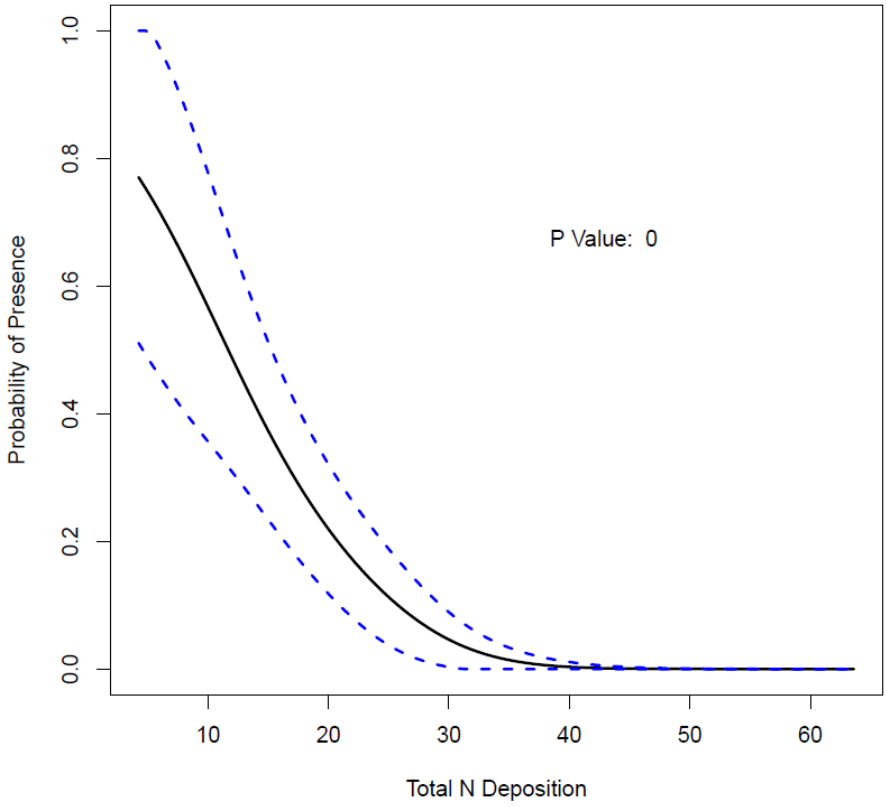

Figure A3.17. Spatial change in the probability of presence of *Cladonia subulata* in heathland with increasing total current inorganic N deposition (kg N ha^{-1} yr^{-1}). Data from BLS.

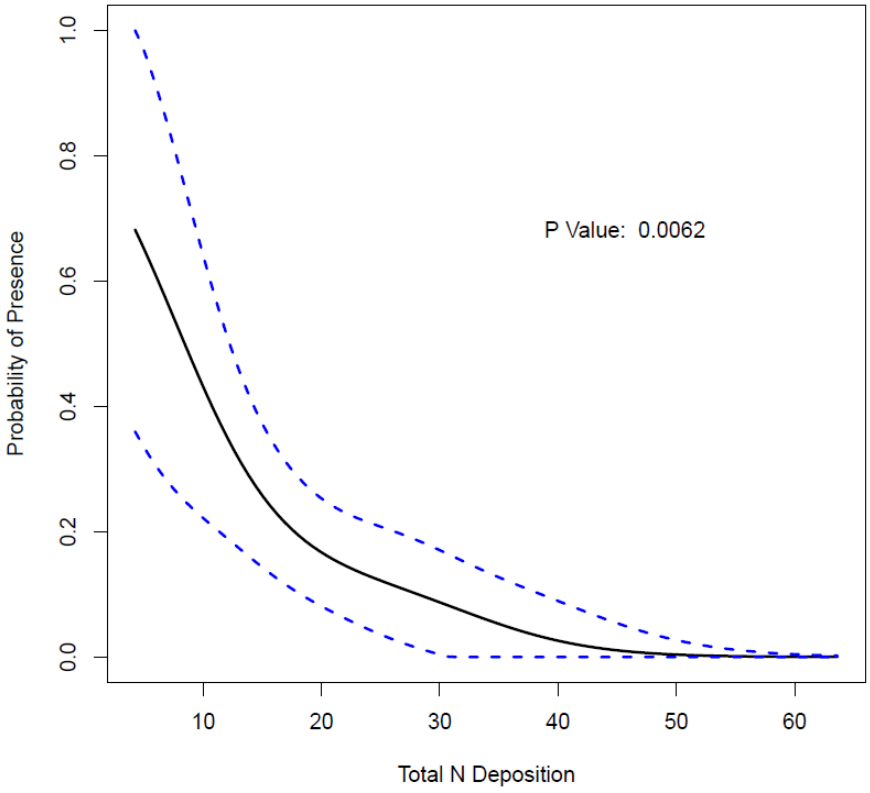

Figure A3.18. Spatial change in the probability of presence of *Cladonia uncialis biuncialis* in heathland with increasing total current inorganic N deposition (kg N ha^{-1} yr^{-1}). Data from BLS.

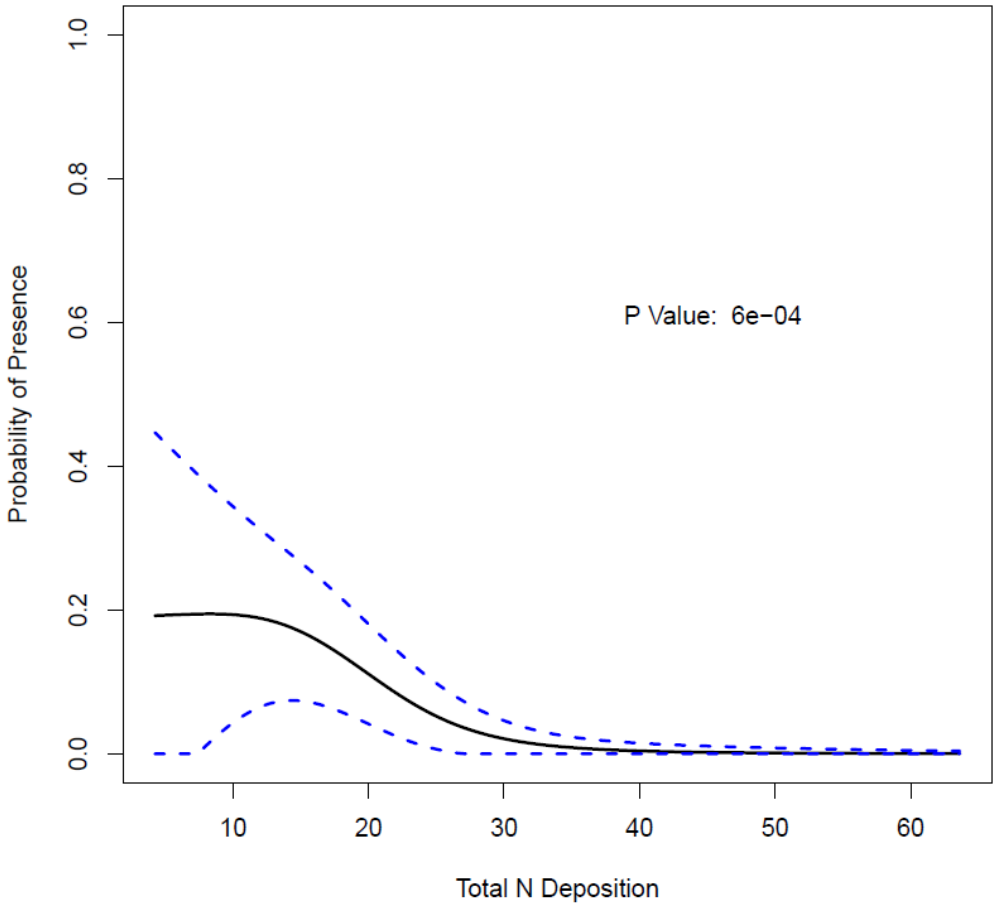

Figure A3.19. Spatial change in the probability of presence of *Dibaeis baeomyces* in heathland with increasing total current inorganic N deposition (kg N ha^{-1} yr^{-1}). Data from BLS.

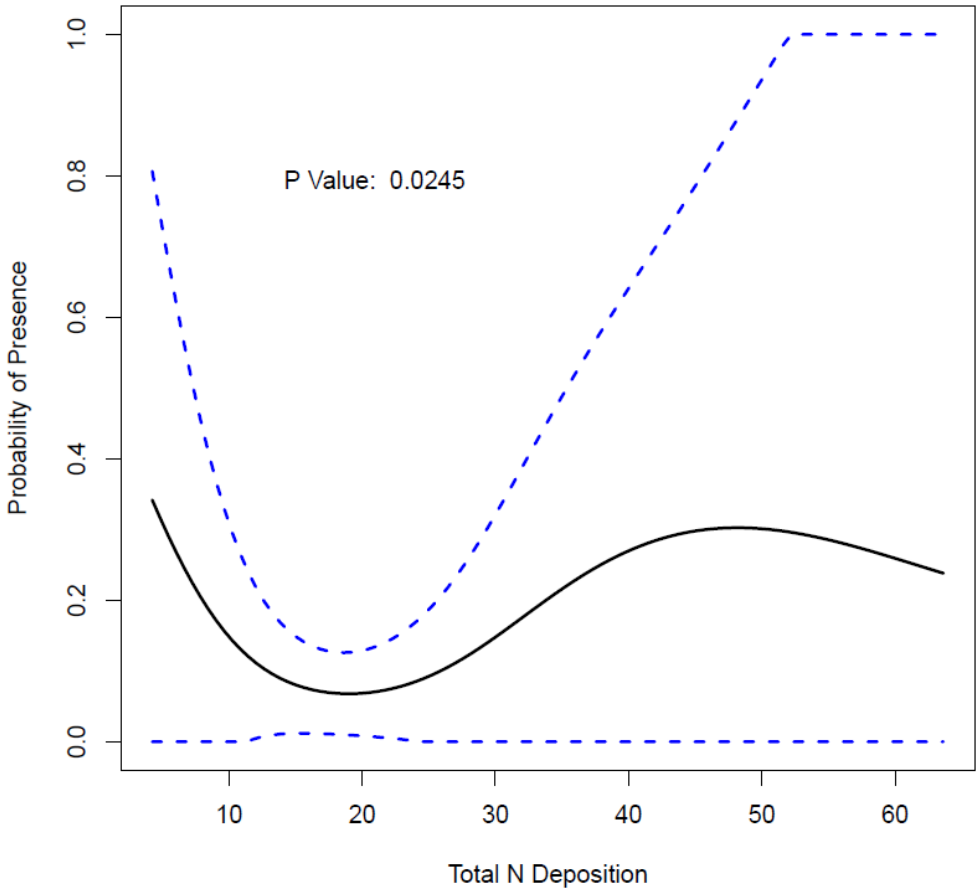

Figure A3.20. Spatial change in the probability of presence of *Diploschistes muscorum* in heathland with increasing total current inorganic N deposition (kg N ha^{-1} yr^{-1}). Data from BLS.

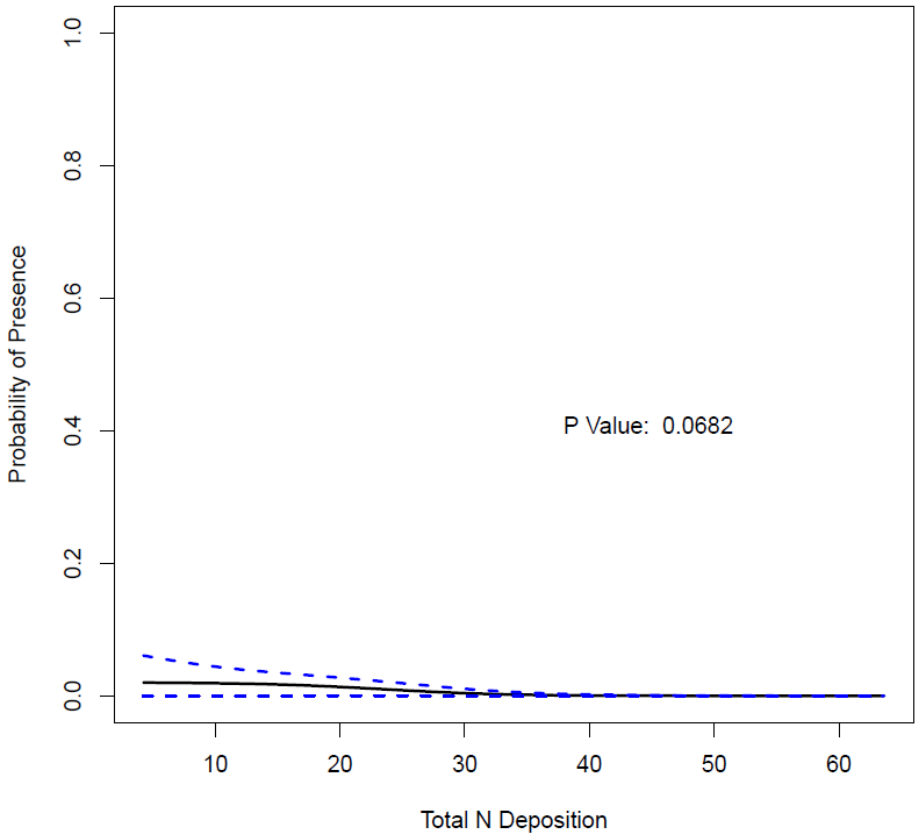

Figure A3.21. Spatial change in the probability of presence of *Lichenomphalia hudsoniana* in heathland with increasing total current inorganic N deposition (kg N ha^{-1} yr^{-1}). Data from BLS.

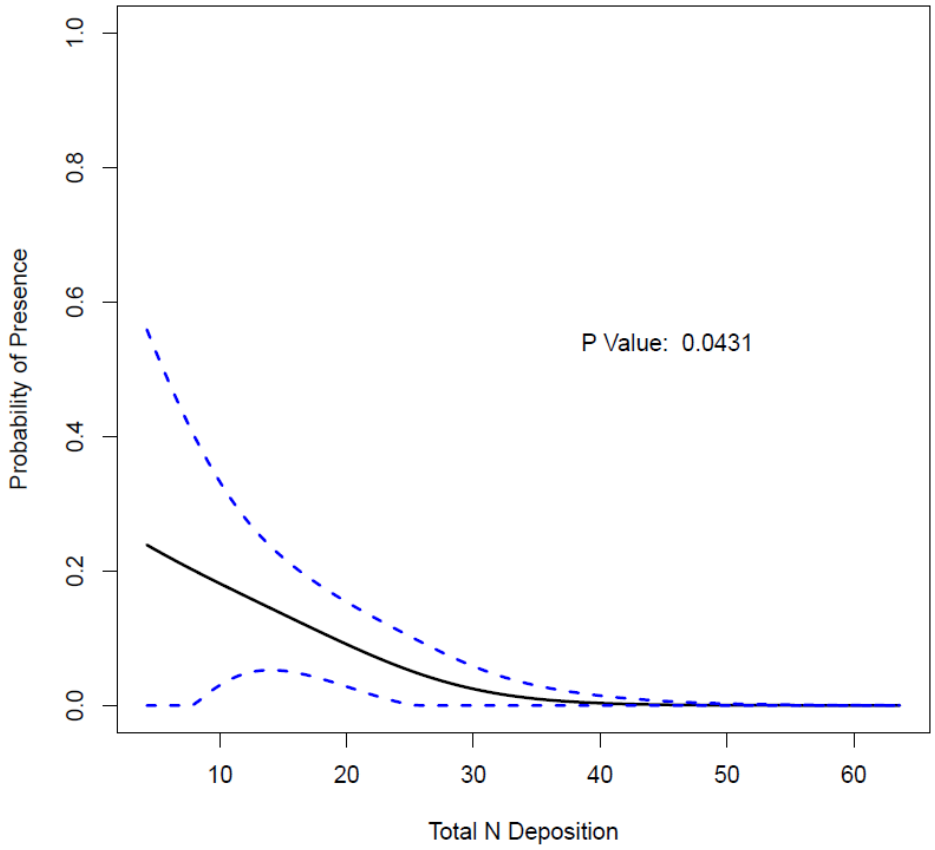

Figure A3.22. Spatial change in the probability of presence of *Lichenomphalia umbellifera* in heathland with increasing total current inorganic N deposition (kg N ha^{-1} yr^{-1}). Data from BLS.

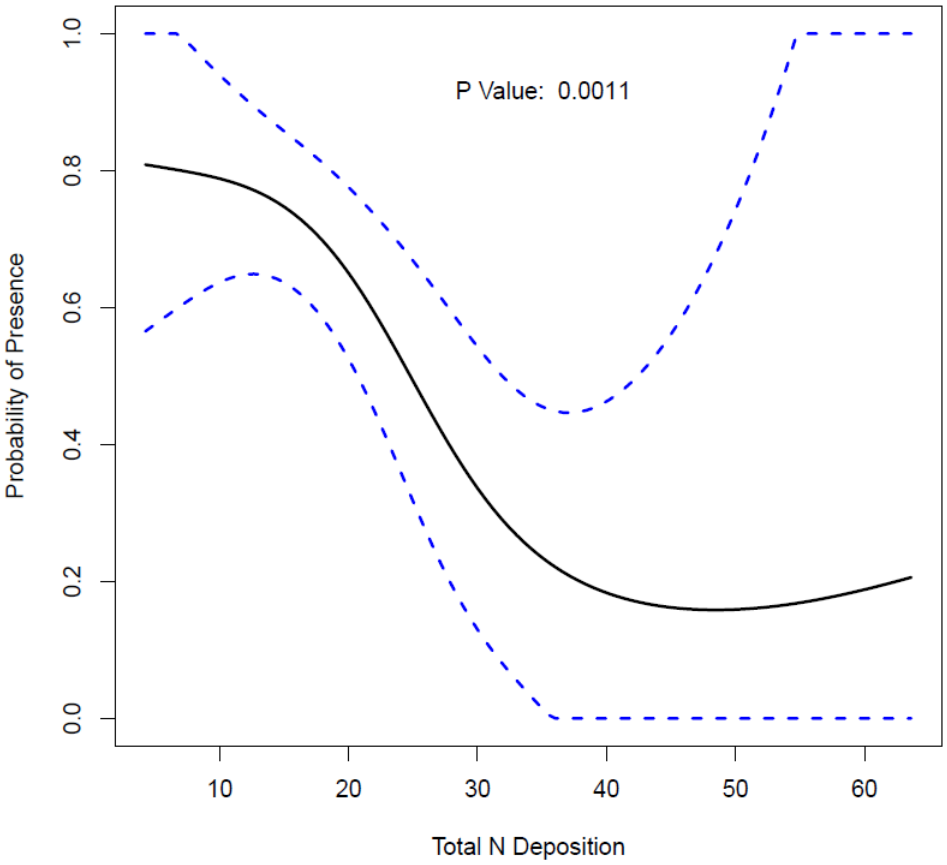

Figure A3.23. Spatial change in the probability of presence of *Peltigera hymenina* in heathland with increasing total current inorganic N deposition (kg N ha^{-1} yr^{-1}). Data from BLS.

Electronic appendix 4

BBS Database.

Acid grassland – upland

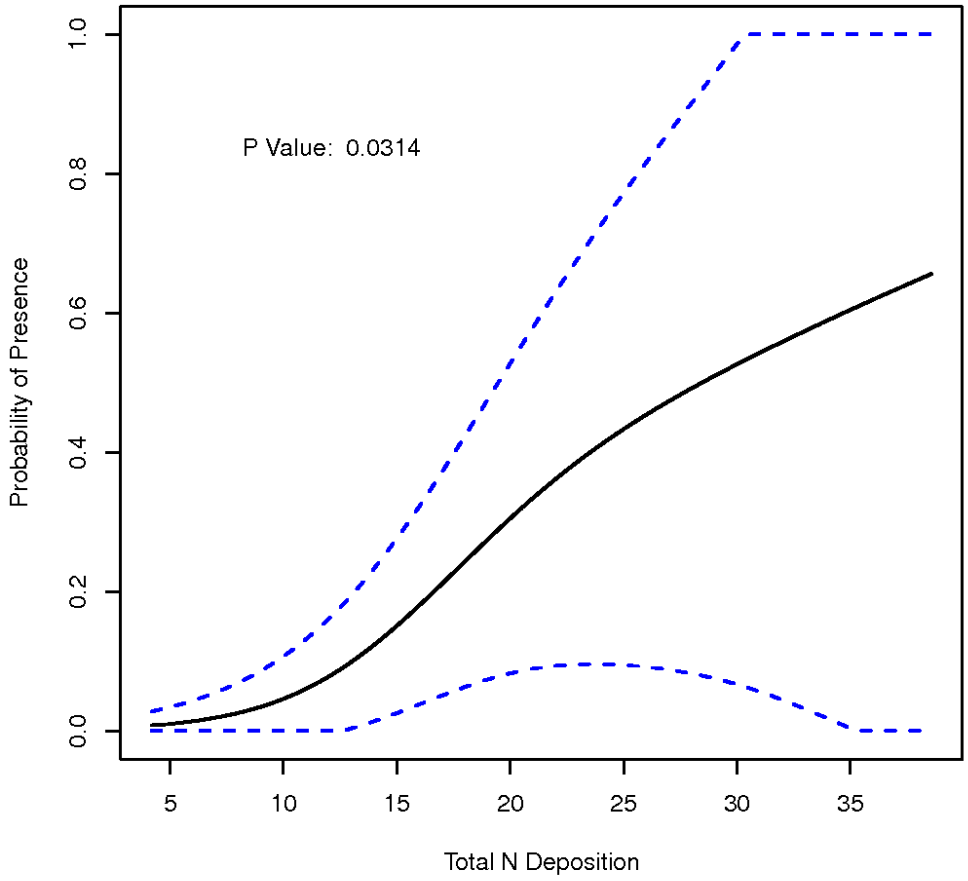

Figure A4.1. Spatial change in the probability of presence of *Archidium alternifolium* in upland acid grassland with increasing total current inorganic N deposition (kg N ha^{-1} yr^{-1}). Data from BBS database.

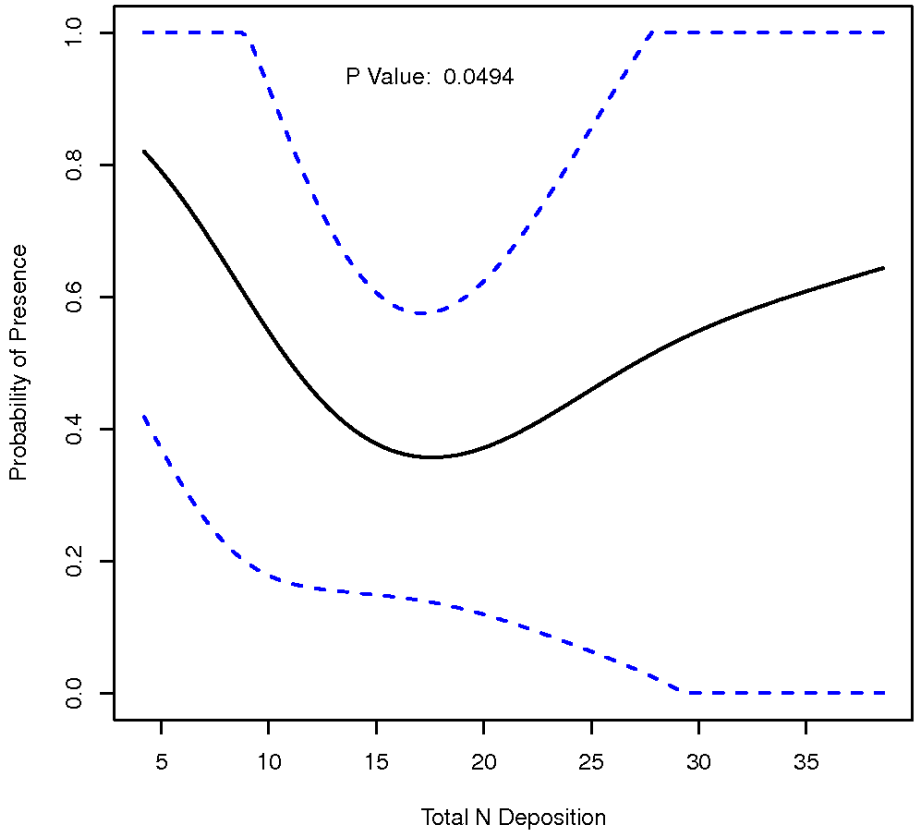

Figure A4.2. Spatial change in the probability of presence of *Dicranum fuscescens* in upland acid grassland with increasing total current inorganic N deposition (kg N ha^{-1} yr^{-1}). Data from BBS database.

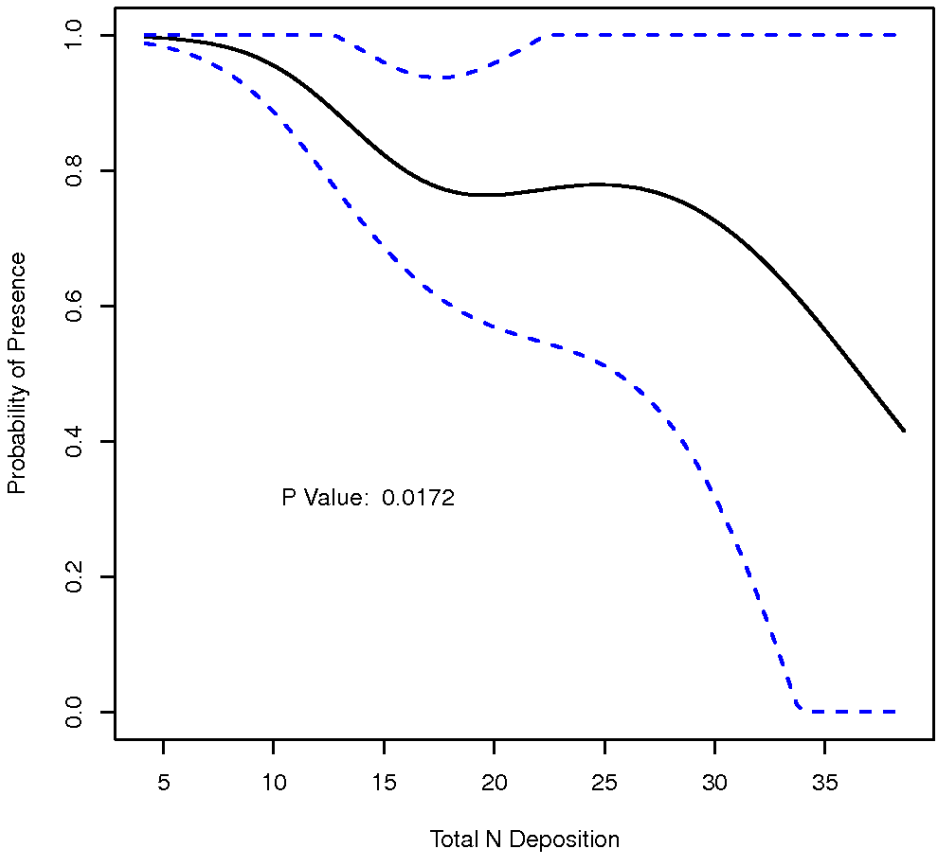

Figure A4.3. Spatial change in the probability of presence of *Frullania tamarisci* in upland acid grassland with increasing total current inorganic N deposition (kg N ha^{-1} yr^{-1}). Data from BBS database.

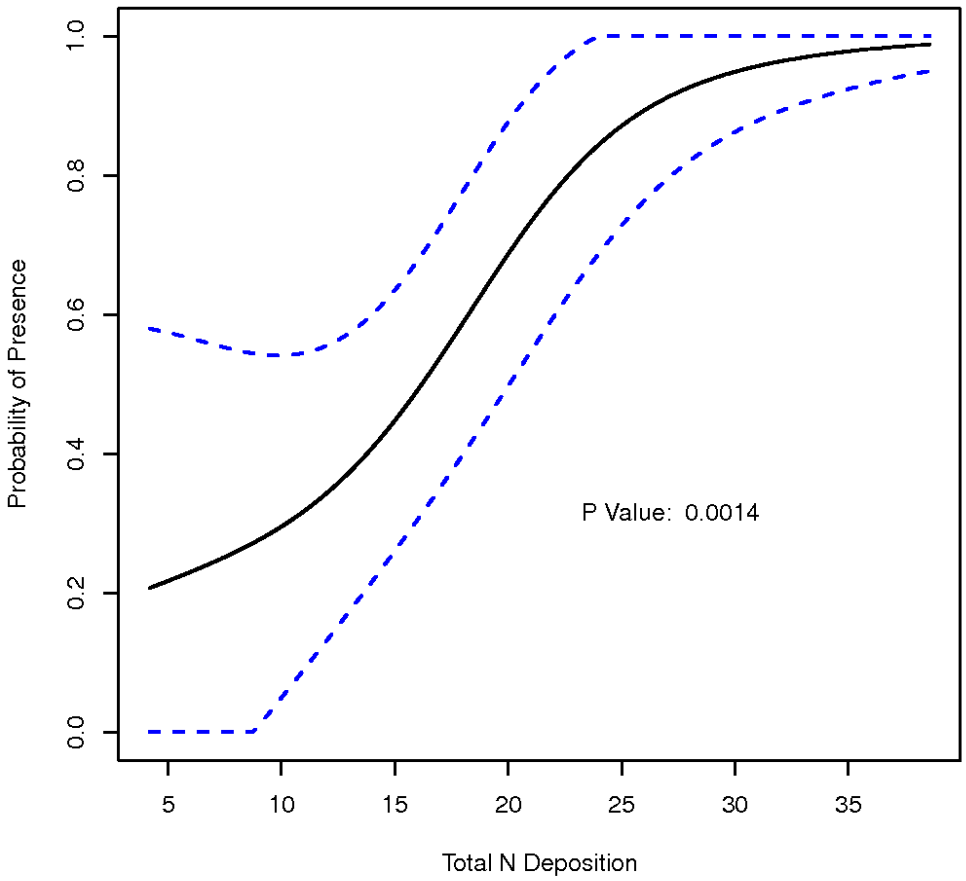

Figure A4.4. Spatial change in the probability of presence of *Gymnocolea inflata* in upland acid grassland with increasing total current inorganic N deposition (kg N ha^{-1} yr^{-1}). Data from BBS database.

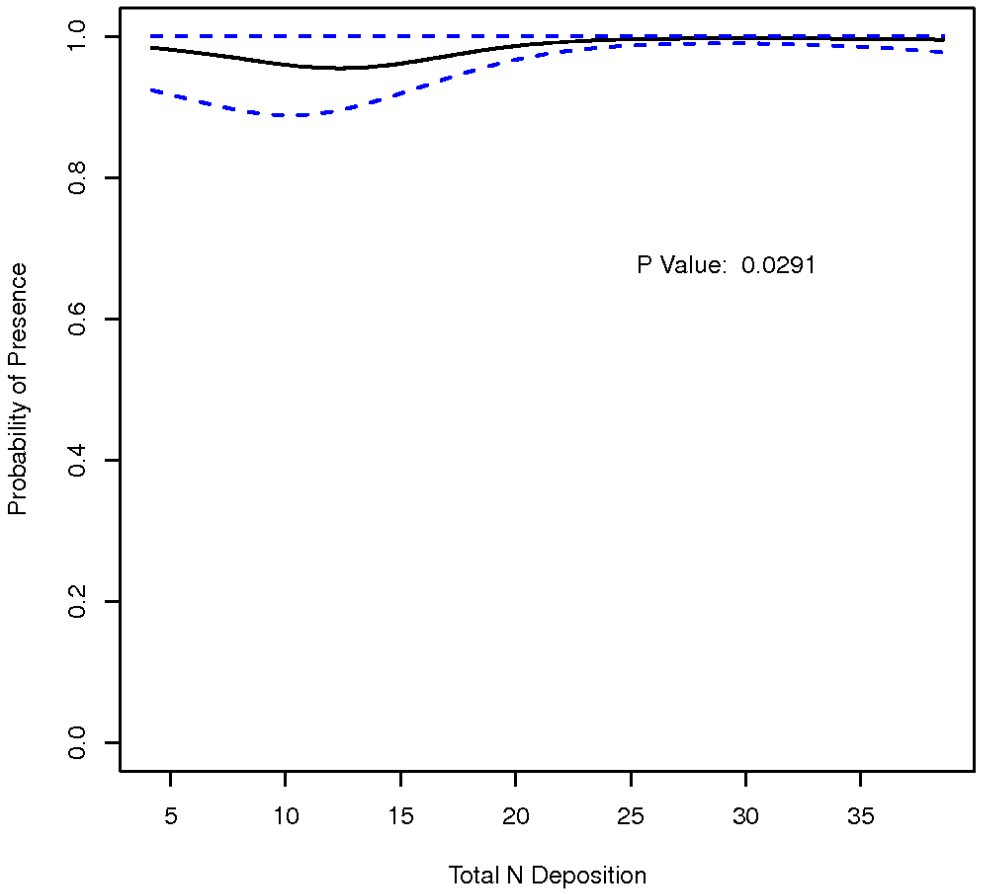

Figure A4.5. Spatial change in the probability of presence of *Hylocomium splendens* in upland acid grassland with increasing total current inorganic N deposition (kg N ha^{-1} yr^{-1}). Data from BBS database.

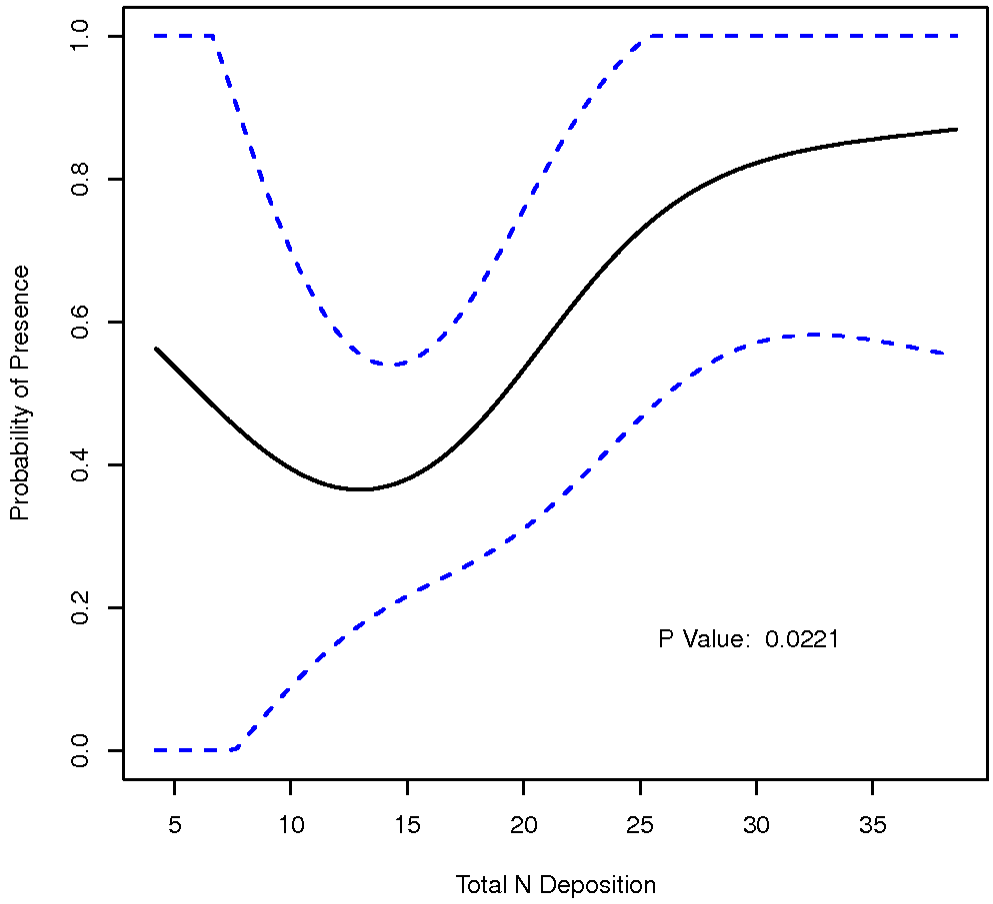

Figure A4.6. Spatial change in the probability of presence of *Leptodontium flexifolium* in upland acid grassland with increasing total current inorganic N deposition (kg N ha^{-1} yr^{-1}). Data from BBS database.

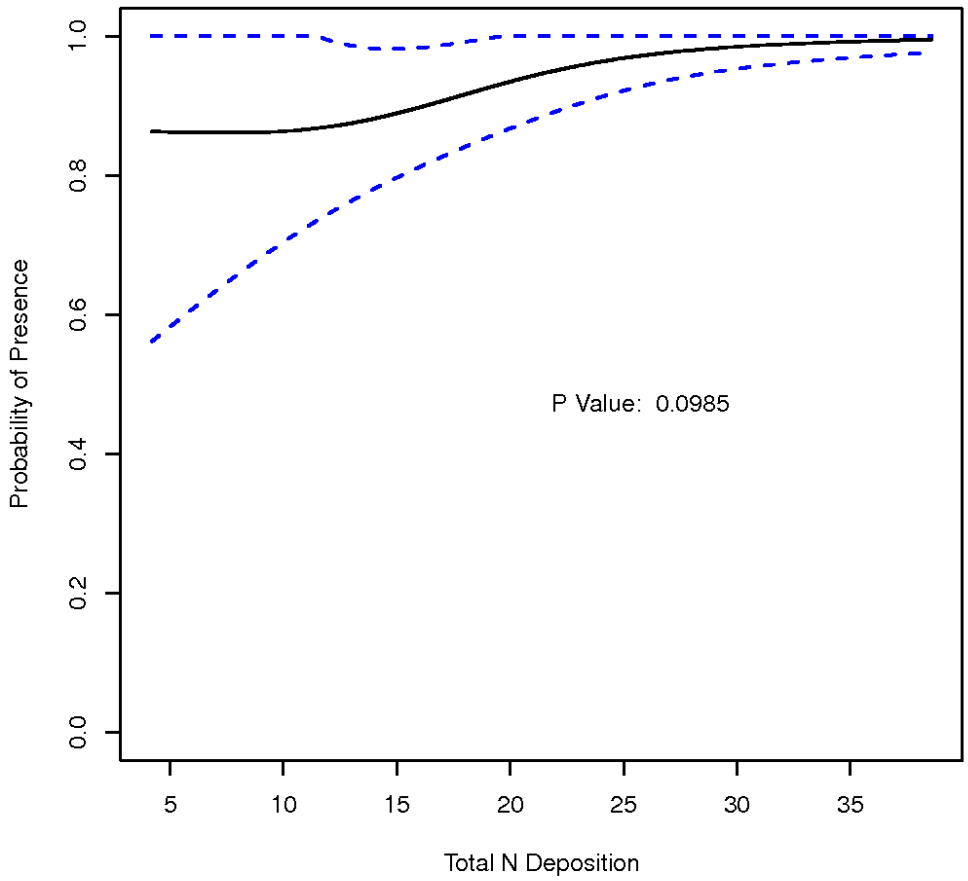

Figure A4.7. Spatial change in the probability of presence of *Lophozia ventricosa* in upland acid grassland with increasing total current inorganic N deposition (kg N ha^{-1} yr^{-1}). Data from BBS database.

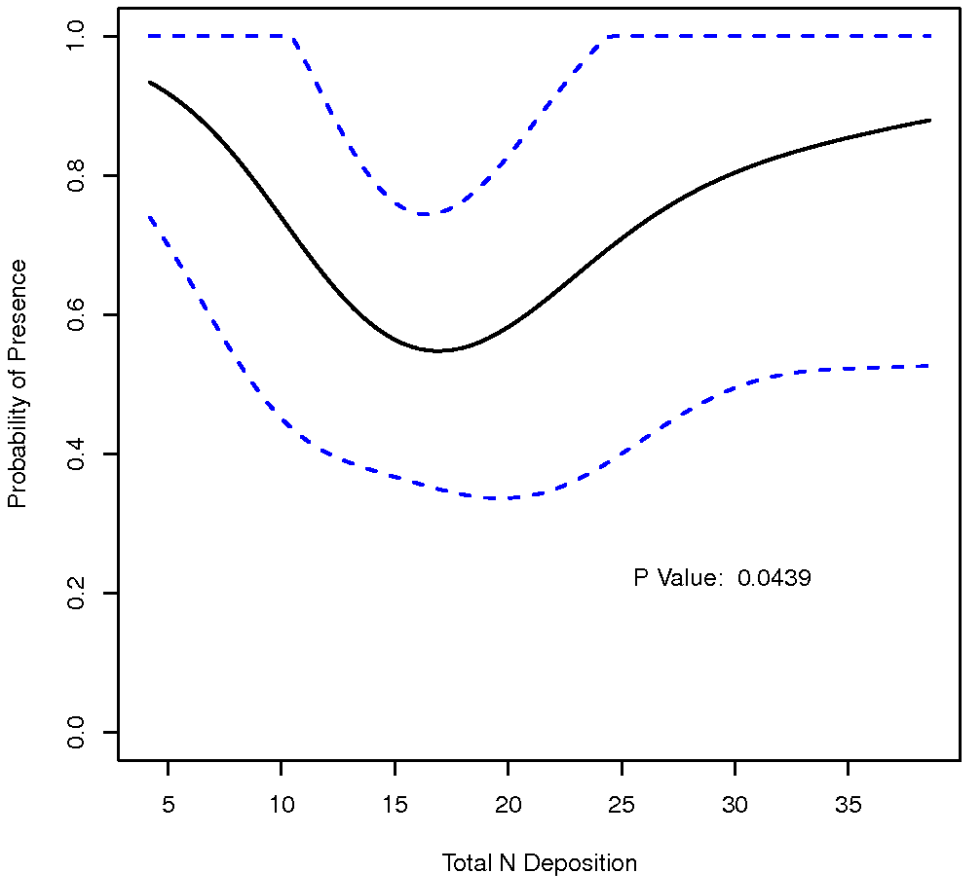

Figure A4.8. Spatial change in the probability of presence of *Marsupella emarginata* in upland acid grassland with increasing total current inorganic N deposition (kg N ha^{-1} yr^{-1}). Data from BBS database.

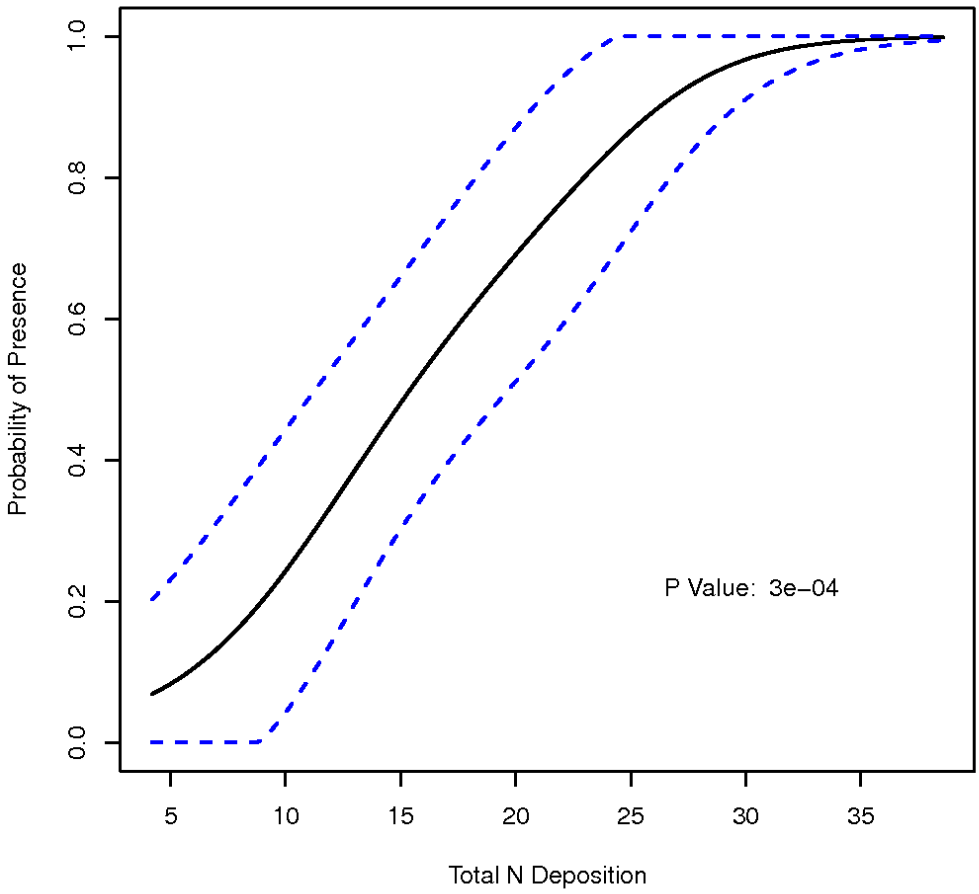

Figure A4.9. Spatial change in the probability of presence of *Racomitrium ericoides* in upland acid grassland with increasing total current inorganic N deposition (kg N ha^{-1} yr^{-1}). Data from BBS database.

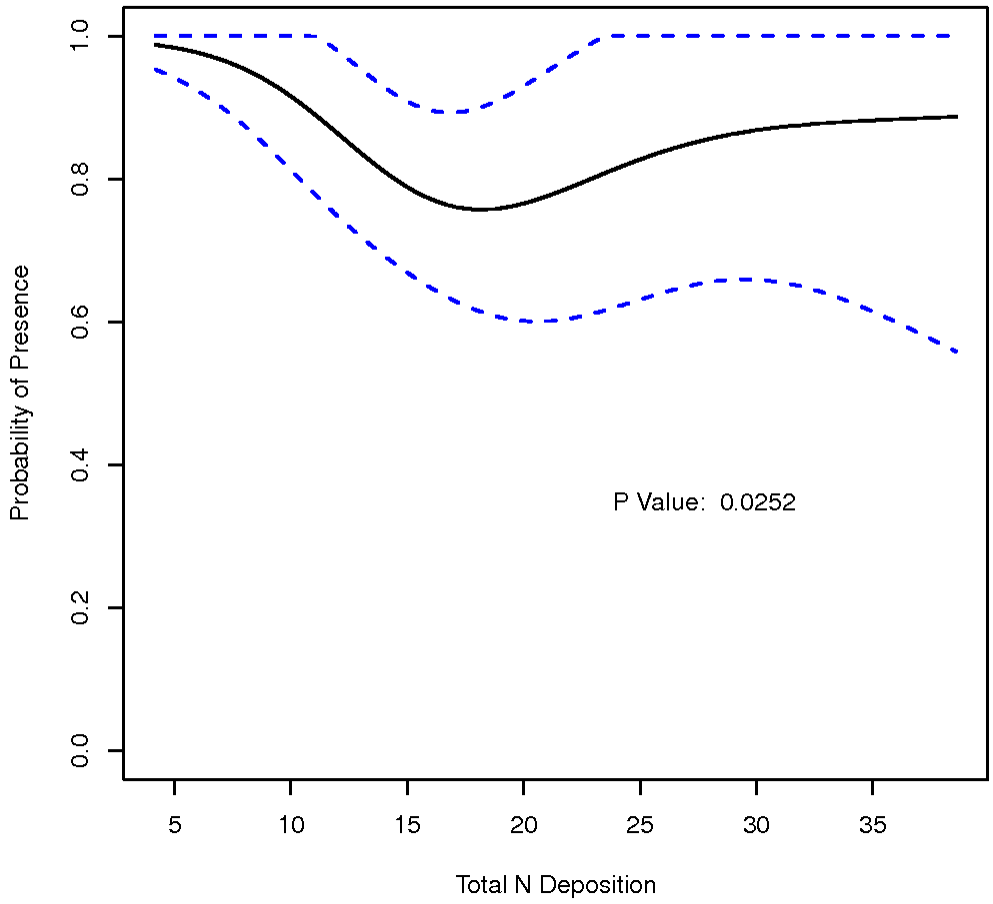

Figure A4.10. Spatial change in the probability of presence of *Racomitrium lanuginosum* in upland acid grassland with increasing total current inorganic N deposition (kg N ha^{-1} yr^{-1}). Data from BBS database.

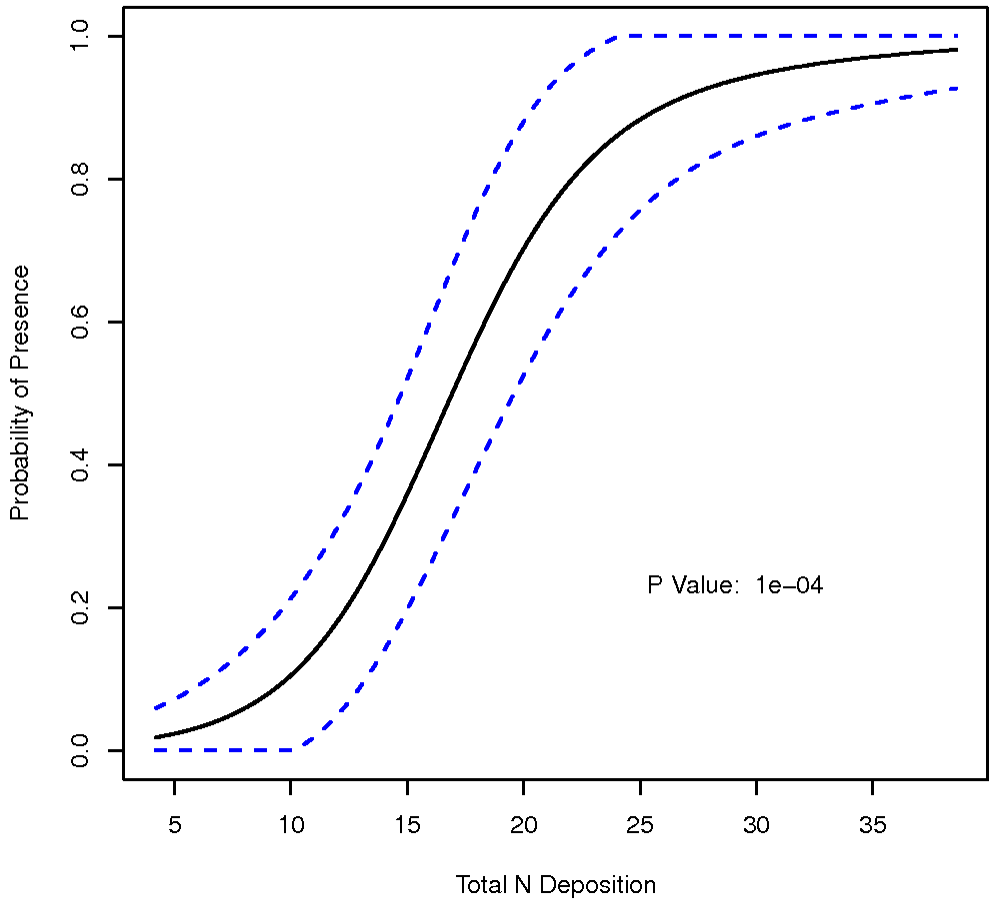

Figure A4.11. Spatial change in the probability of presence of *Sanionia uncinata* in upland acid grassland with increasing total current inorganic N deposition (kg N ha^{-1} yr^{-1}). Data from BBS database.

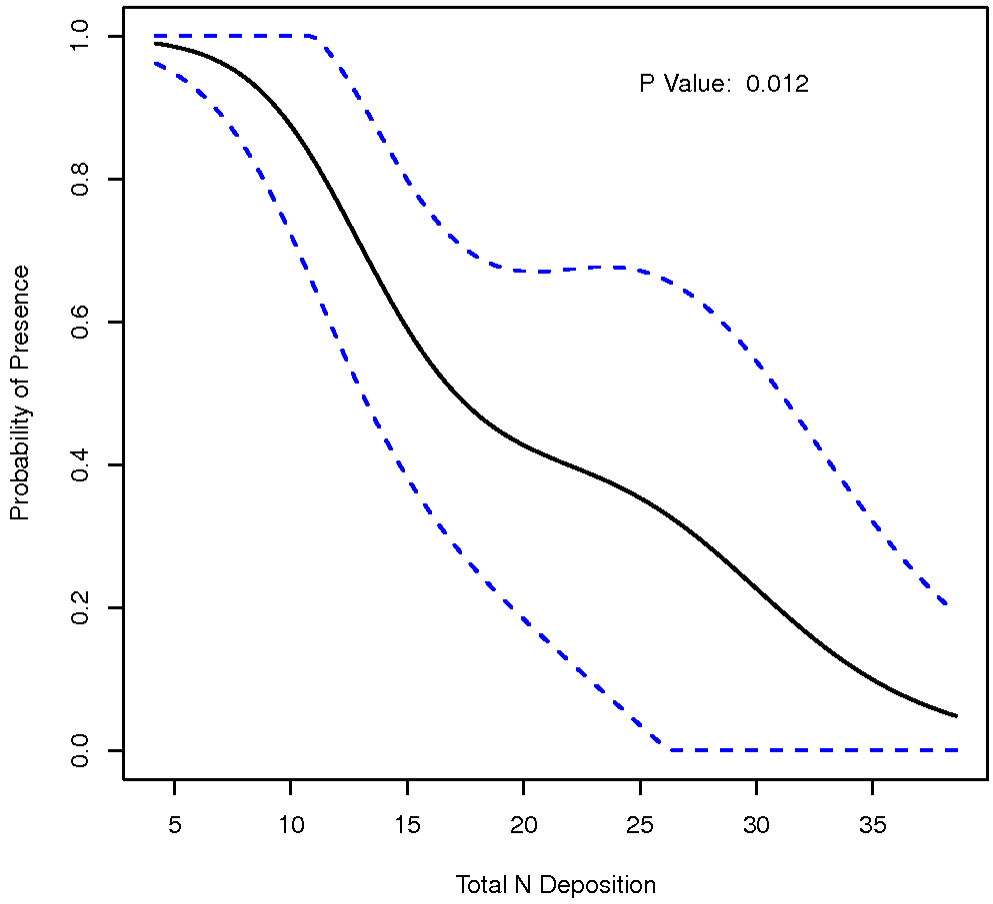

Figure A4.12. Spatial change in the probability of presence of *Scapania gracilis* in upland acid grassland with increasing total current inorganic N deposition (kg N ha^{-1} yr^{-1}). Data from BBS database.

Calcareous grassland – upland

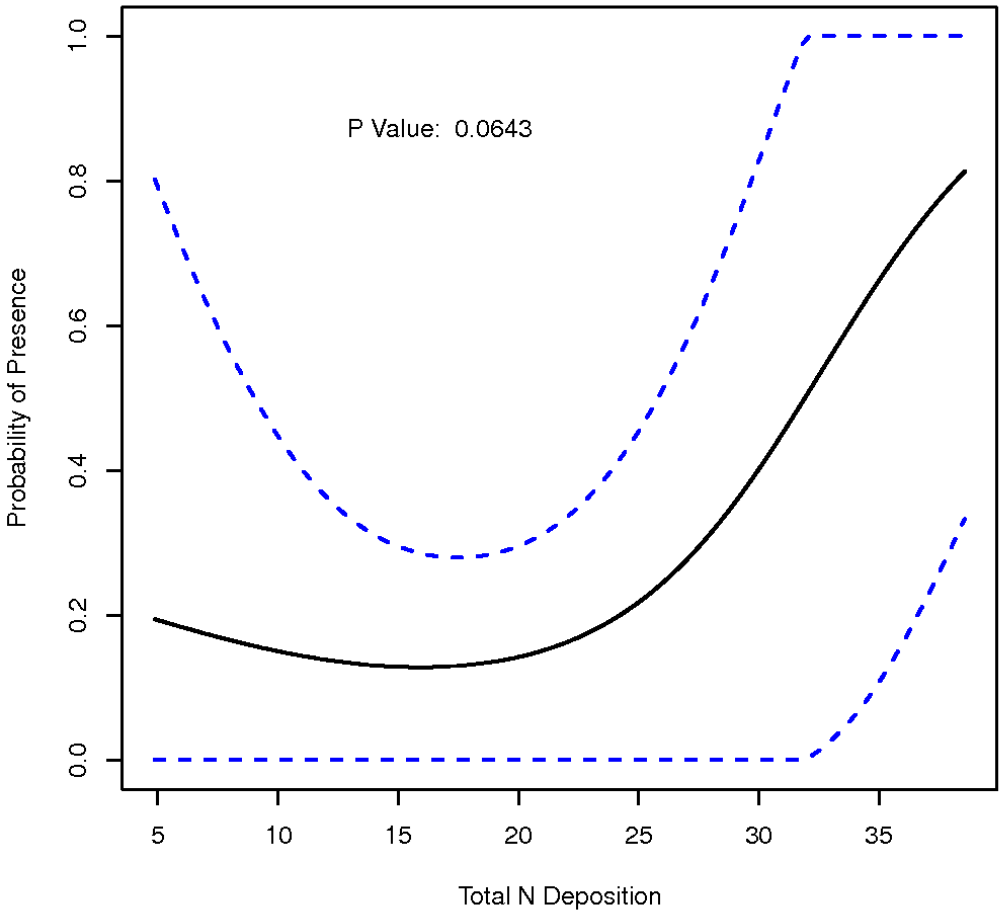

Figure A4.13. Spatial change in the probability of presence of *Didymodon vinealis* in upland calcareous grassland with increasing total current inorganic N deposition (kg N ha^{-1} yr^{-1}). Data from BBS database.

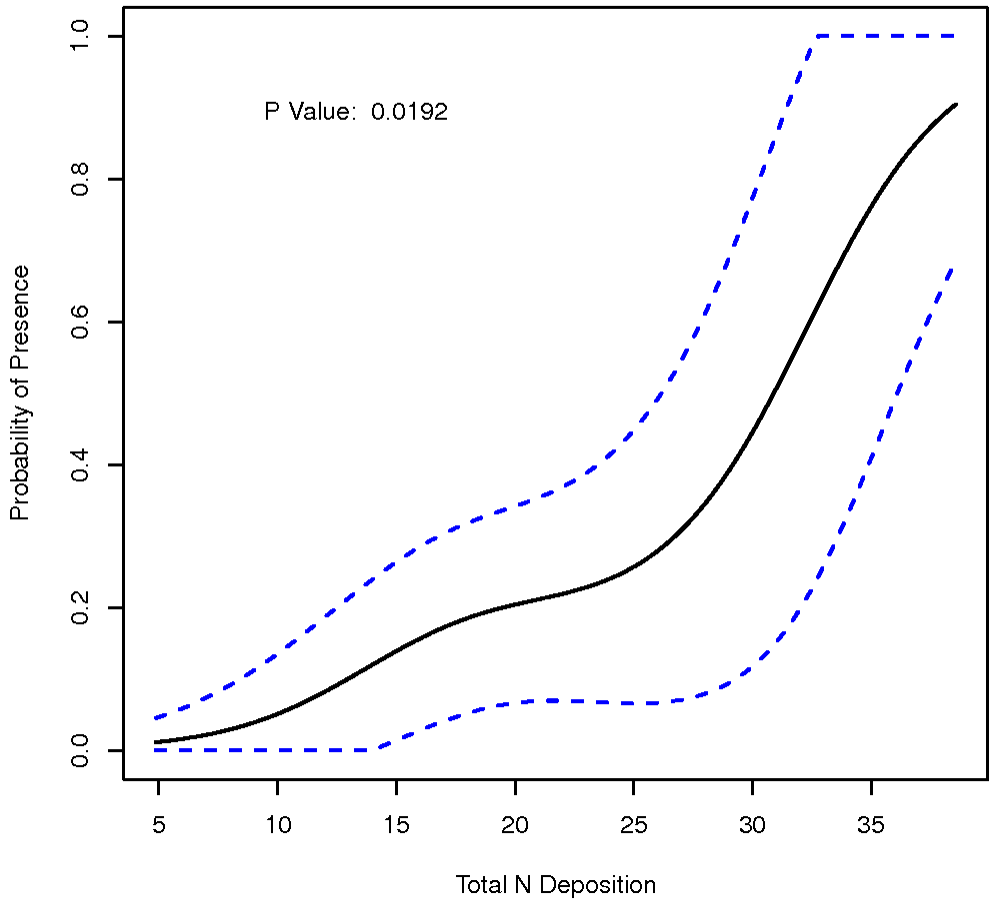

Figure A4.14. Spatial change in the probability of presence of *Leiocolea turbinata* in upland calcareous grassland with increasing total current inorganic N deposition (kg N ha^{-1} yr^{-1}). Data from BBS database.

Bog – upland

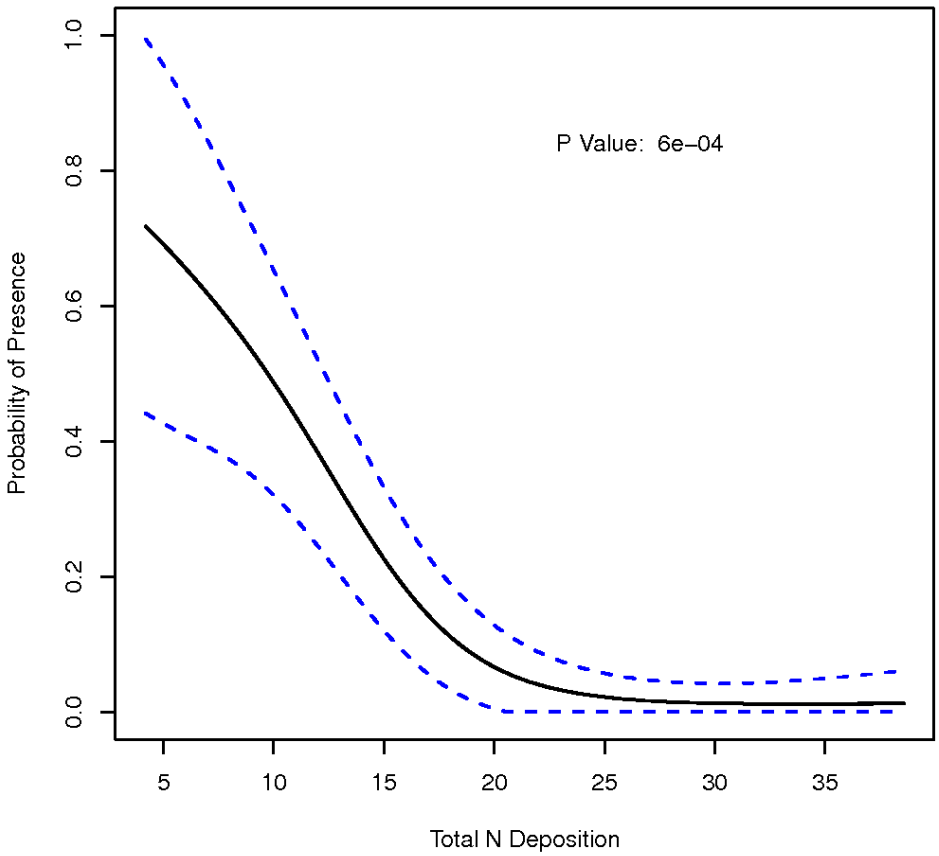

Figure A15. Spatial change in the probability of presence of *Anastrophyllum minutum* in upland bog with increasing total current inorganic N deposition (kg N ha^{-1} yr^{-1}). Data from BBS database.

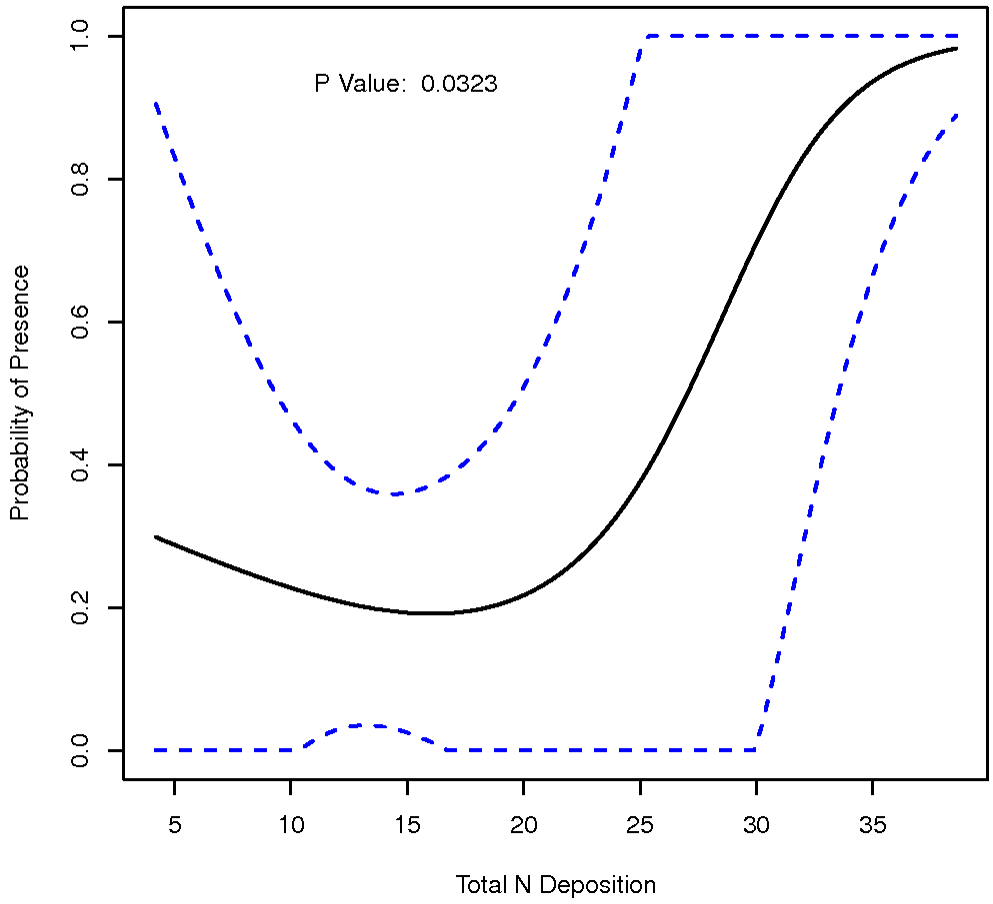

Figure A16. Spatial change in the probability of presence of *Calypogeia neesiana* in upland bog with increasing total current inorganic N deposition (kg N ha^{-1} yr^{-1}). Data from BBS database.

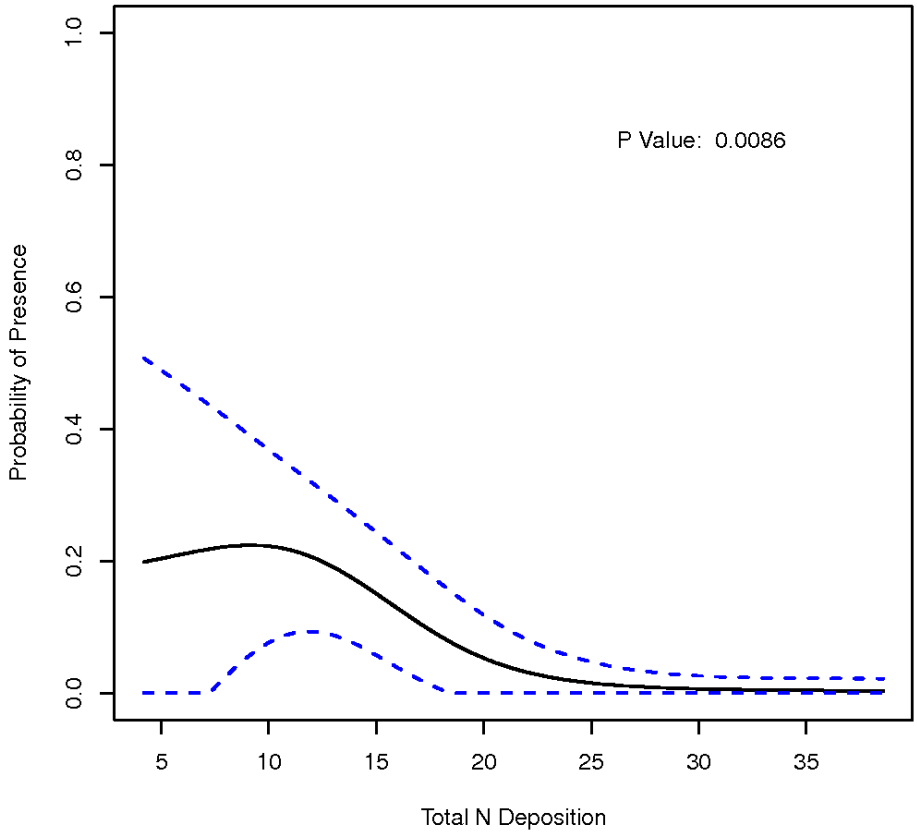

Figure A17. Spatial change in the probability of presence of *Calypogeia sphagnicola* in upland bog with increasing total current inorganic N deposition (kg N ha^{-1} yr^{-1}). Data from BBS database.

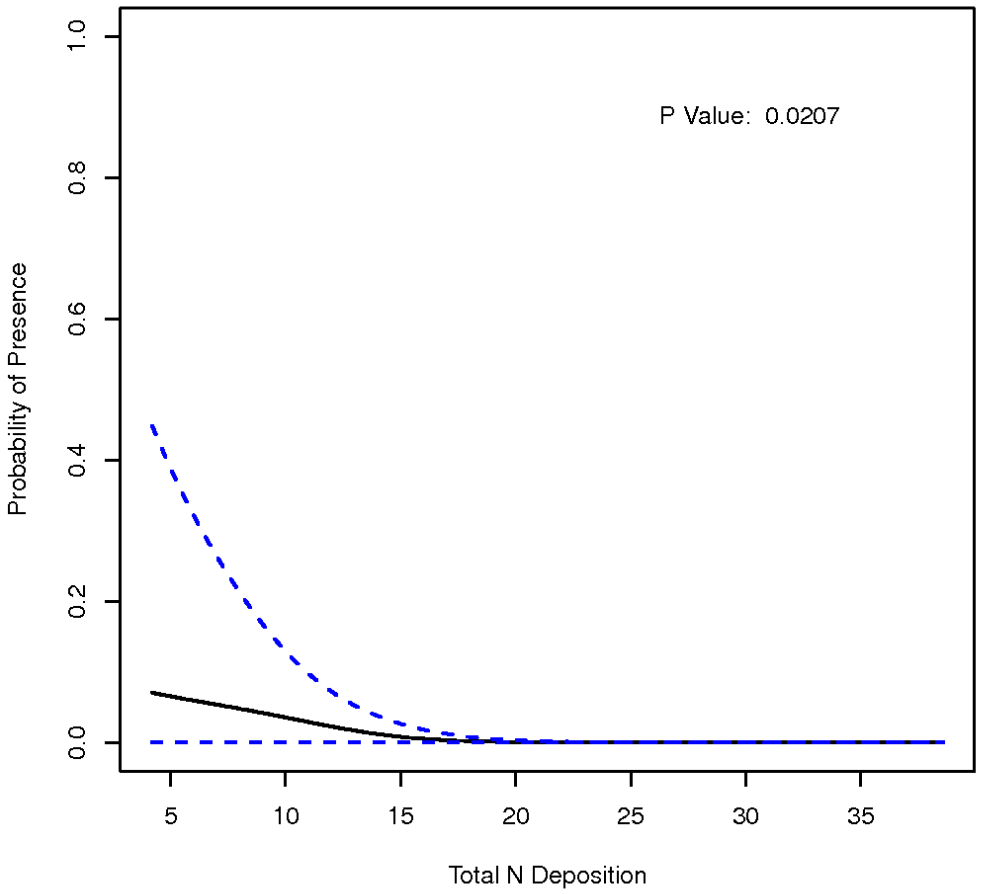

Figure A18. Spatial change in the probability of presence of *Cladopodiella fluitans* in upland bog with increasing total current inorganic N deposition (kg N ha^{-1} yr^{-1}). Data from BBS database.

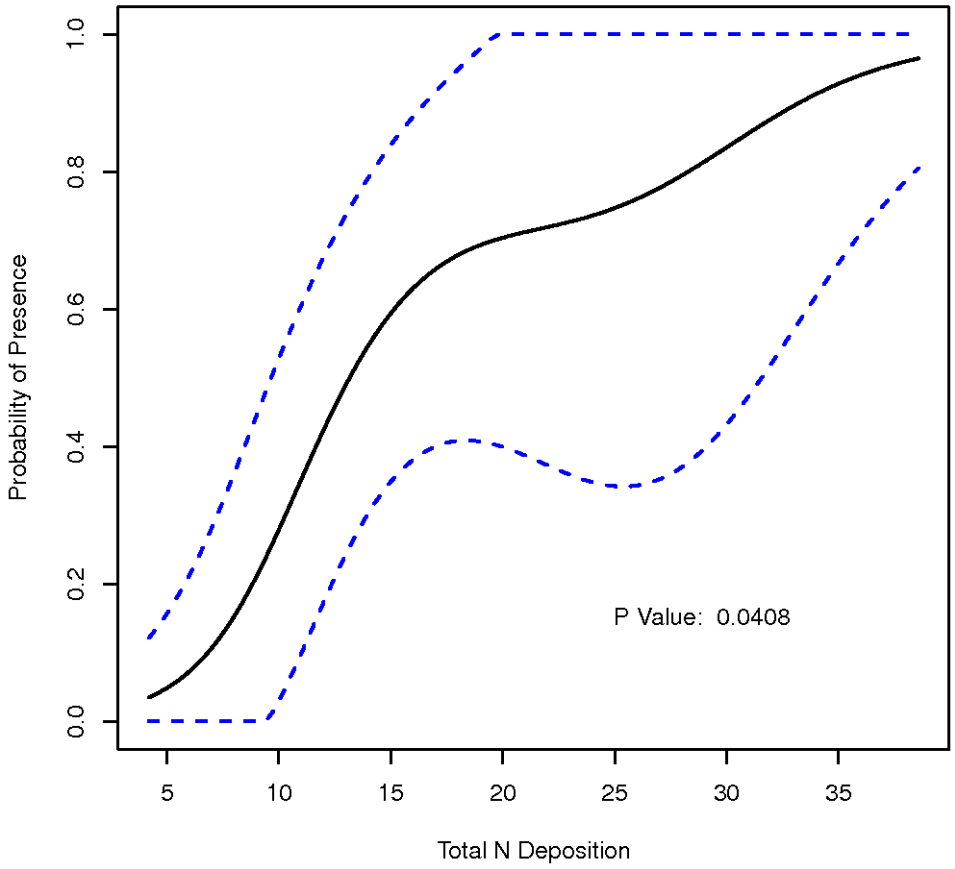

Figure A19. Spatial change in the probability of presence of *Dicranum bonjeanii* in upland bog with increasing total current inorganic N deposition (kg N ha^{-1} yr^{-1}). Data from BBS database.

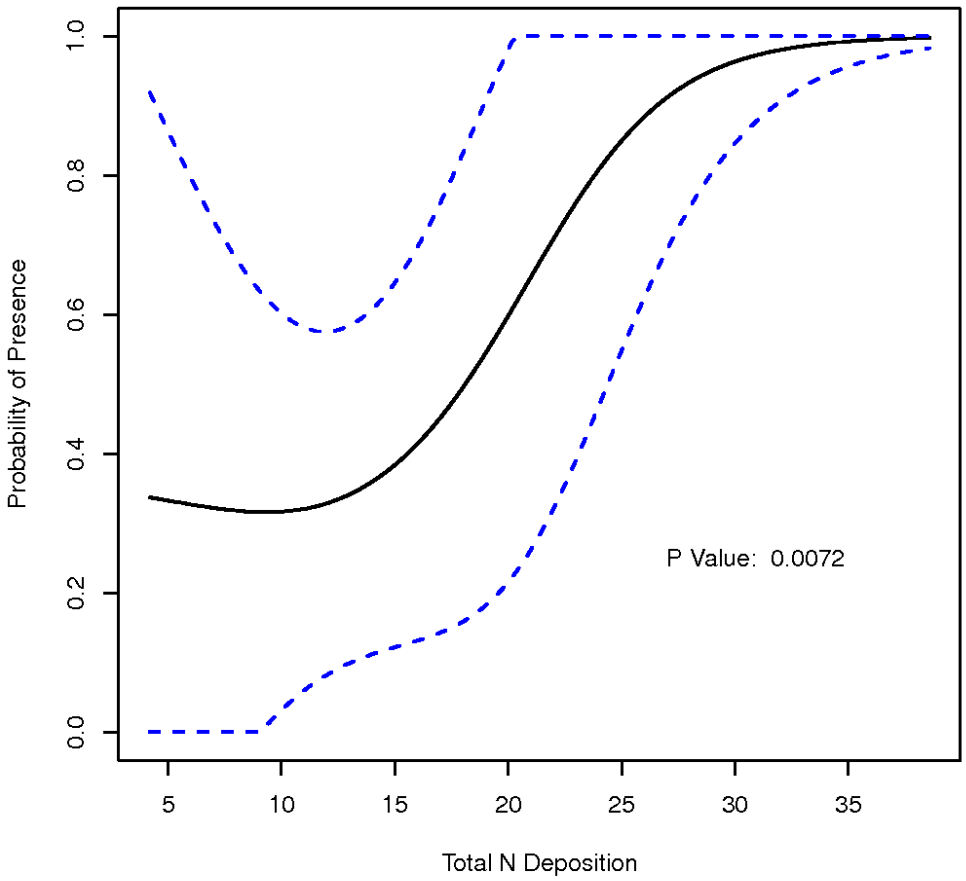

Figure A20. Spatial change in the probability of presence of *Gymnocolea inflata* in upland bog with increasing total current inorganic N deposition (kg N ha^{-1} yr^{-1}). Data from BBS database.

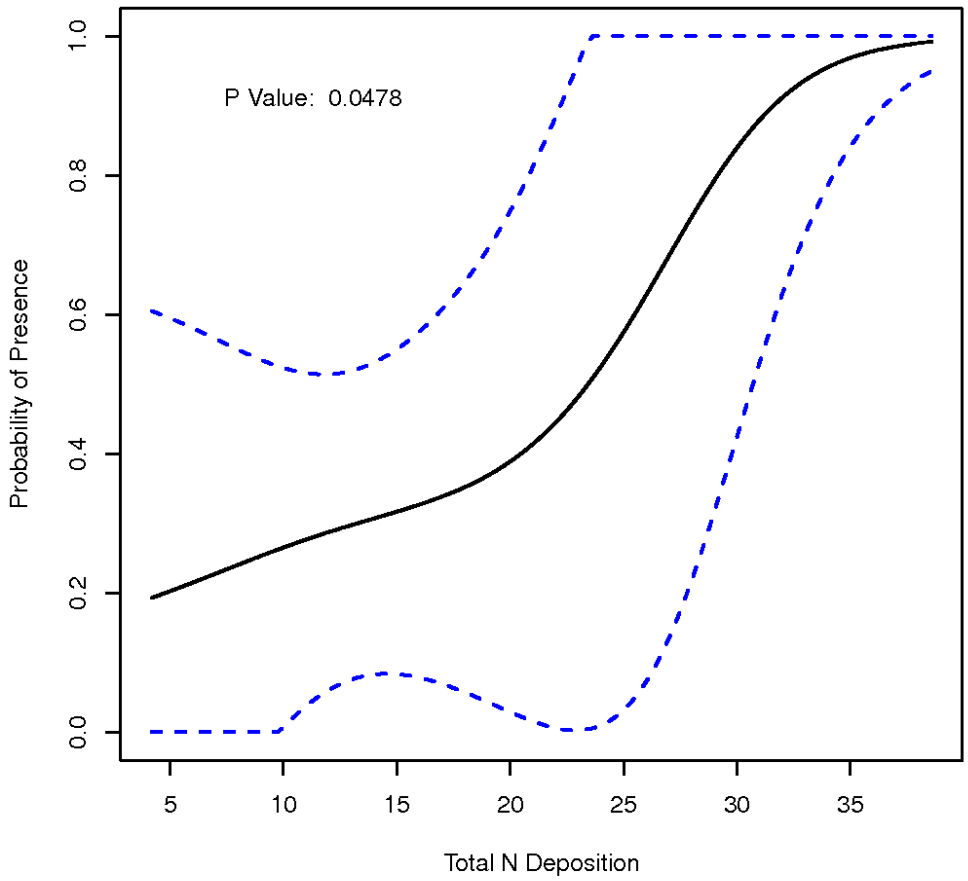

Figure A21. Spatial change in the probability of presence of *Lophozia incisa* in upland bog with increasing total current inorganic N deposition (kg N ha^{-1} yr^{-1}). Data from BBS database.

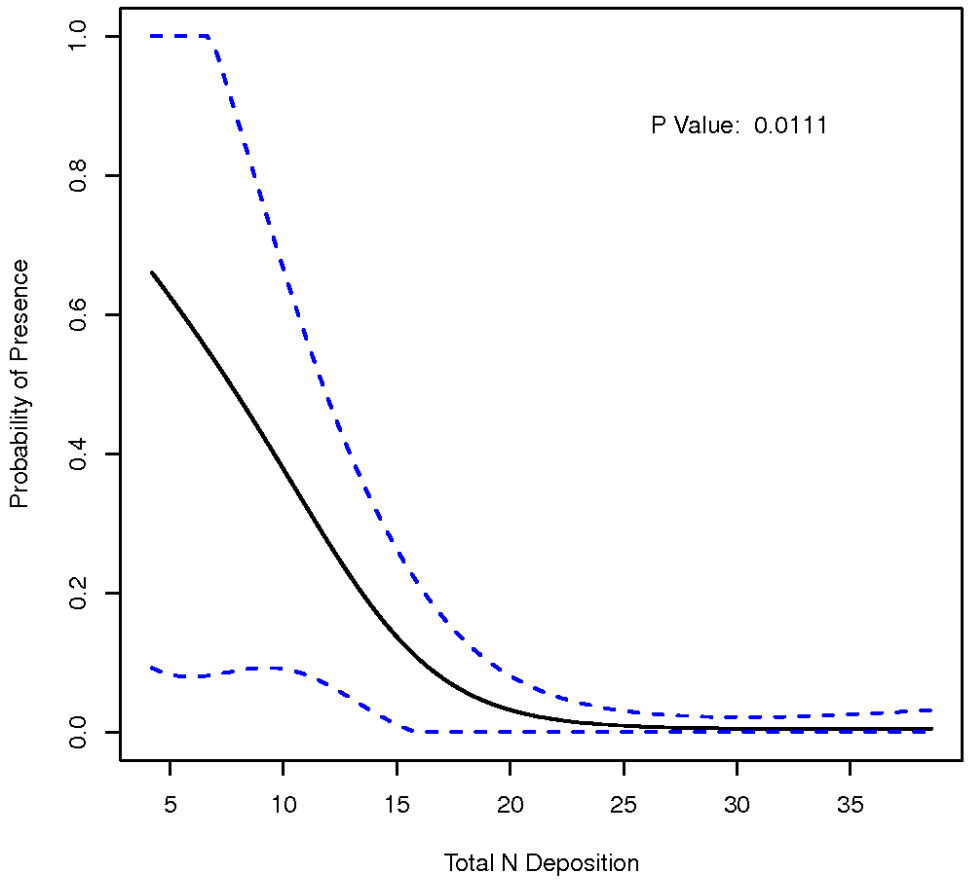

Figure A22. Spatial change in the probability of presence of *Odontoschisma denudatum* in upland bog with increasing total current inorganic N deposition (kg N ha^{-1} yr^{-1}). Data from BBS database.

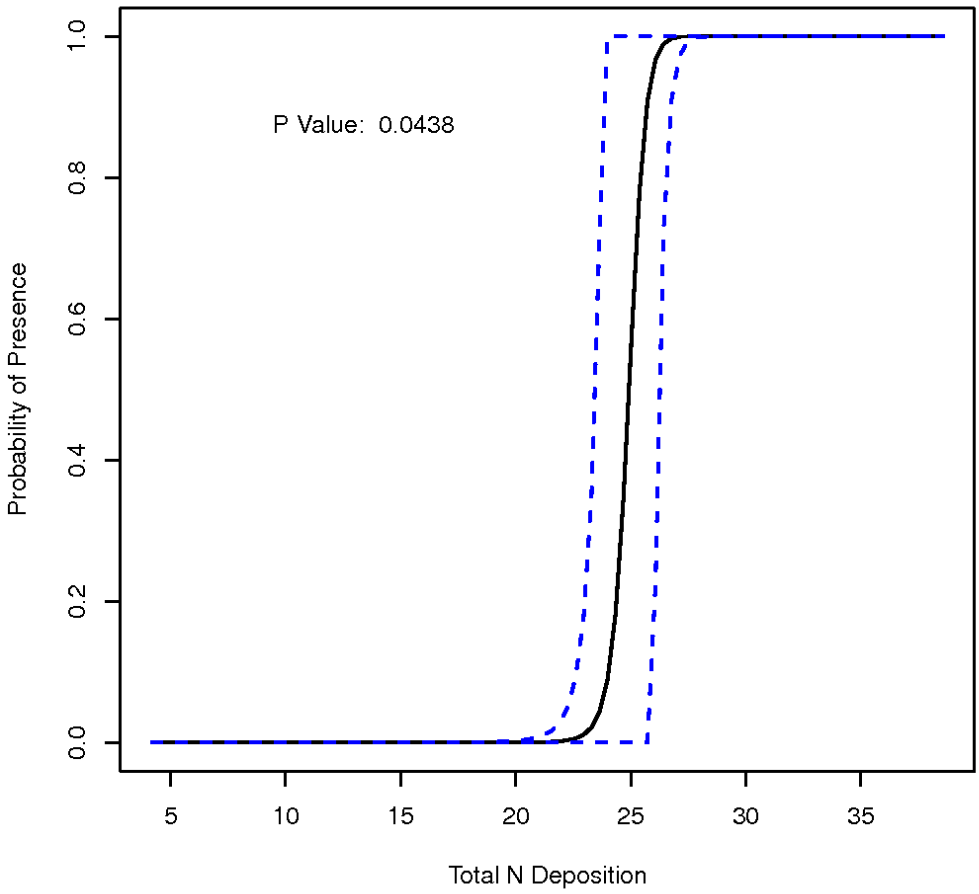

Figure A23. Spatial change in the probability of presence of *Pleurozia purpurea* in upland bog with increasing total current inorganic N deposition (kg N ha^{-1} yr^{-1}). Data from BBS database.

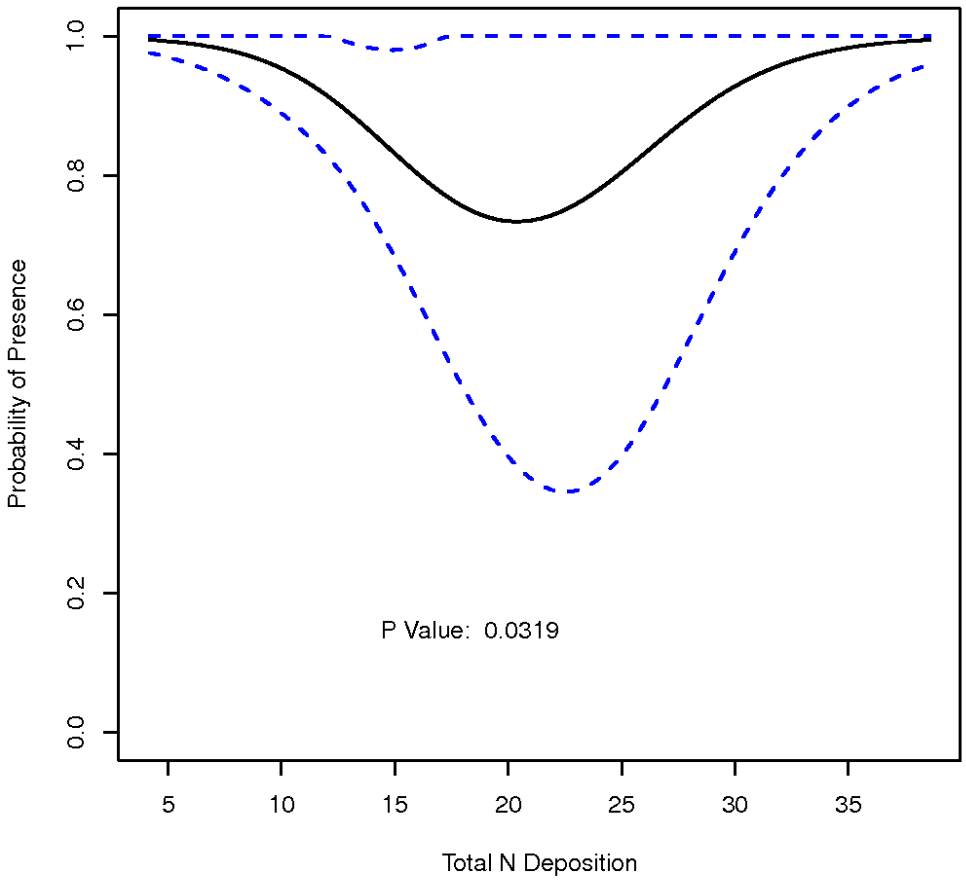

Figure A24. Spatial change in the probability of presence of *Racomitrium lanuginosum* in upland bog with increasing total current inorganic N deposition (kg N ha^{-1} yr^{-1}). Data from BBS database.

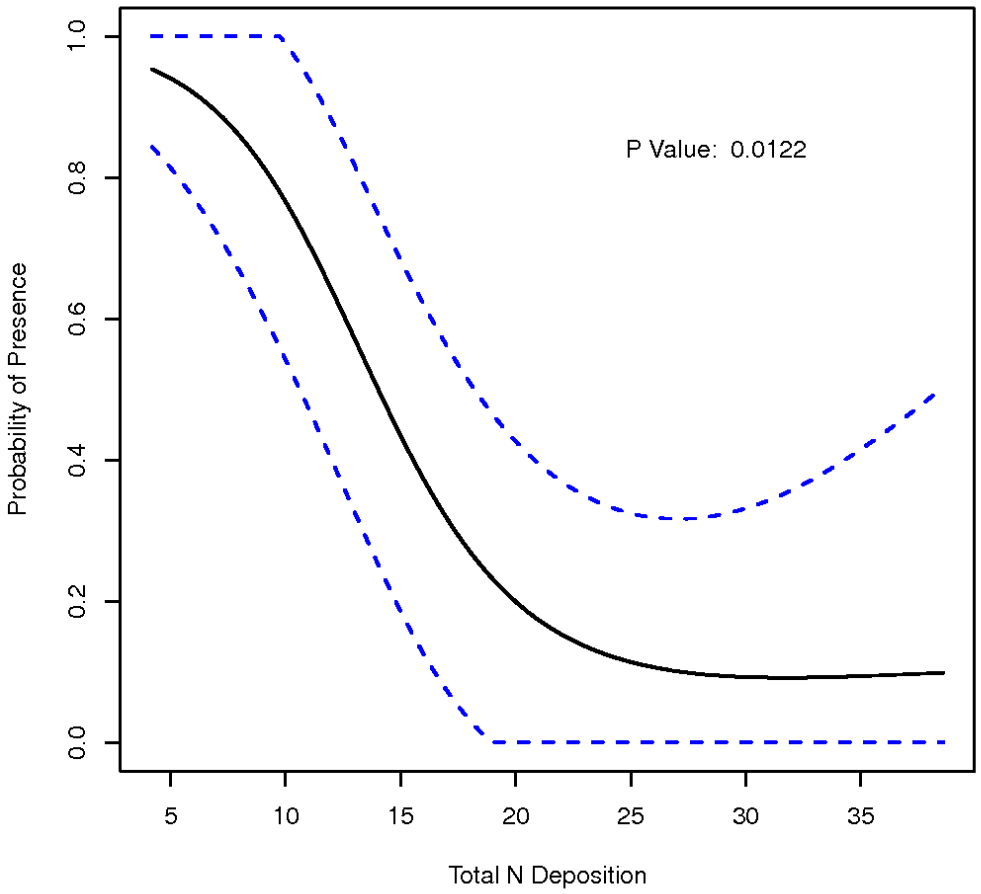

Figure A25. Spatial change in the probability of presence of *Scapania umbrosa* in upland bog with increasing total current inorganic N deposition (kg N ha^{-1} yr^{-1}). Data from BBS database.

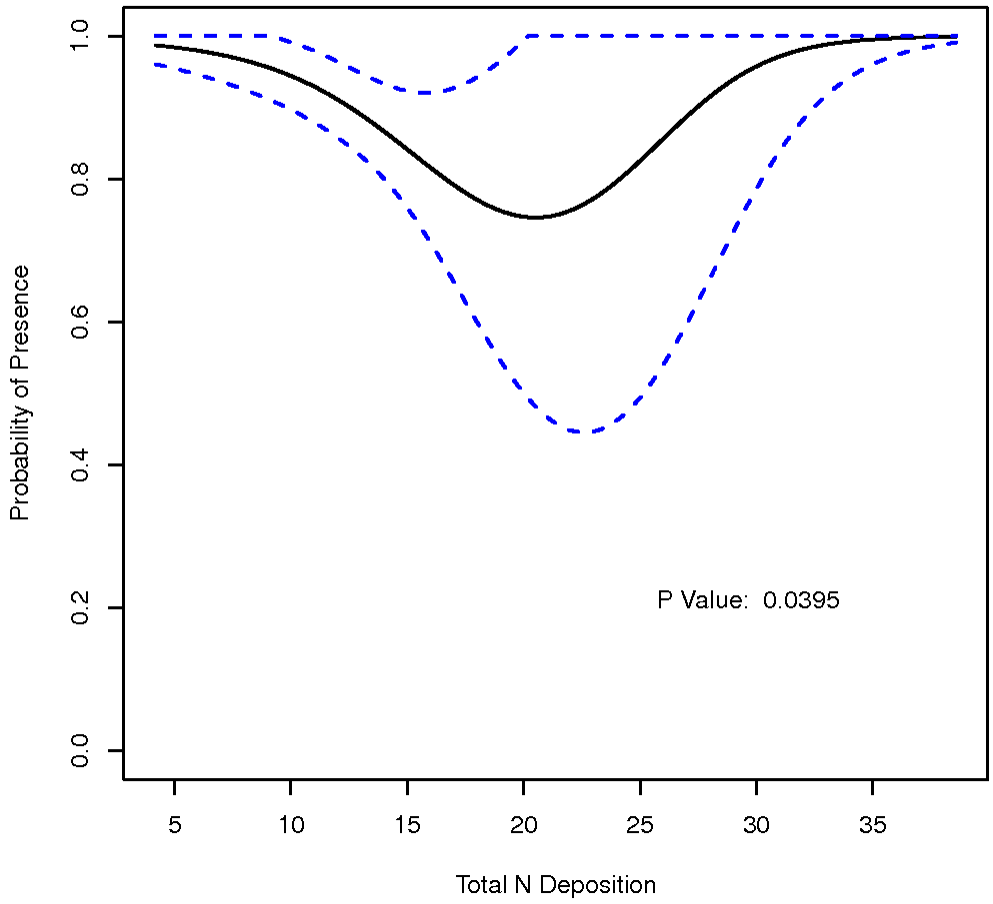

Figure A26. Spatial change in the probability of presence of *Scapania undulata* in upland bog with increasing total current inorganic N deposition (kg N ha^{-1} yr^{-1}). Data from BBS database.

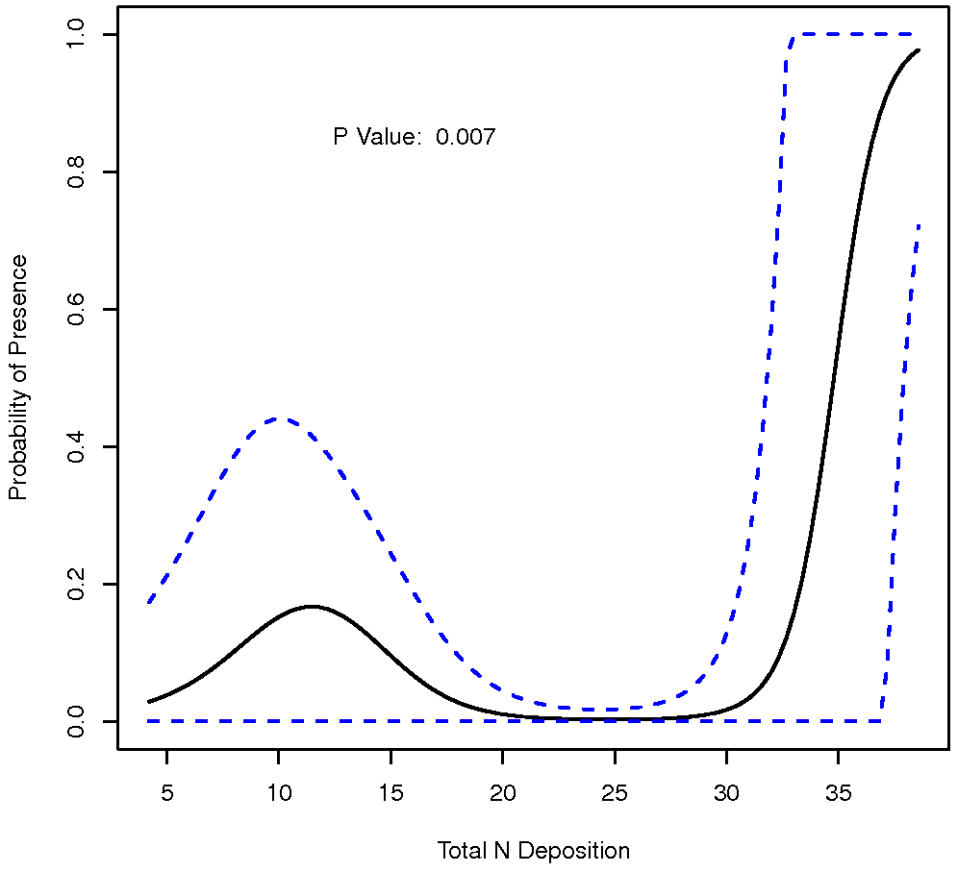

Figure A27. Spatial change in the probability of presence of *Sphagnum austinii* in upland bog with increasing total current inorganic N deposition (kg N ha^{-1} yr^{-1}). Data from BBS database.

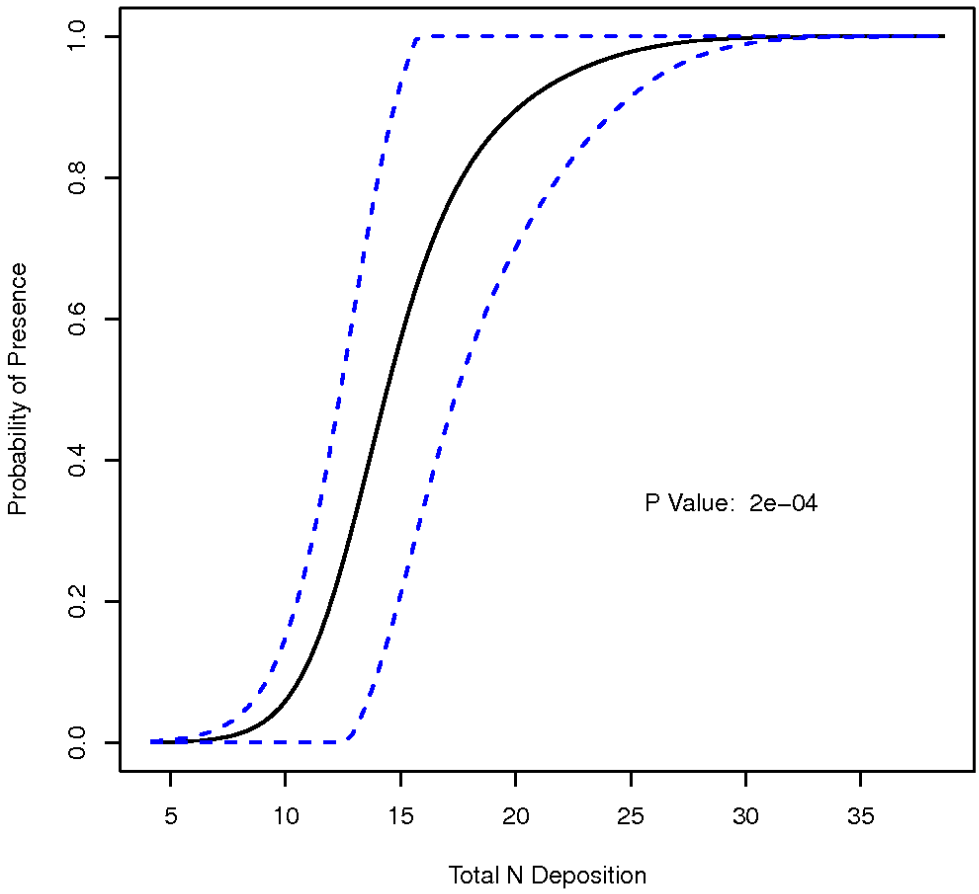

Figure A28. Spatial change in the probability of presence of *Warnstorfia fluitans* in upland bog with increasing total current inorganic N deposition (kg N ha^{-1} yr^{-1}). Data from BBS database.

Heathland – upland

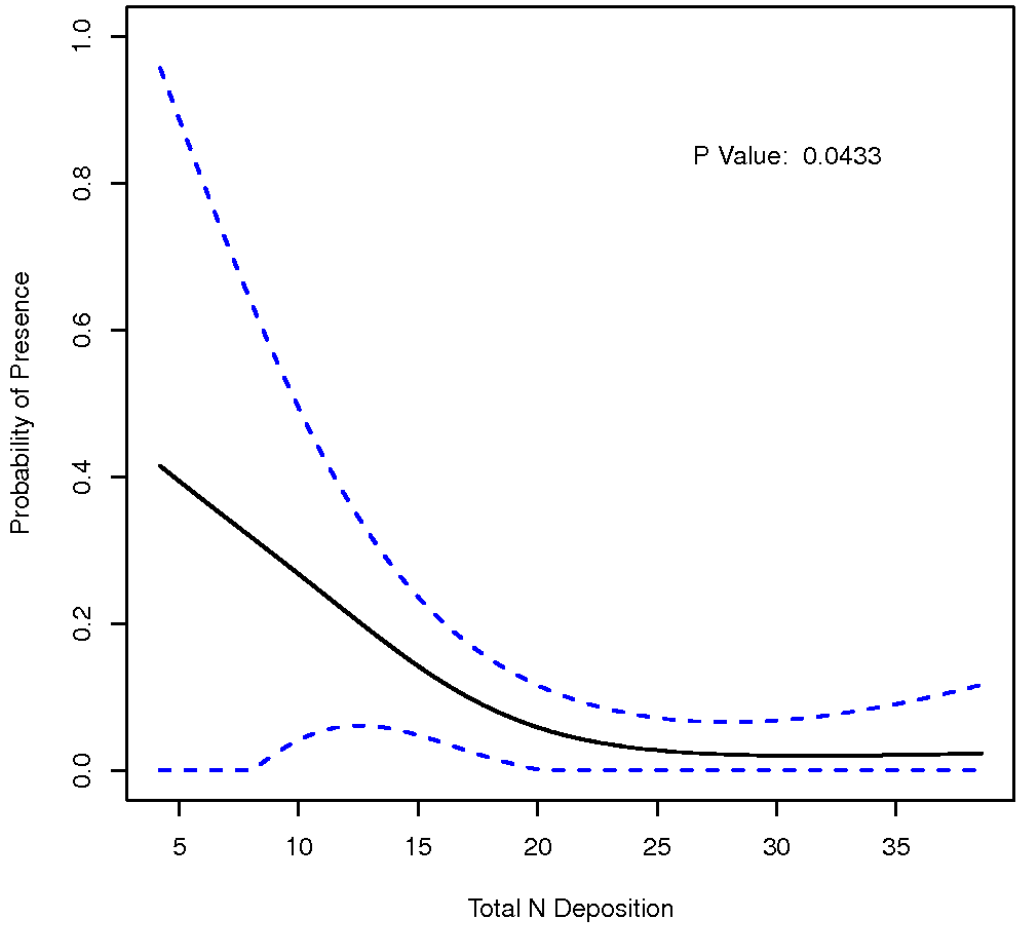

Figure A29. Spatial change in the probability of presence of *Anastrophyllum minutum* in upland heathland with increasing total current inorganic N deposition (kg N ha^{-1} yr^{-1}). Data from BBS database.

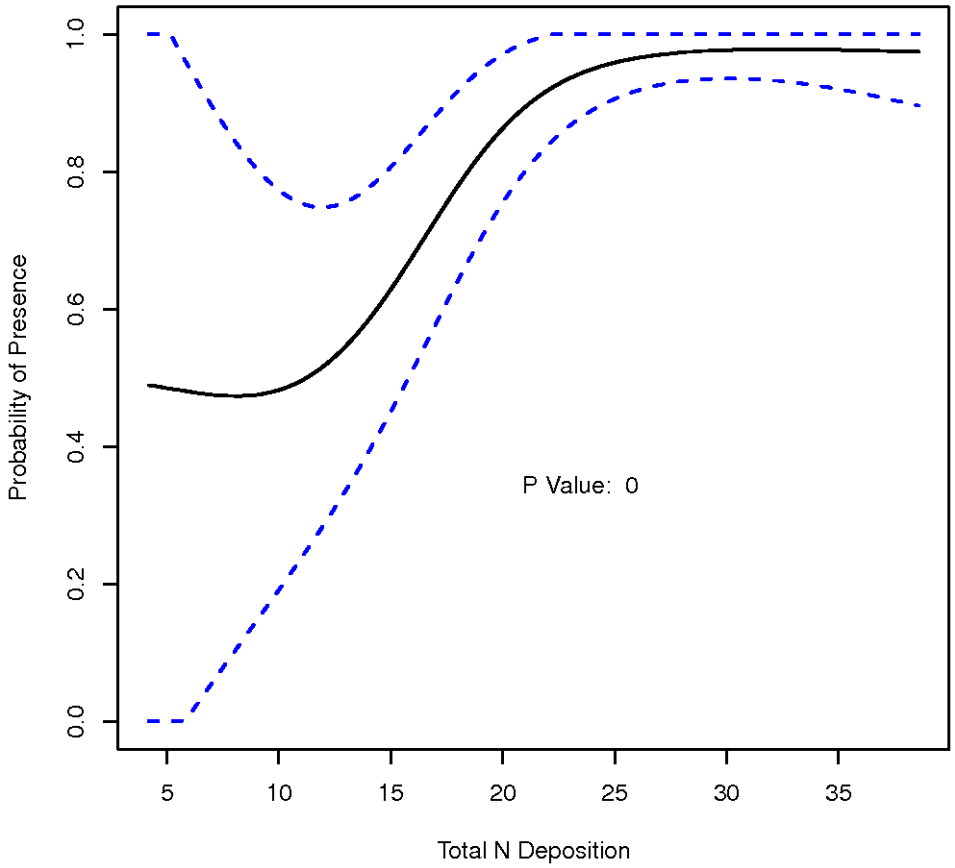

Figure A30. Spatial change in the probability of presence of *Aulacomnium palustre* in upland heathland with increasing total current inorganic N deposition (kg N ha^{-1} yr^{-1}). Data from BBS database.

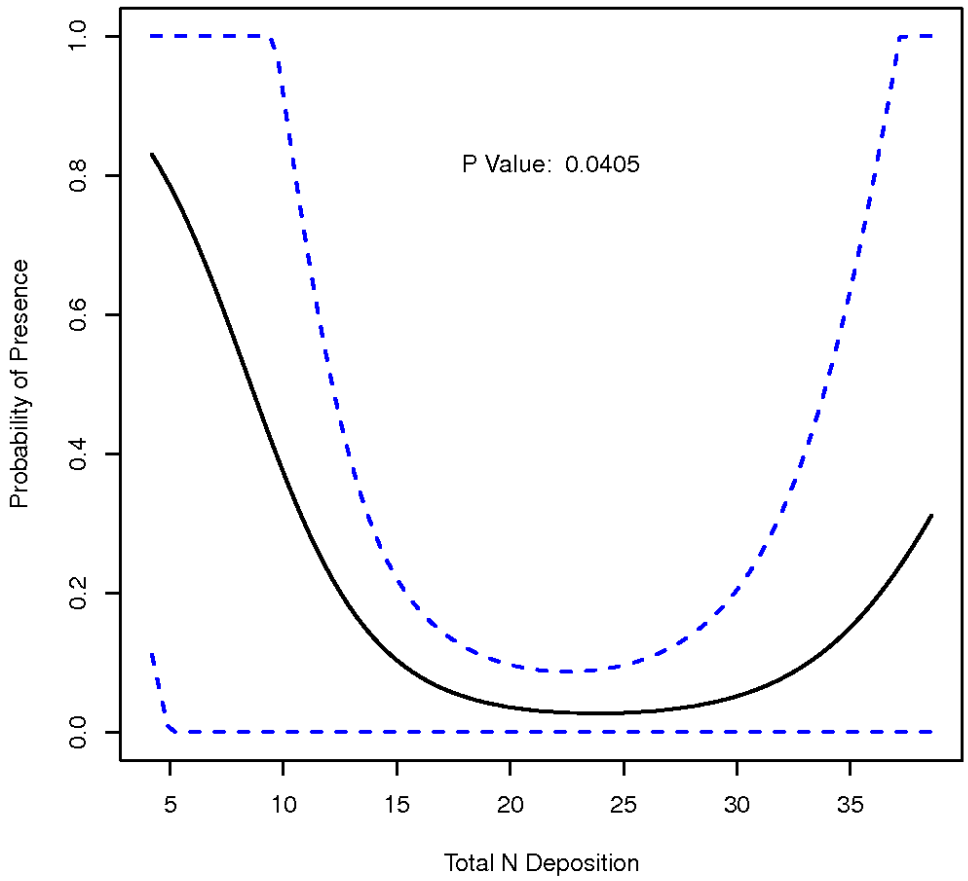

Figure A31. Spatial change in the probability of presence of *Barbilophozia atlantica* in upland heathland with increasing total current inorganic N deposition (kg N ha^{-1} yr^{-1}). Data from BBS database.

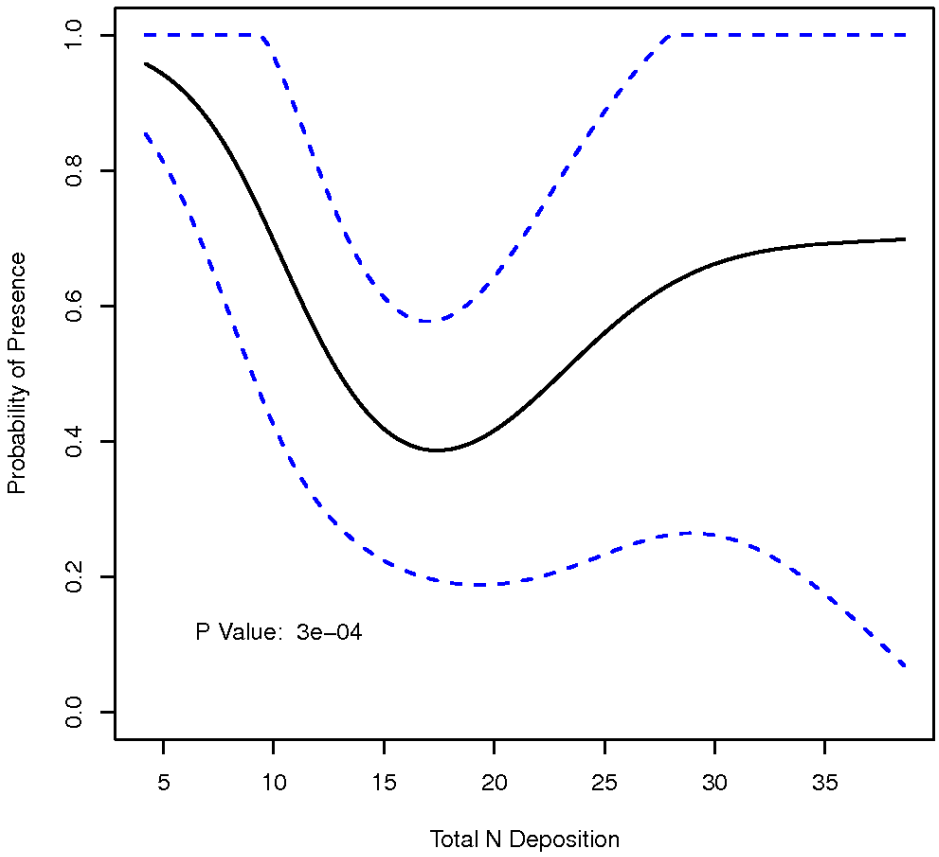

Figure A32. Spatial change in the probability of presence of *Barbilophozia attenuate* in upland heathland with increasing total current inorganic N deposition (kg N ha^{-1} yr^{-1}). Data from BBS database.

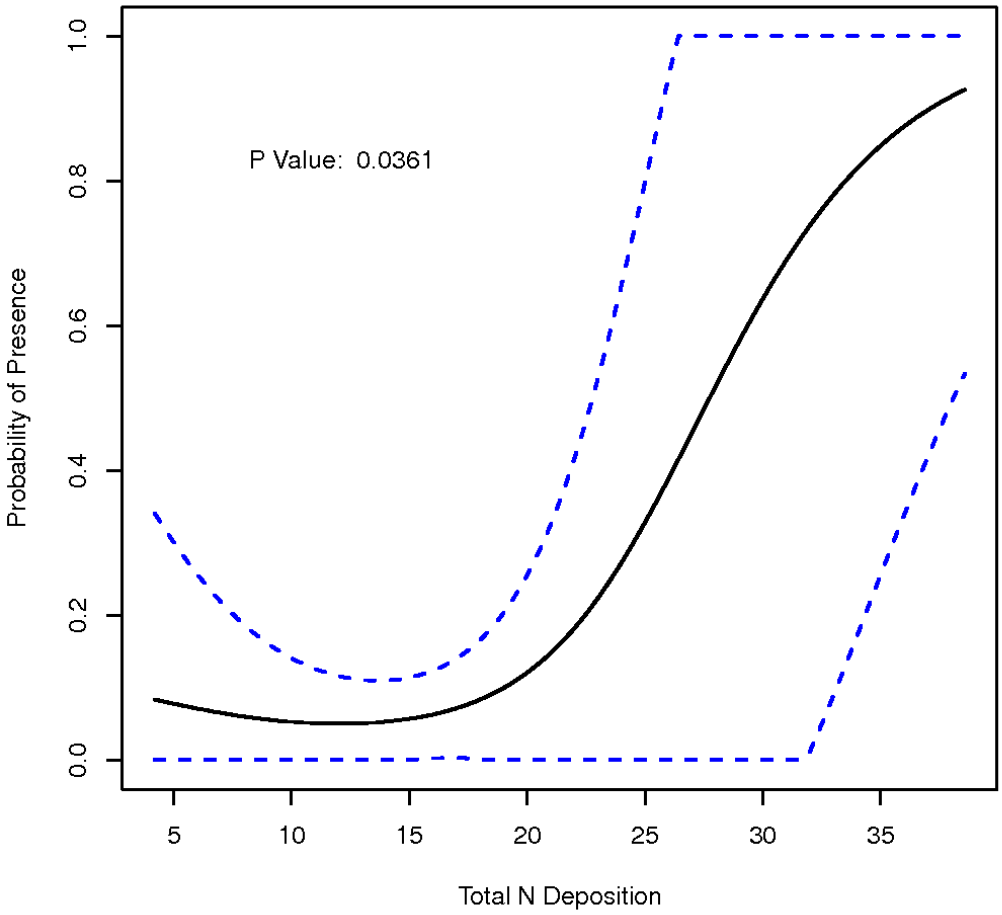

Figure A33. Spatial change in the probability of presence of *Barbilophozia hatcheri* in upland heathland with increasing total current inorganic N deposition (kg N ha^{-1} yr^{-1}). Data from BBS database.

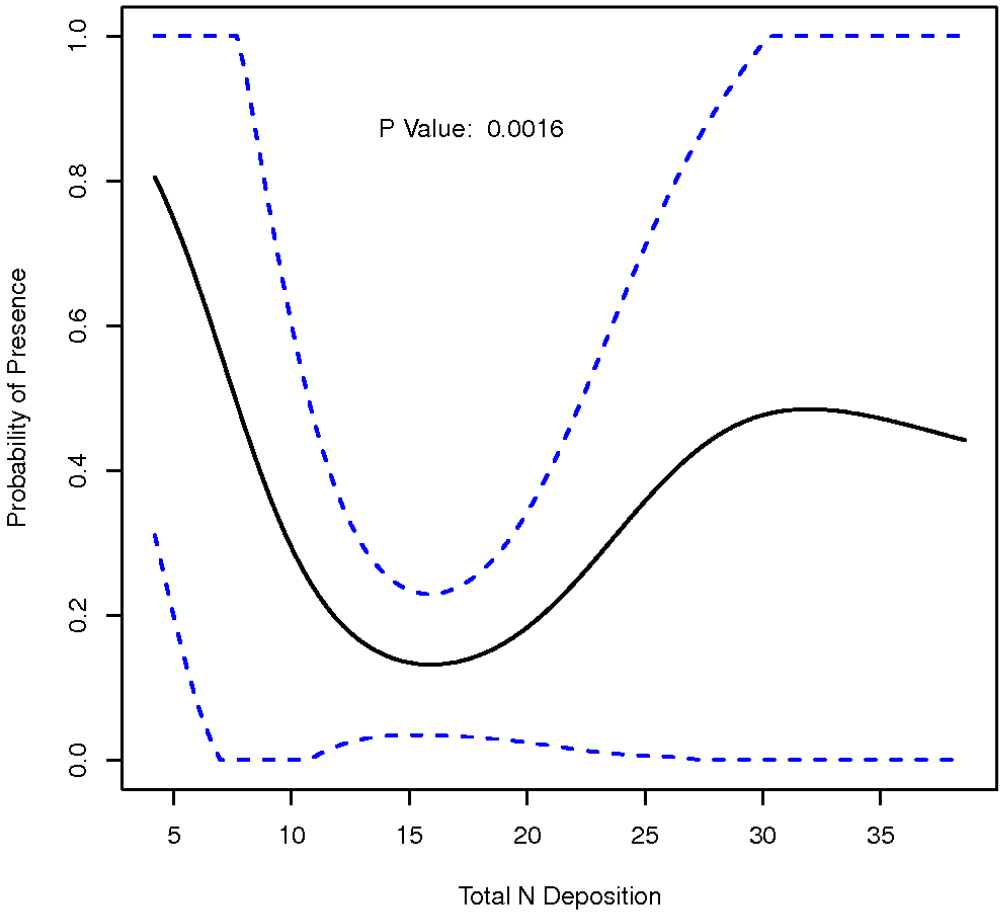

Figure A34. Spatial change in the probability of presence of *Bryum alpinum* in upland heathland with increasing total current inorganic N deposition (kg N ha^{-1} yr^{-1}). Data from BBS database.

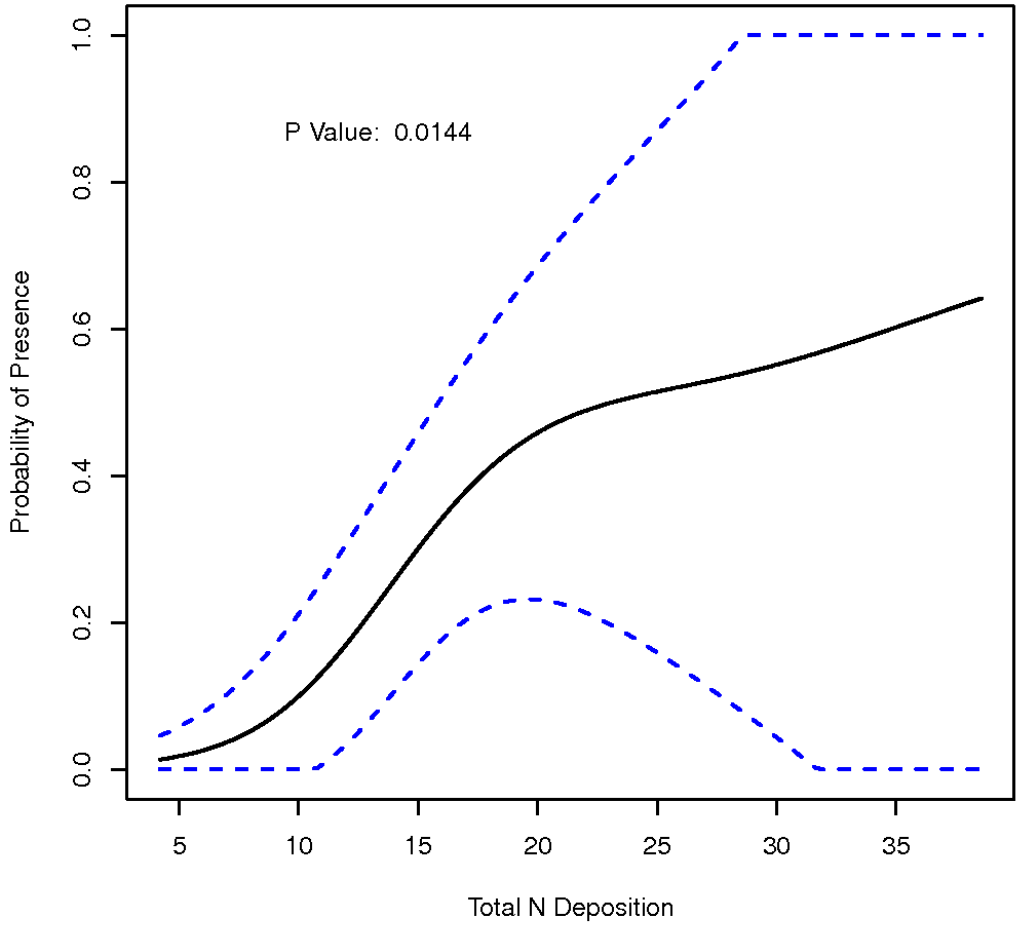

Figure A35. Spatial change in the probability of presence of *Calypogeia arguta* in upland heathland with increasing total current inorganic N deposition (kg N ha^{-1} yr^{-1}). Data from BBS database.

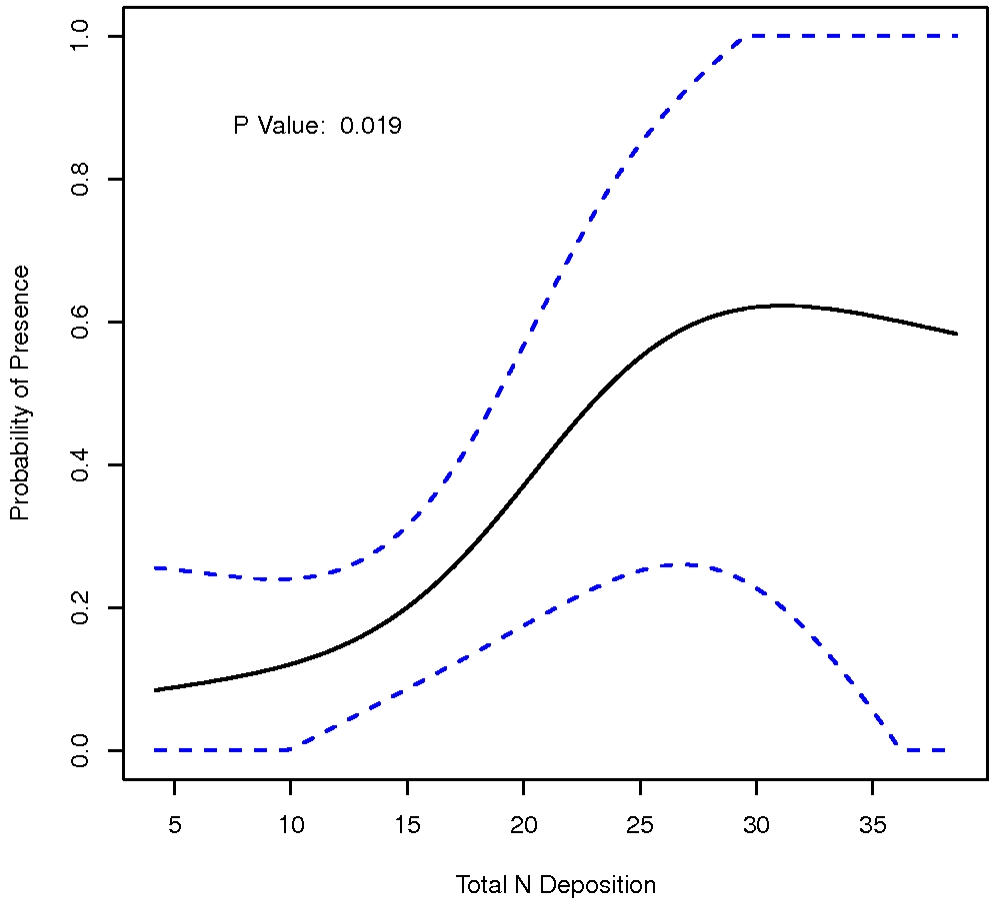

Figure A36. Spatial change in the probability of presence of *Cephalozia connivens* in upland heathland with increasing total current inorganic N deposition (kg N ha^{-1} yr^{-1}). Data from BBS database.

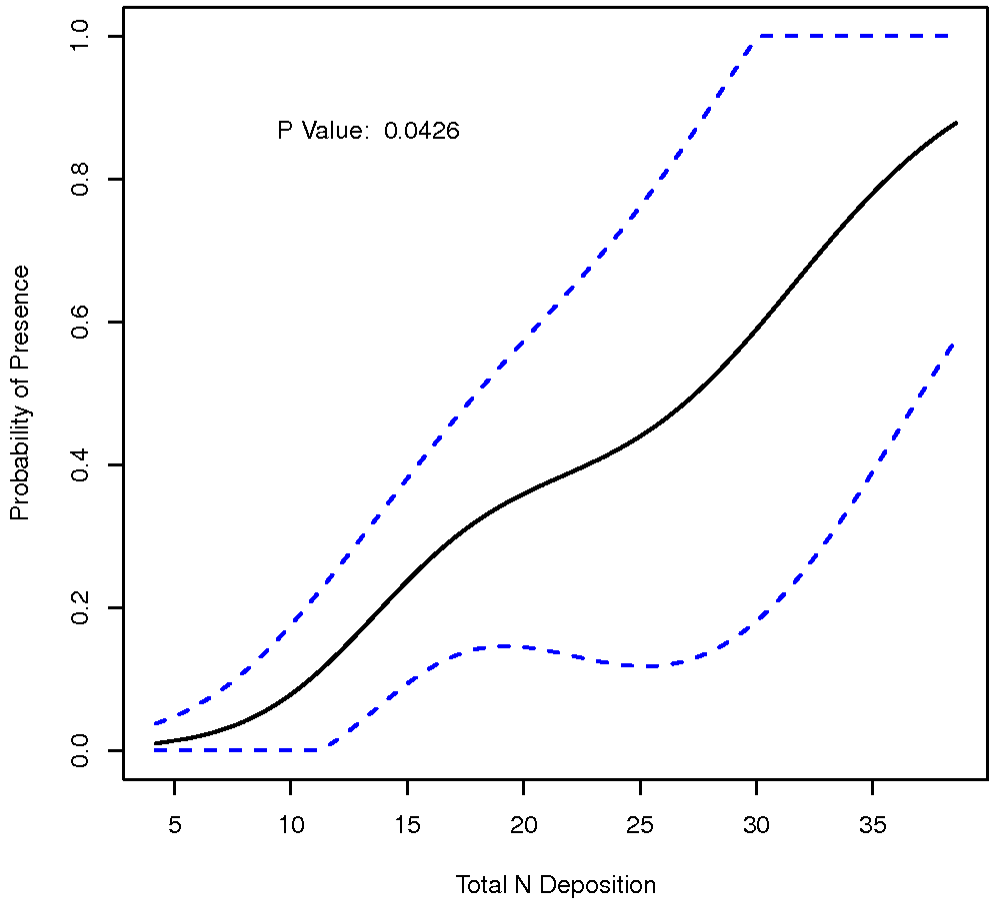

Figure A37. Spatial change in the probability of presence of *Dicranella schreberiana* in upland heathland with increasing total current inorganic N deposition (kg N ha^{-1} yr^{-1}). Data from BBS database.

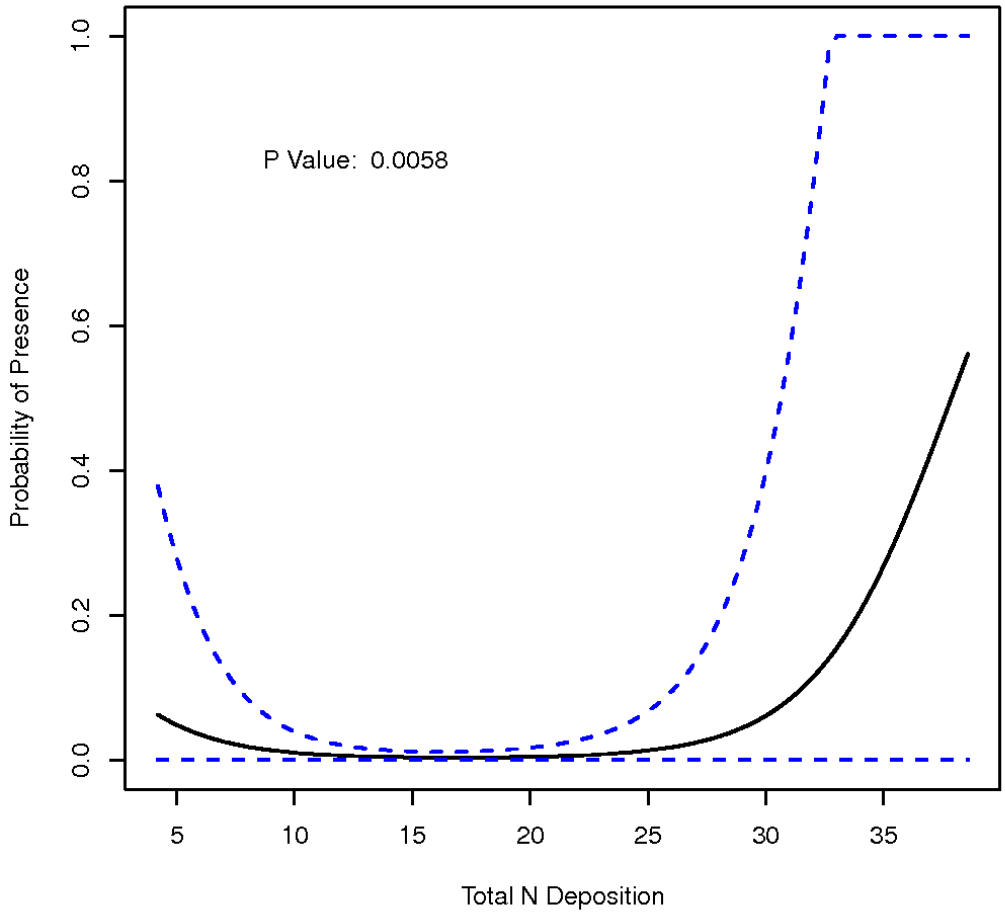

Figure A38. Spatial change in the probability of presence of *Douinia ovate* in upland heathland with increasing total current inorganic N deposition (kg N ha^{-1} yr^{-1}). Data from BBS database.

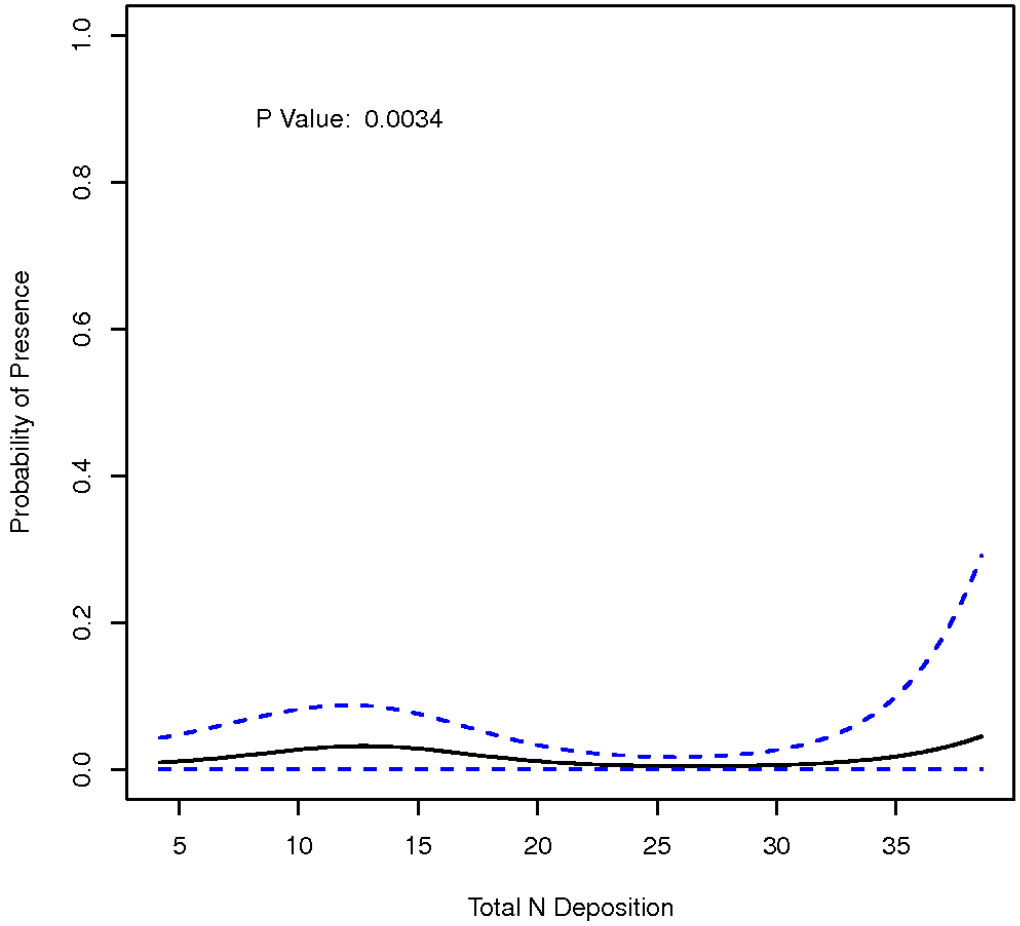

Figure A39. Spatial change in the probability of presence of *Entosthodon attenuates* in upland heathland with increasing total current inorganic N deposition (kg N ha^{-1} yr^{-1}). Data from BBS database.

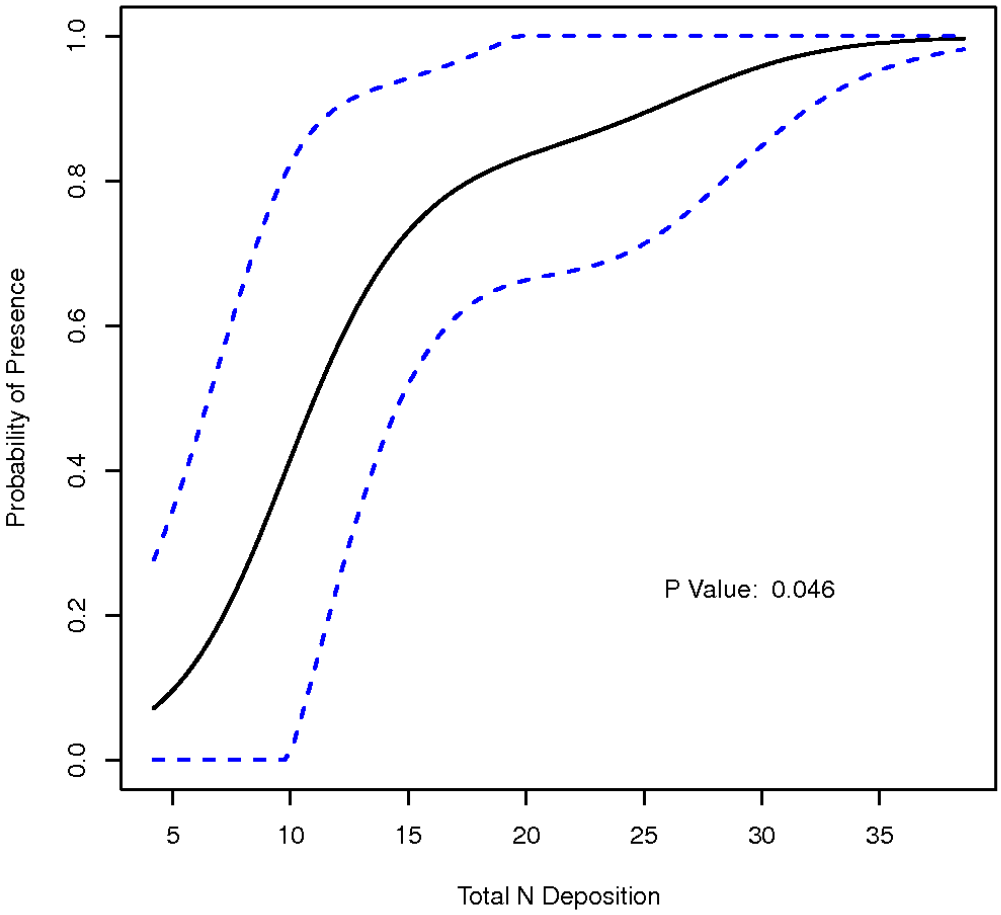

Figure A40. Spatial change in the probability of presence of *Fissidens bryoides s.l.* in upland heathland with increasing total current inorganic N deposition (kg N ha^{-1} yr^{-1}). Data from BBS database.

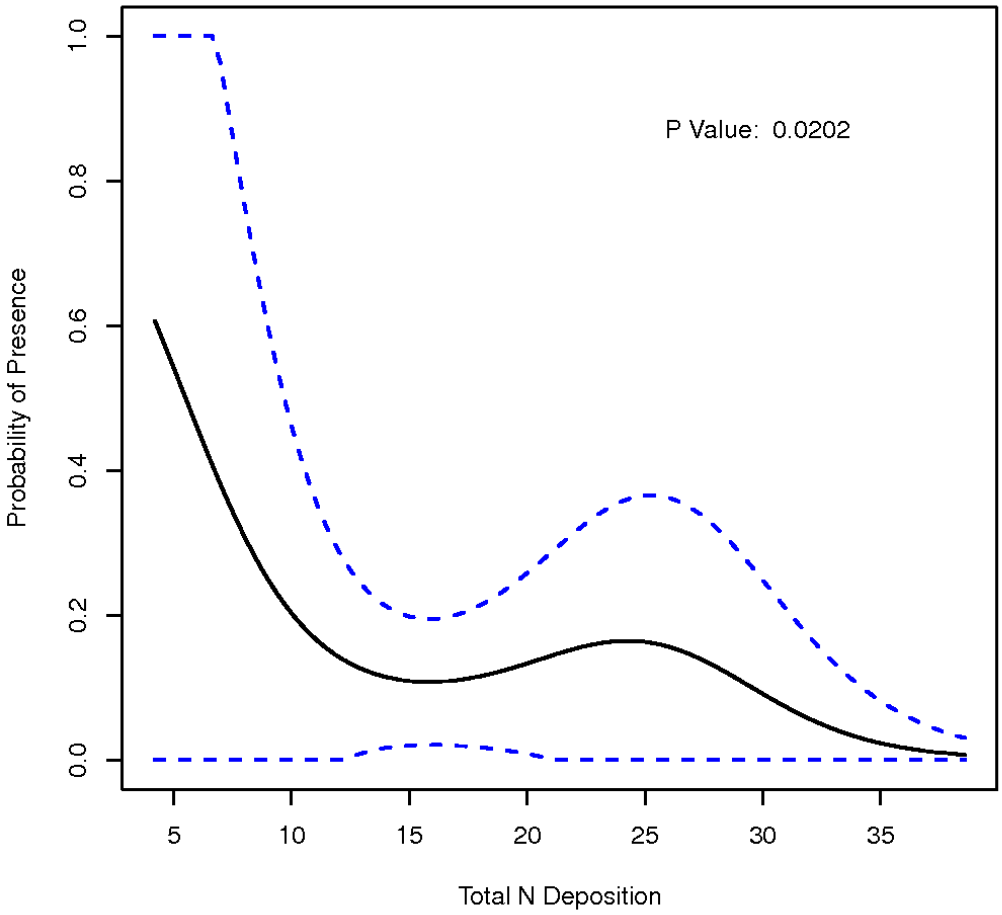

Figure A41. Spatial change in the probability of presence of *Fossombronia wondraczekii* in upland heathland with increasing total current inorganic N deposition (kg N ha^{-1} yr^{-1}). Data from BBS database.

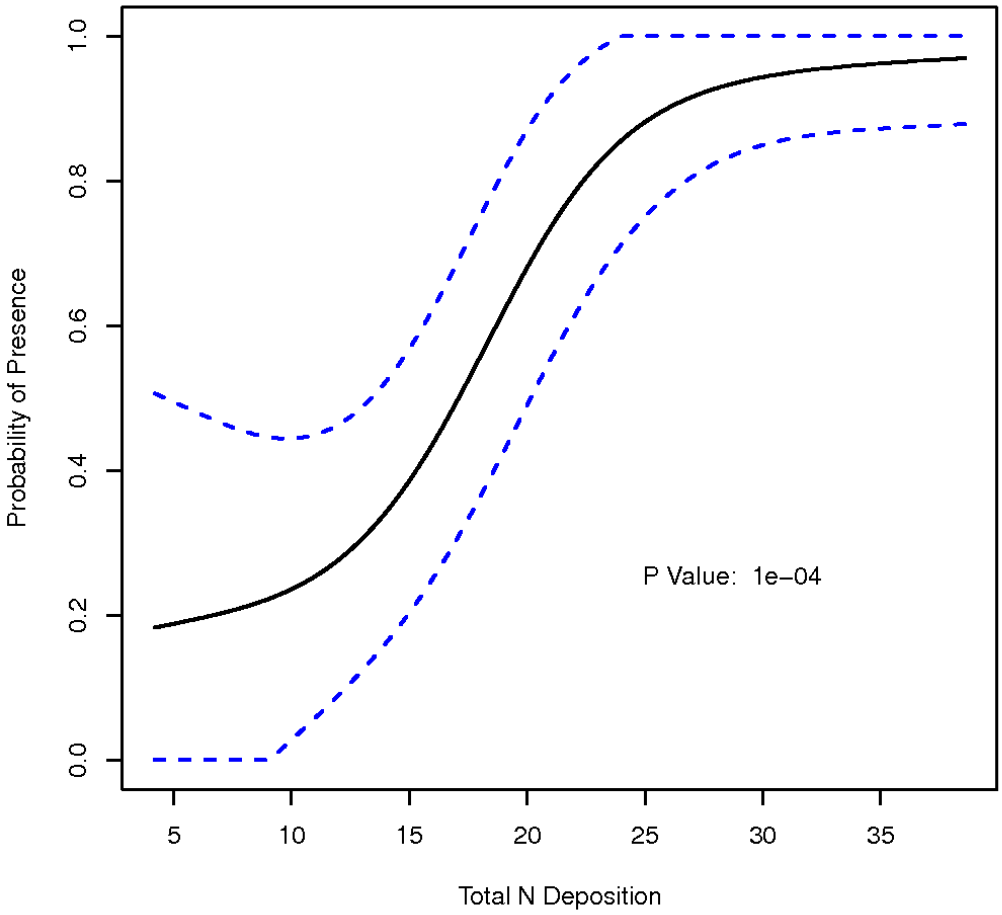

Figure A42. Spatial change in the probability of presence of *Gymnocolea inflata* in upland heathland with increasing total current inorganic N deposition (kg N ha^{-1} yr^{-1}). Data from BBS database.

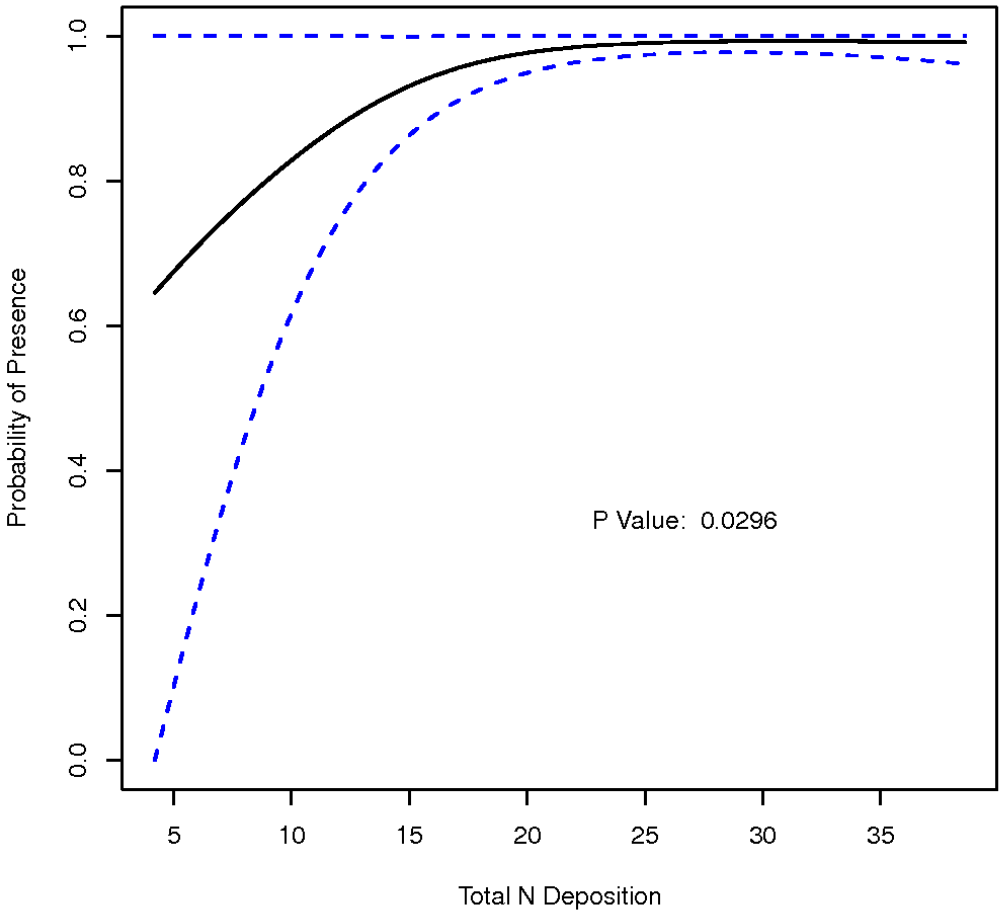

Figure A43. Spatial change in the probability of presence of *Hylocomium splendens* in upland heathland with increasing total current inorganic N deposition (kg N ha^{-1} yr^{-1}). Data from BBS database.

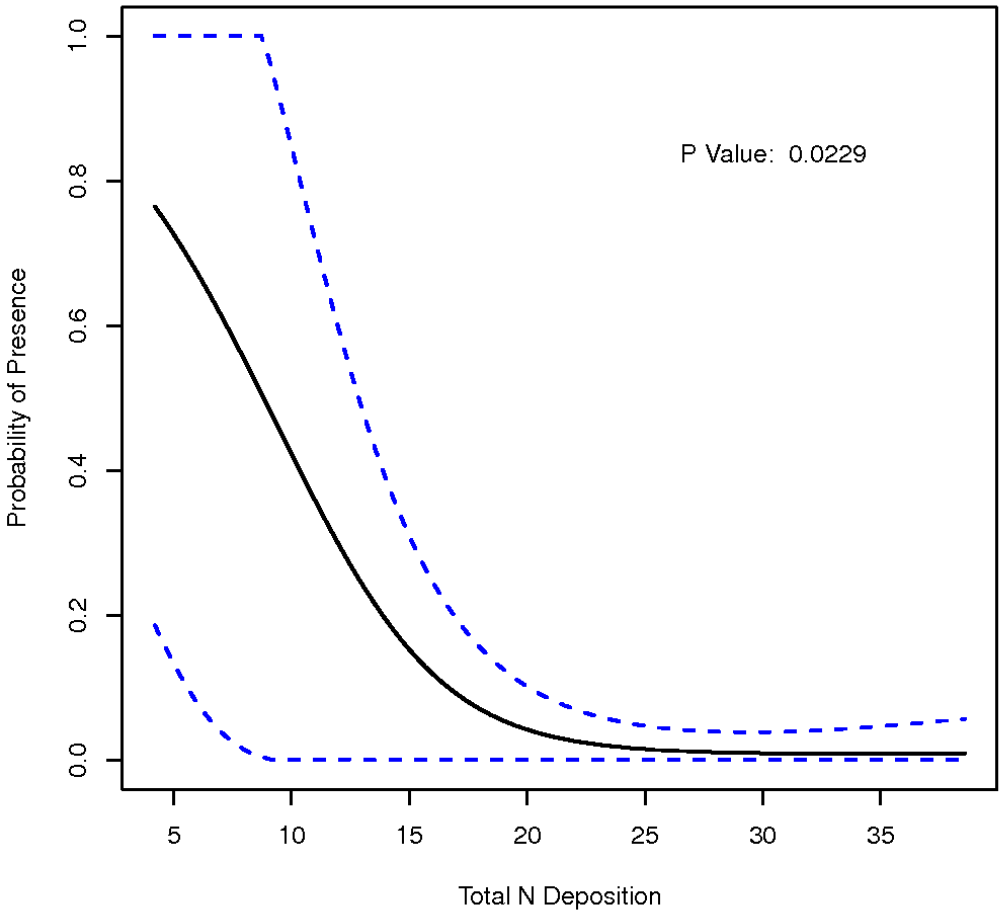

Figure A44. Spatial change in the probability of presence of *Lepidozia pearsonii* in upland heathland with increasing total current inorganic N deposition (kg N ha^{-1} yr^{-1}). Data from BBS database.

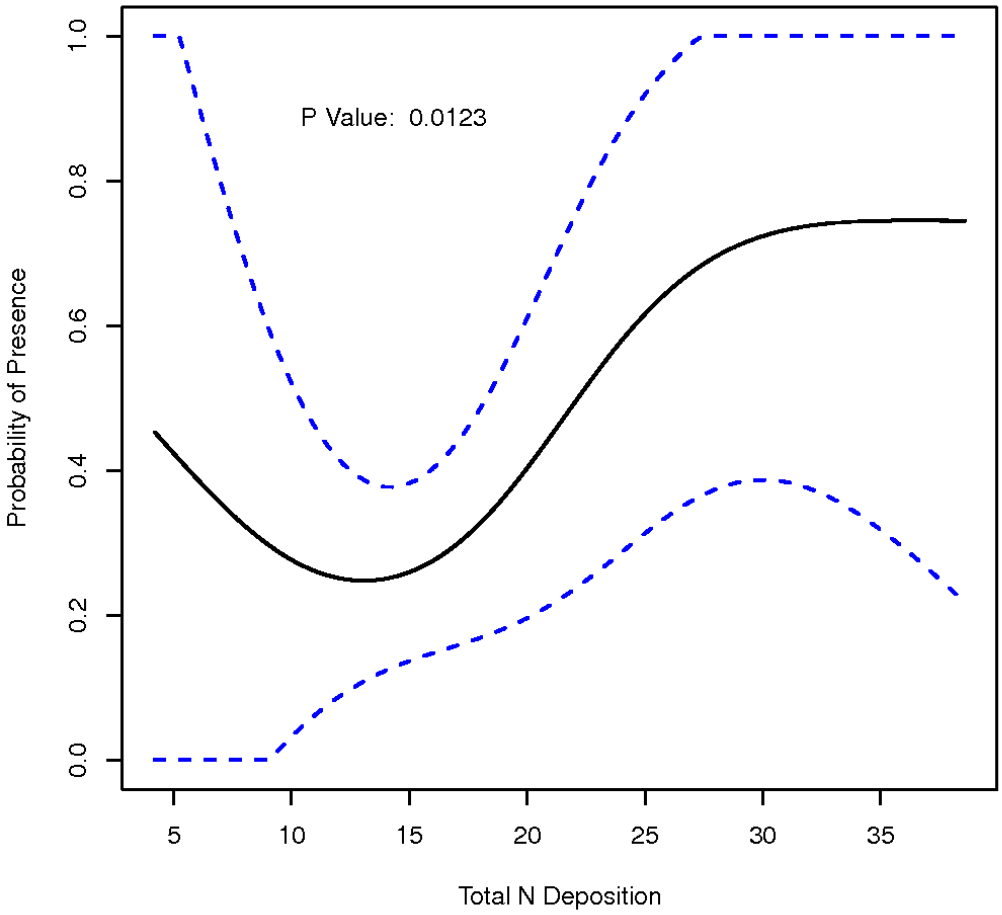

Figure A45. Spatial change in the probability of presence of *Leptodontium flexifolium* in upland heathland with increasing total current inorganic N deposition (kg N ha^{-1} yr^{-1}). Data from BBS database.

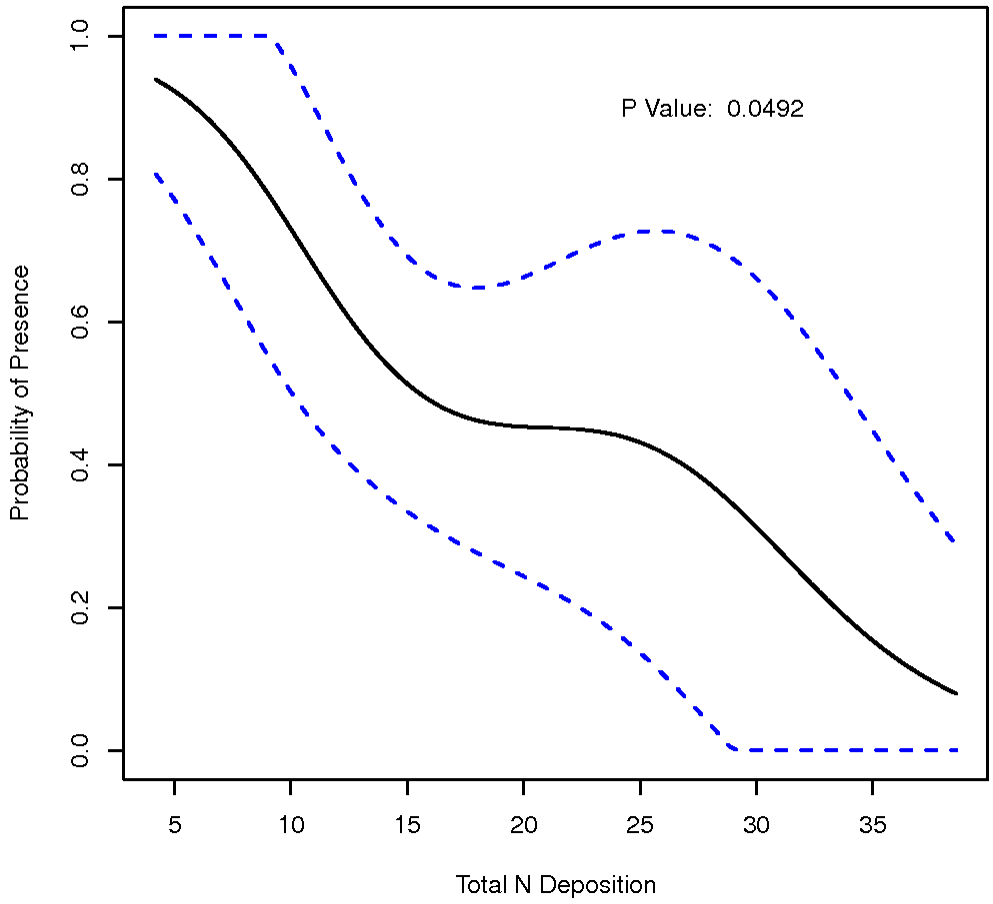

Figure A46. Spatial change in the probability of presence of *Leucobryum glaucum* in upland heathland with increasing total current inorganic N deposition (kg N ha^{-1} yr^{-1}). Data from BBS database.

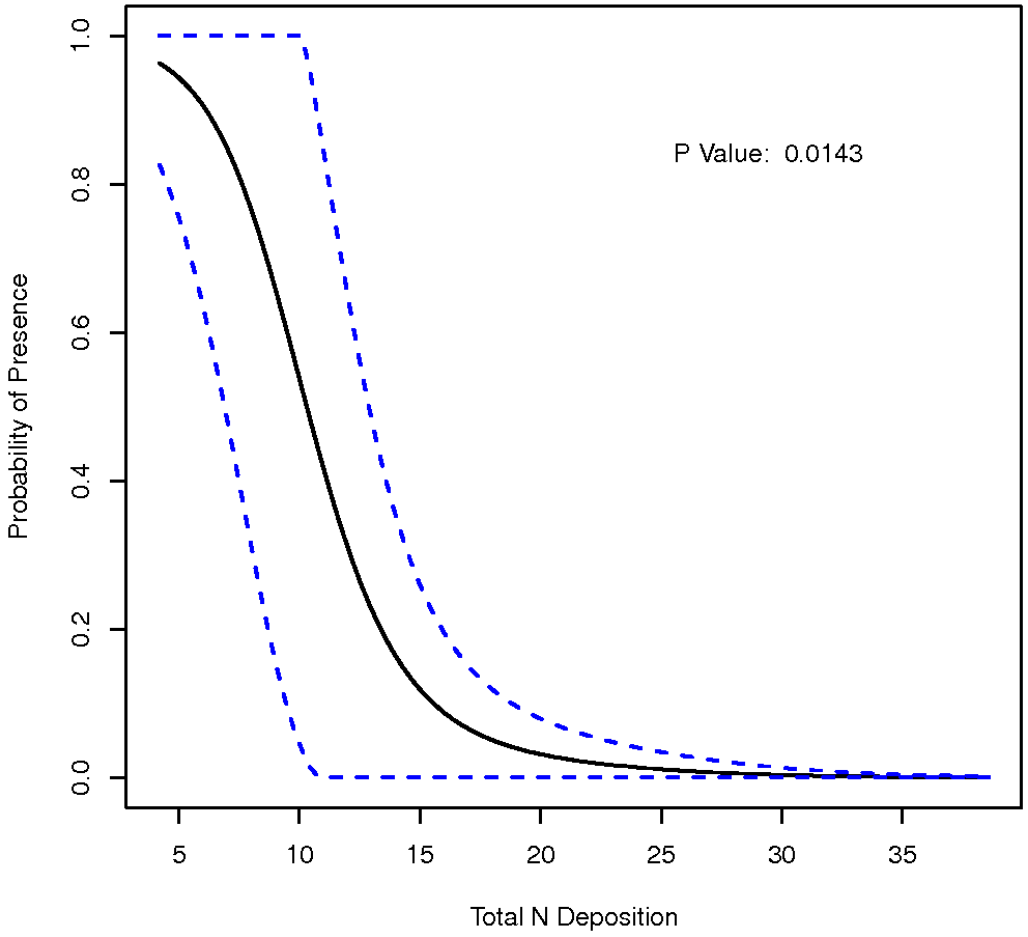

Figure A47. Spatial change in the probability of presence of *Microlejeunea ulicina* in upland heathland with increasing total current inorganic N deposition (kg N ha^{-1} yr^{-1}). Data from BBS database.

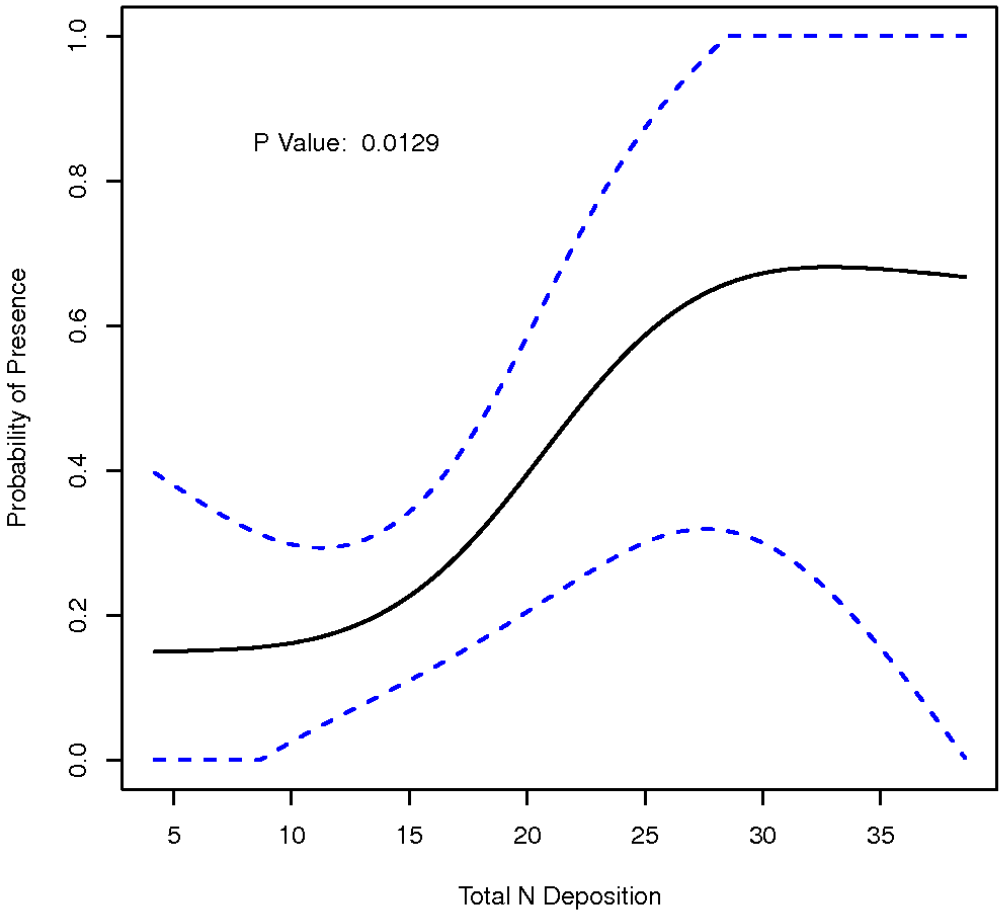

Figure A48. Spatial change in the probability of presence of *Mylia anomala* in upland heathland with increasing total current inorganic N deposition (kg N ha^{-1} yr^{-1}). Data from BBS database.

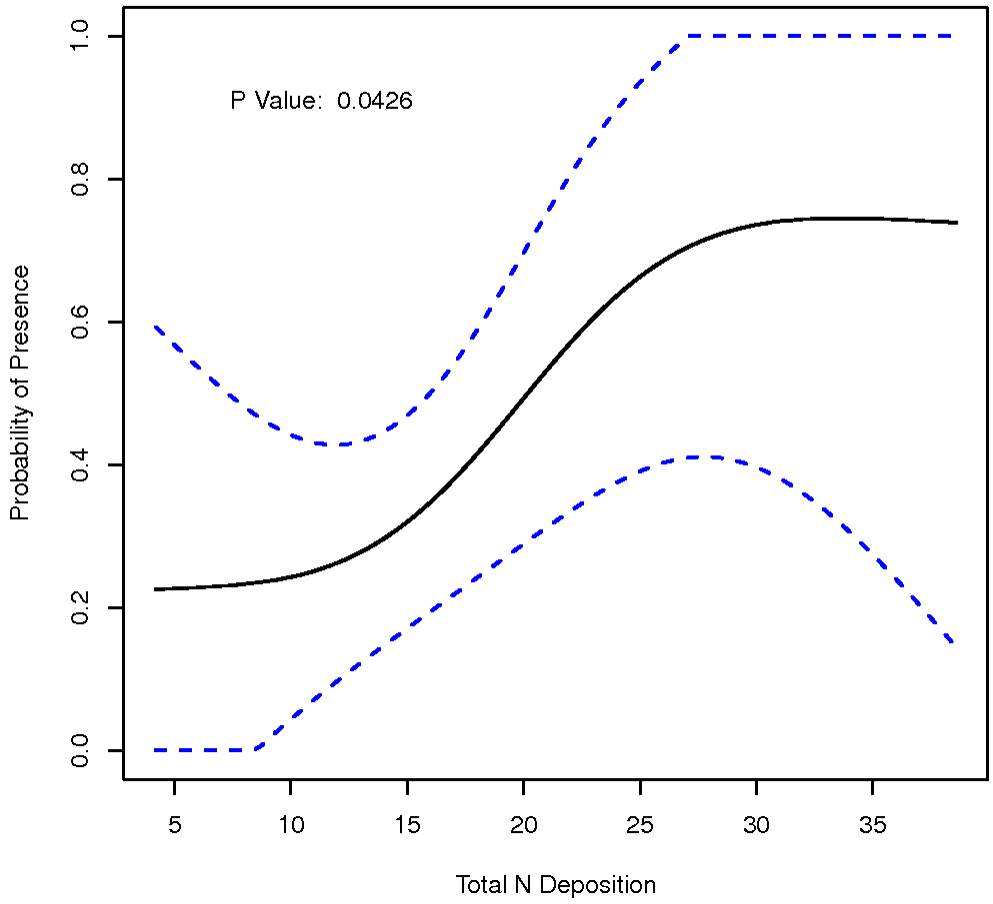

Figure A49. Spatial change in the probability of presence of *Odontoschisma sphagni* in upland heathland with increasing total current inorganic N deposition (kg N ha^{-1} yr^{-1}). Data from BBS database.

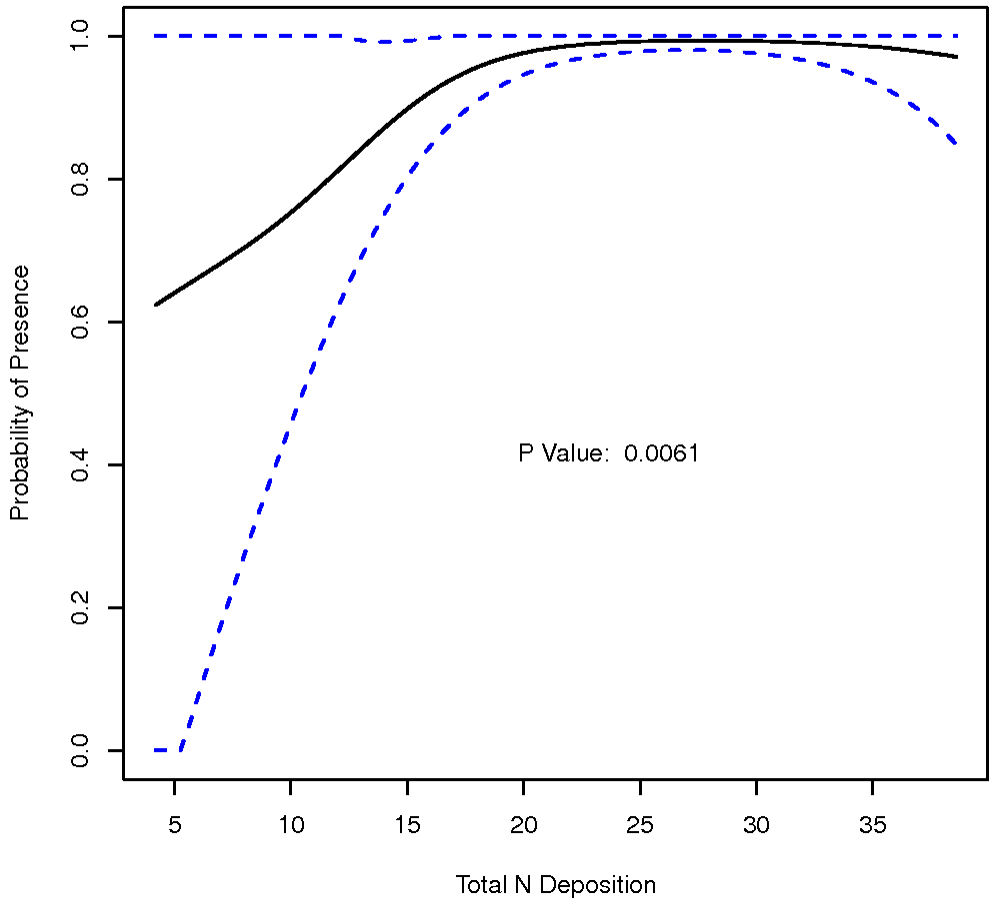

Figure A50. Spatial change in the probability of presence of *Polytrichum commune* in upland heathland with increasing total current inorganic N deposition (kg N ha^{-1} yr^{-1}). Data from BBS database.

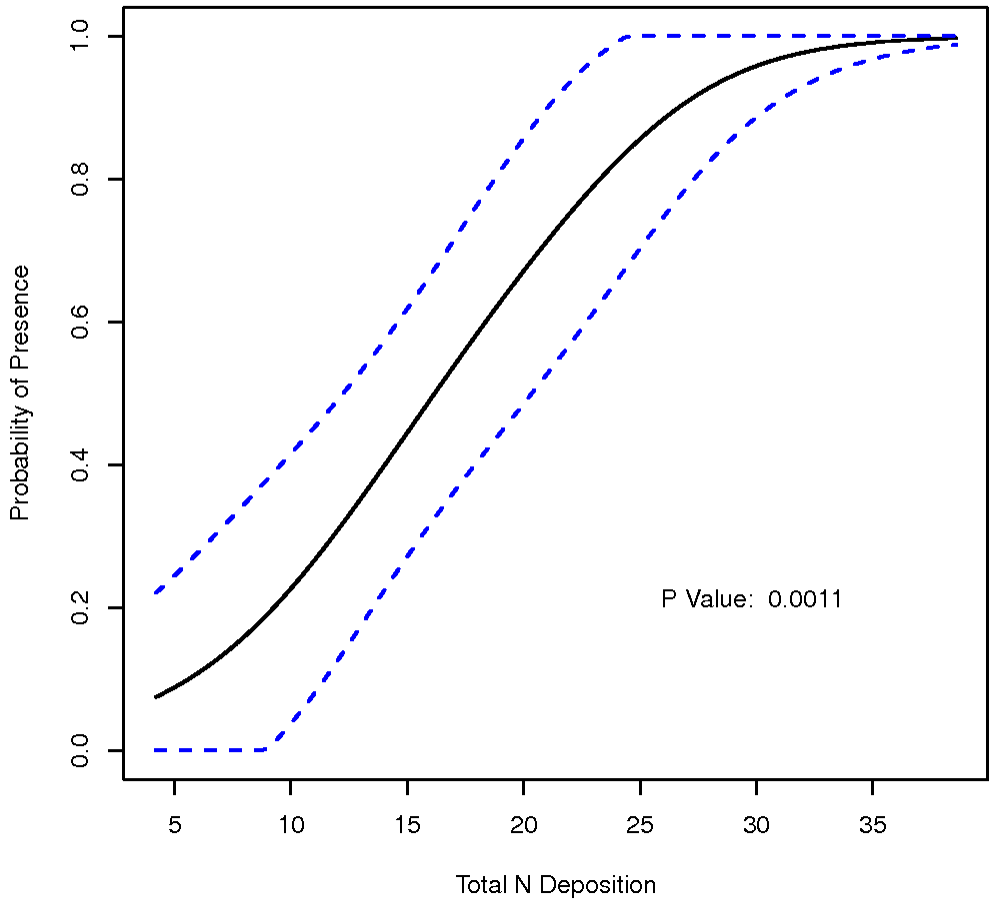

Figure A51. Spatial change in the probability of presence of *Racomitrium ericoides* in upland heathland with increasing total current inorganic N deposition (kg N ha^{-1} yr^{-1}). Data from BBS database.

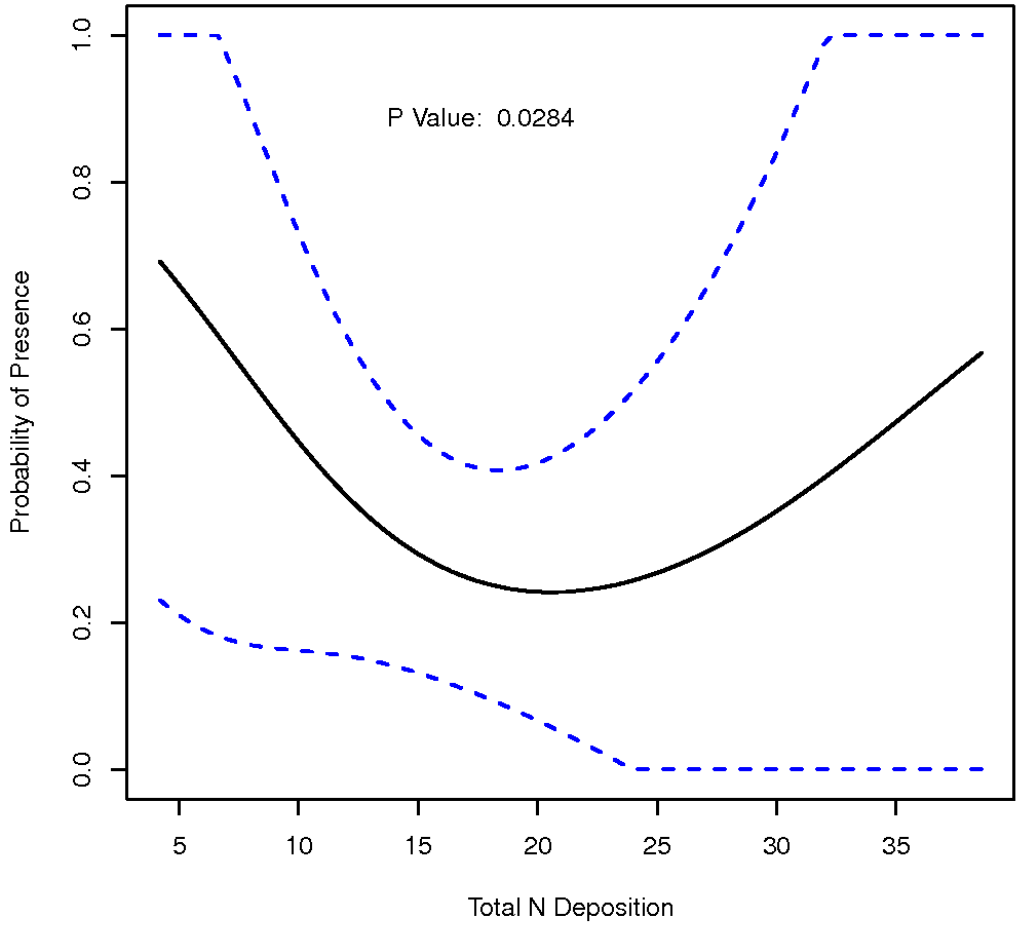

Figure A52. Spatial change in the probability of presence of *Riccardia palmate* in upland heathland with increasing total current inorganic N deposition (kg N ha^{-1} yr^{-1}). Data from BBS database.

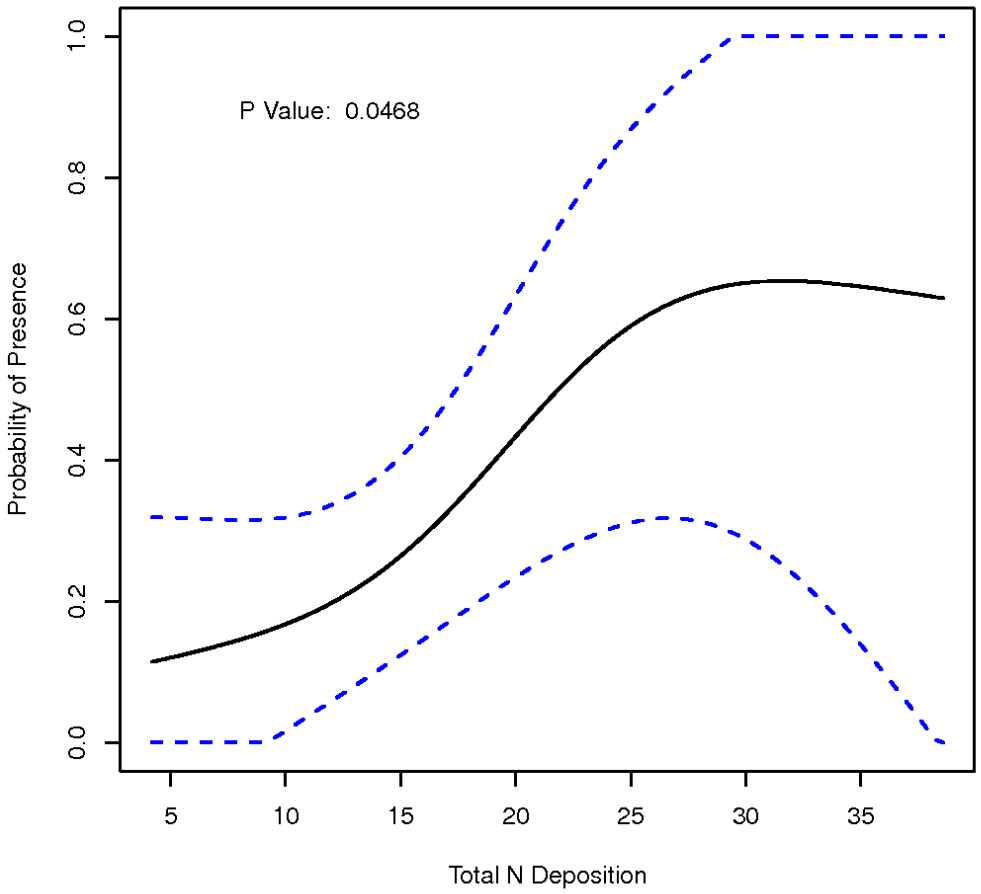

Figure A53. Spatial change in the probability of presence of *Scapania irrigua* in upland heathland with increasing total current inorganic N deposition (kg N ha^{-1} yr^{-1}). Data from BBS database.

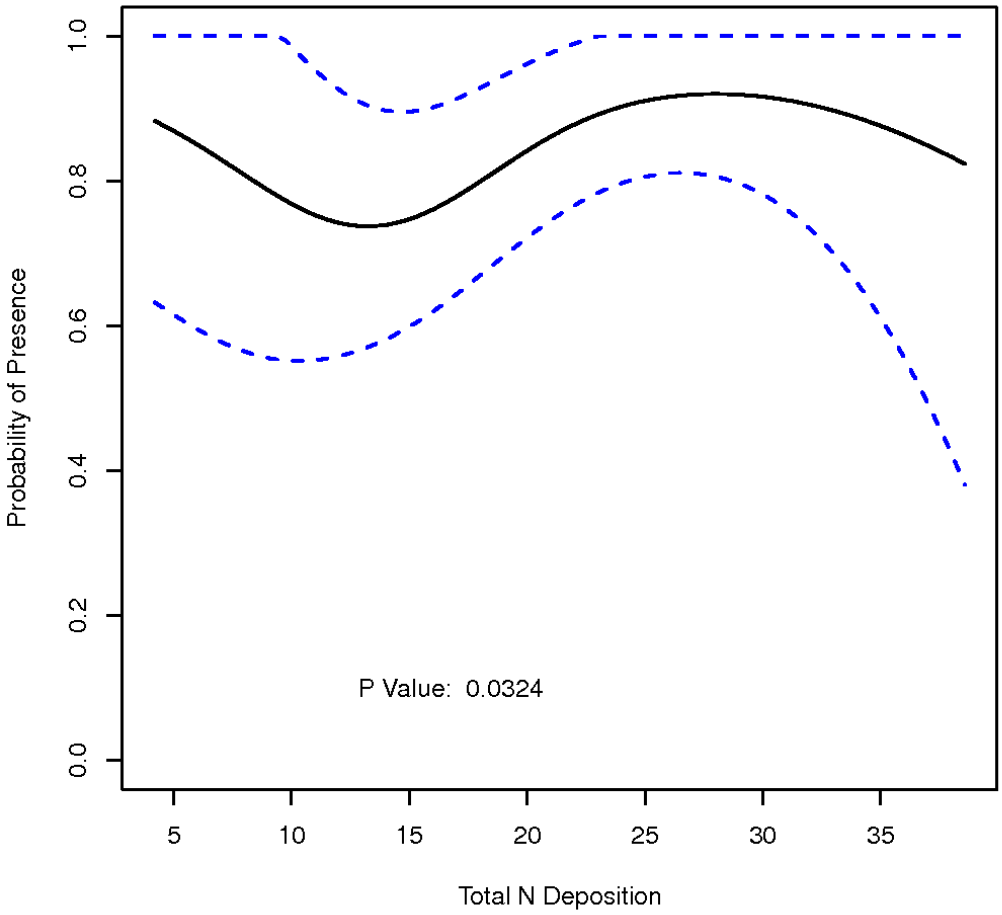

Figure A54. Spatial change in the probability of presence of *Sphagnum capillifolium* in upland heathland with increasing total current inorganic N deposition (kg N ha^{-1} yr^{-1}). Data from BBS database.

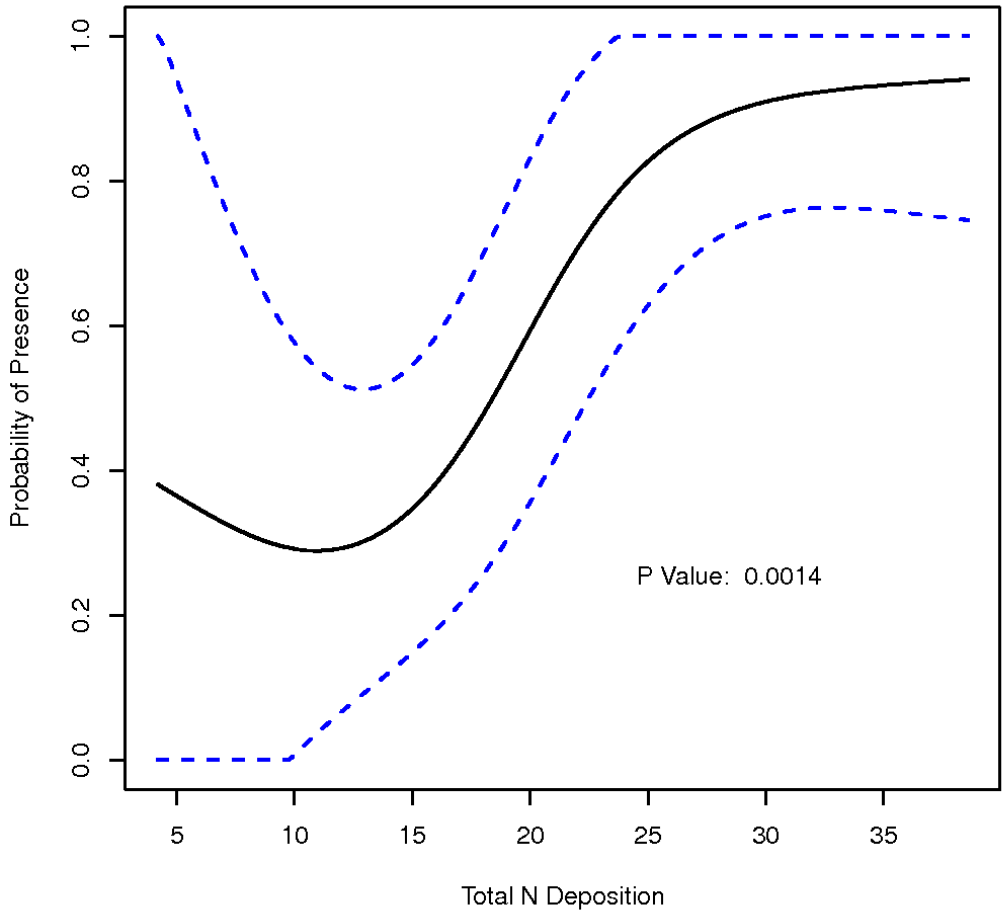

Figure A55. Spatial change in the probability of presence of *Sphagnum denticulatum* in upland heathland with increasing total current inorganic N deposition (kg N ha^{-1} yr^{-1}). Data from BBS database.

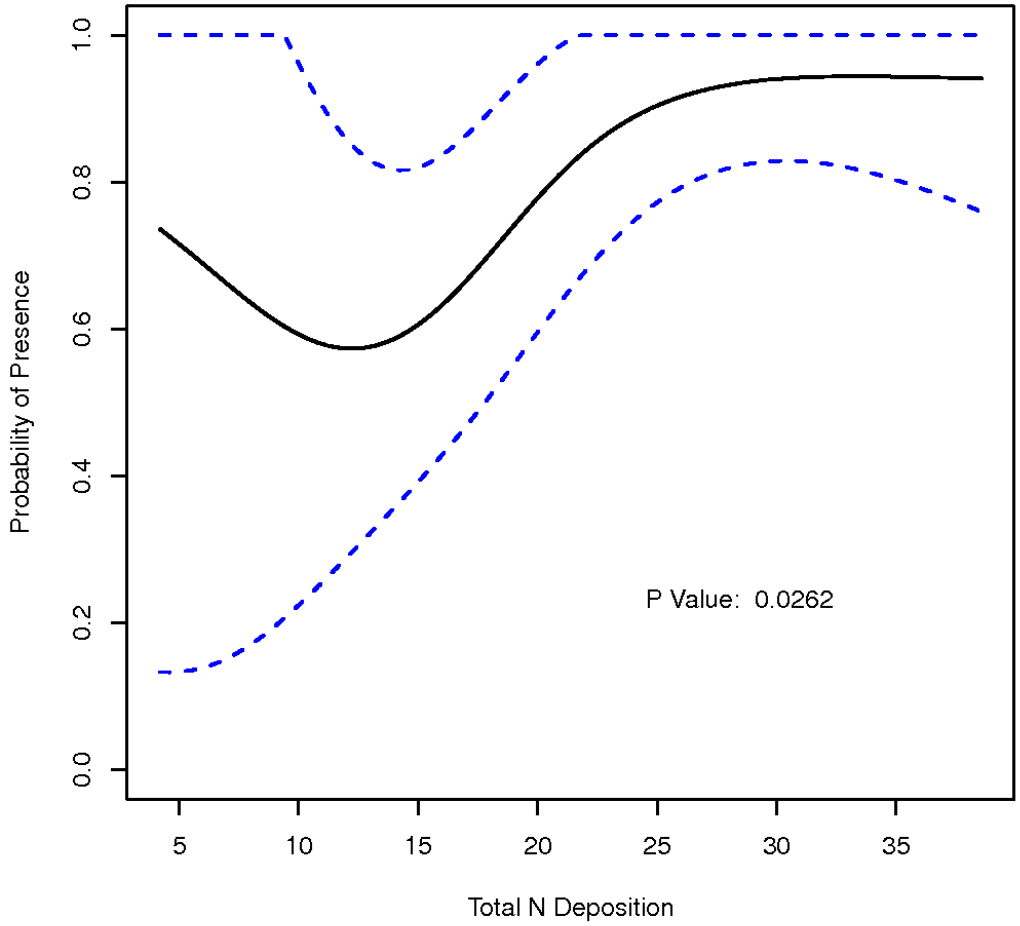

Figure A56. Spatial change in the probability of presence of *Sphagnum fallax* in upland heathland with increasing total current inorganic N deposition (kg N ha^{-1} yr^{-1}). Data from BBS database.

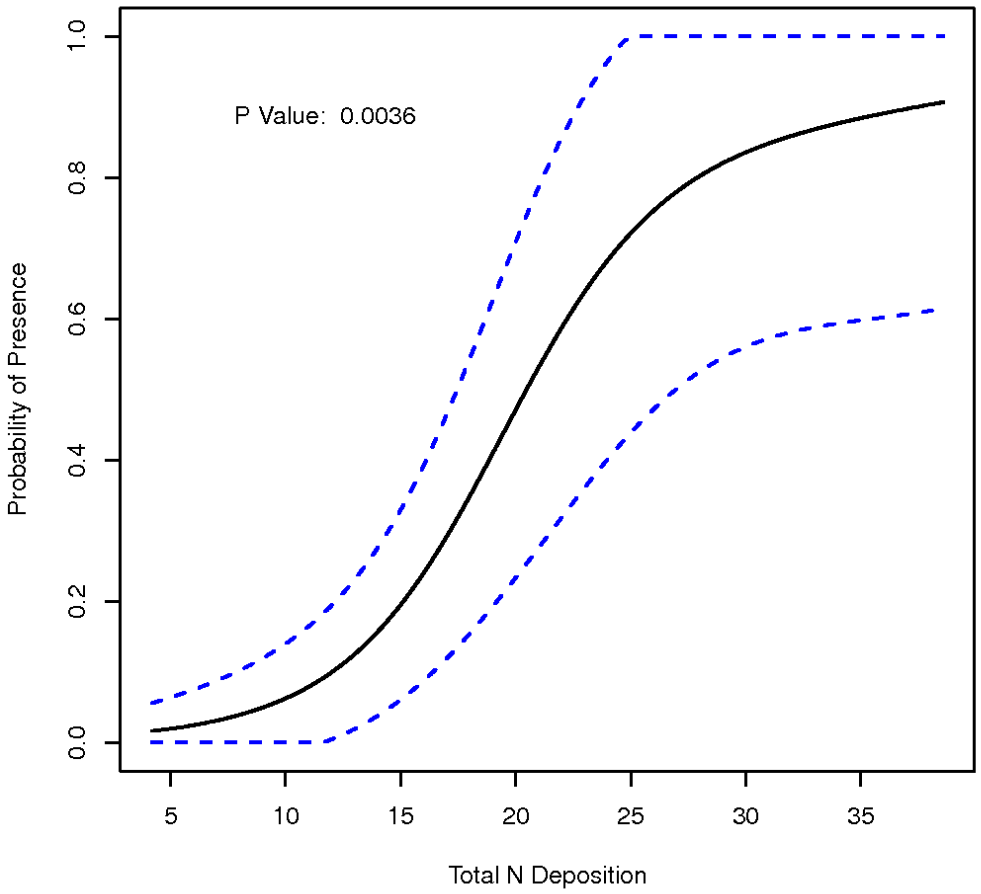

Figure A57. Spatial change in the probability of presence of *Sphagnum russowii* in upland heathland with increasing total current inorganic N deposition (kg N ha^{-1} yr^{-1}). Data from BBS database.

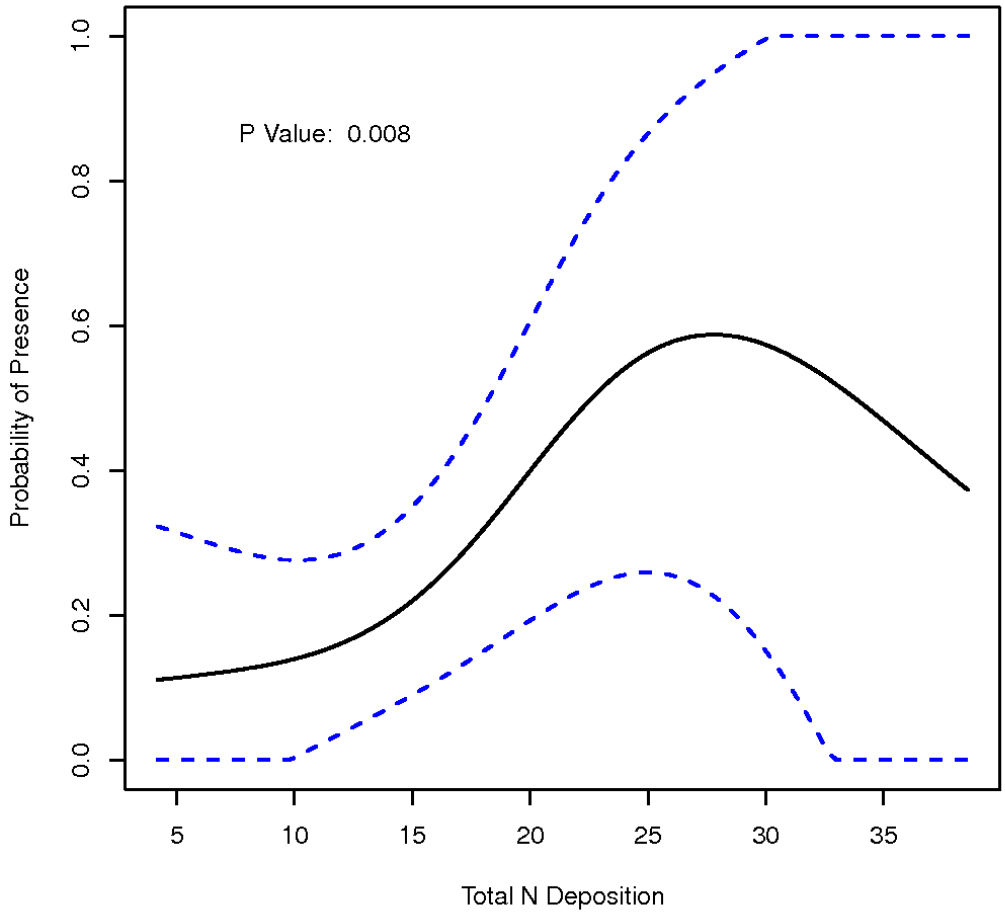

Figure A58. Spatial change in the probability of presence of *Sphagnum squarrosum* in upland heathland with increasing total current inorganic N deposition (kg N ha^{-1} yr^{-1}). Data from BBS database.

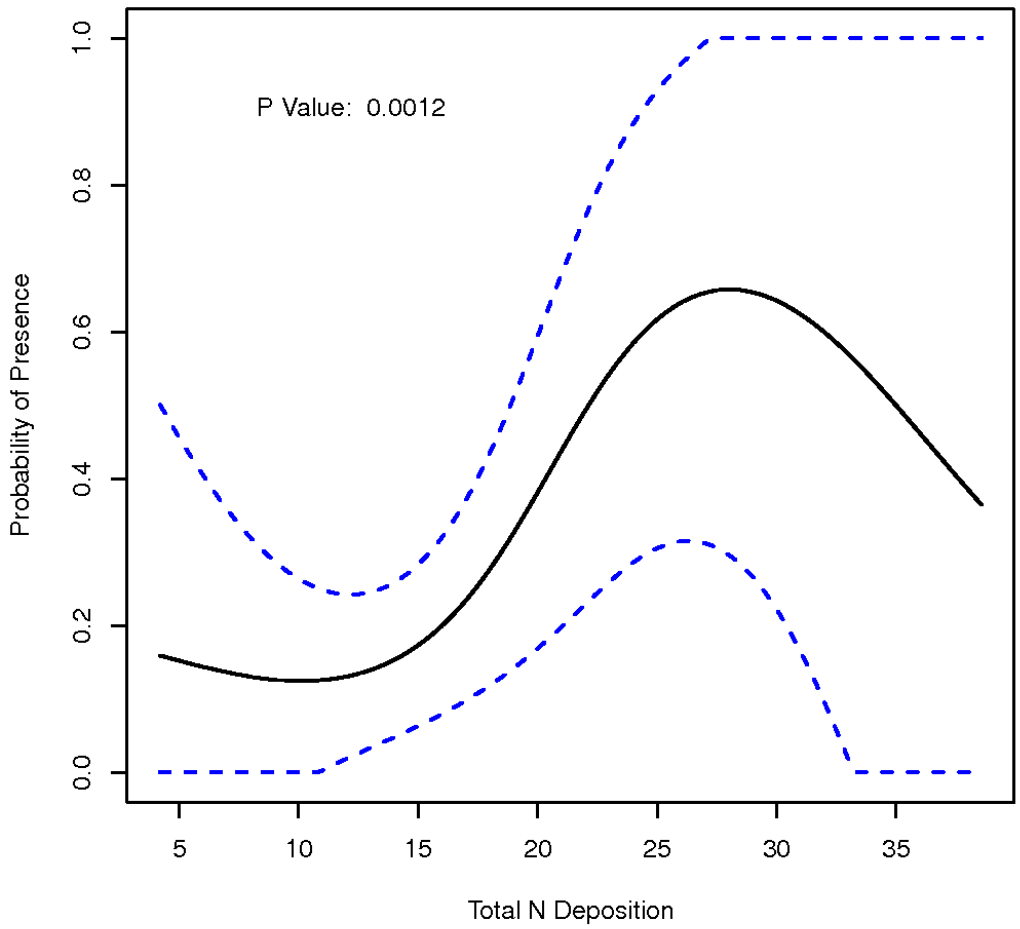

Figure A59. Spatial change in the probability of presence of *Sphagnum subnitens* in upland heathland with increasing total current inorganic N deposition (kg N ha^{-1} yr^{-1}). Data from BBS database.

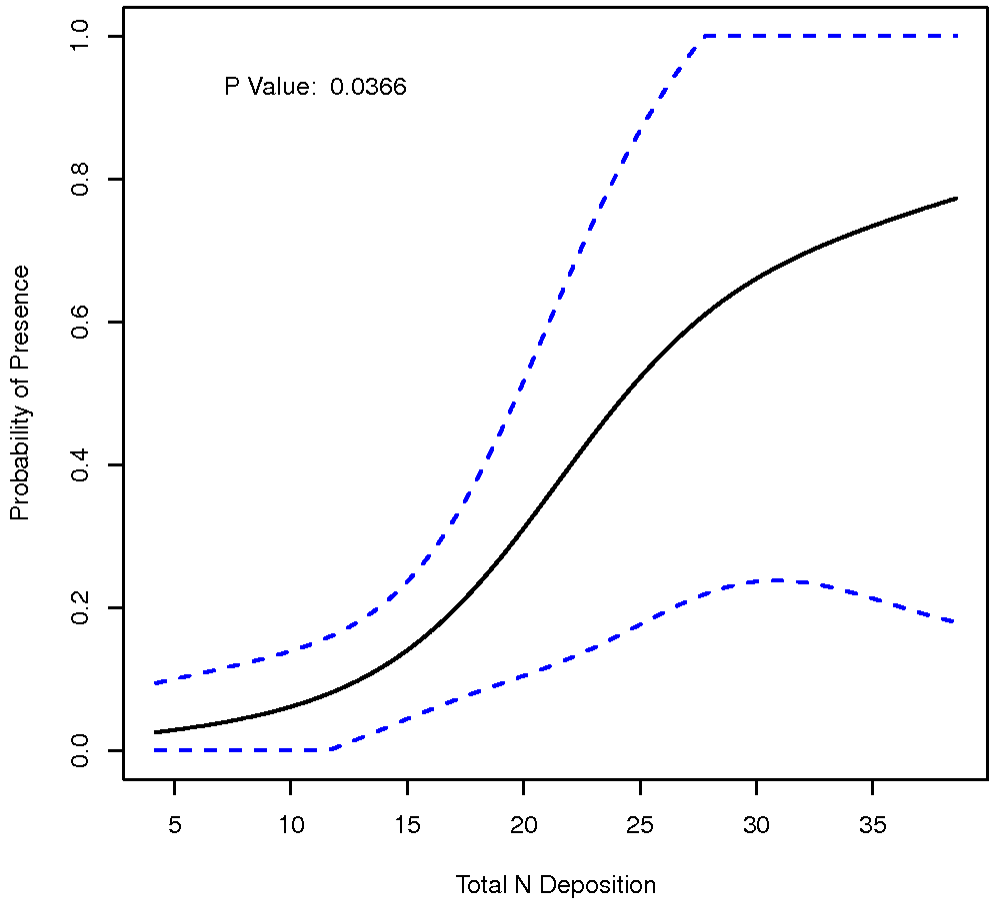

Figure A60. Spatial change in the probability of presence of *Sphagnum tenellum* in upland heathland with increasing total current inorganic N deposition (kg N ha^{-1} yr^{-1}). Data from BBS database.

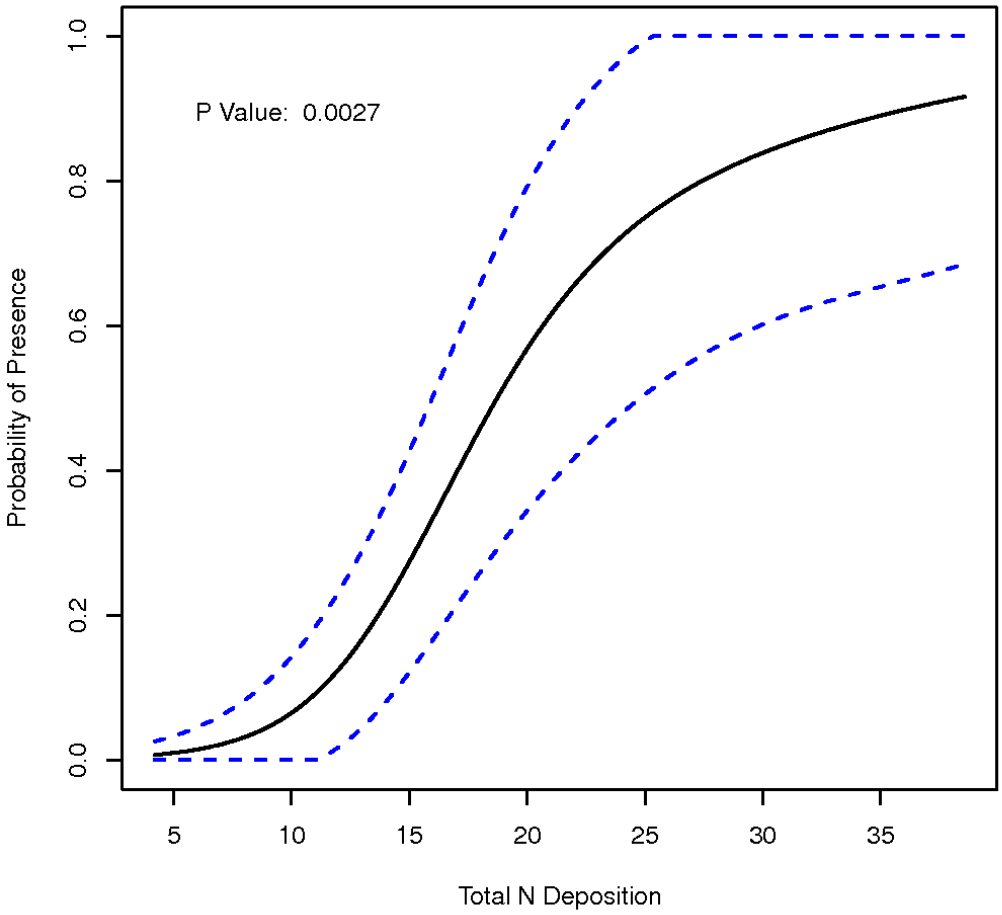

Figure A61. Spatial change in the probability of presence of *Warnstorfia fluitans* in upland heathland with increasing total current inorganic N deposition (kg N ha^{-1} yr^{-1}). Data from BBS database.